THE DESIGN AND CONSTRUCTION OF A COBALT IRRADIATION CELL AND ITS APPLICATION TO A STUDY OF THE EFFECTS OF GAMMA RADIATION ON ION EXCHANGE RESINS

by

M. Streat, B.Sc.Tech., A.M.C.T.

A Thesis submitted for the degree of
Doctor of Philosophy
of the University of London

Department of Chemical Engineering
and Chemical Technology,
Imperial College,
London S.W.7.

June, 1961.

ABSTRACT

The design and construction of a kilocurie cobalt-60 irradiation cell is described in detail. This consists of a concrete shielded chamber, into which the source is pushed by means of an electrically driven flexible cable. The source chamber is approached through a labyrinth corridor. The source capsule is stored in a large concrete tower outside the irradiation chamber when not in use. Elaborate safety precautions are provided to ensure that there is no risk of any radiation health hazard. When in operation, the source provides dose rates up to 1 Mr/hr, which is sufficient for many radiation chemistry studies.

This source has been used to irradiate ion exchange resins with gamma radiation at doses of up to 500 Mr. The work reported here describes the breakdown of strong-base polystyrene resins with quaternary ammonium functional groups. The loss in strong-base capacity has been related to the total dose received. An increase in weak-base capacity, resulting from the loss of a methyl group from the strong-base quarternary structure, has been found. The basic products liberated on irradiation have been separately determined as tertiary, secondary and

primary aliphatic amines and ammonia. A trace of formaldehyde is also detected.

Free radical mechanisms have been suggested for the radiation decomposition reactions observed. The thermal stability of the anion exchange resin has also been examined, and decomposition follows the general Hofmann degradation reaction.

ACKNOWLEDGEMENTS

The author wishes to thank Mr. G. R. Hall for his invaluable assistance and guidance throughout this work. The helpful advice of Dr. A. J. Swallow on the radiation chemistry aspects of this work is acknowledged. The author also wishes to thank Mr. P. R. Natarajan for permission to refer to his unpublished results on the nitrate form of resins and for his collaboration in developing some of the analytical procedures.

The co-operation of Messrs. Teleflex Products Limited, Atomic Energy of Canada Limited, Dr. G. S. Murray and his colleagues at the Wantage Radiation Laboratories, Mr. A. C. V. Sweeting and his staff, in various aspects of the design and installation of the cobalt source, is greatly appreciated.

Acknowledgement is also made to Esso Petroleum Company Limited for a studentship.

CONTENTS

		PAGE
	DESIGN OF A COBALT IRRADIATION CELL	
SECTION 1	INTRODUCTION	1
SECTION 2	DESCRIPTION OF SOURCE TRAVEL	13
SECTION 3	CONCRETE FOR RADIATION SHIELDING	19
SECTION 4	DESIGN OF CONCRETE SHIELD	28
SECTION 5	BUILDING OF THE CONCRETE SHIELD	33
SECTION 6	SOURCE CAPSULE DESIGN	36
SECTION 7	DESIGN OF SOURCE TRAVEL MECHANISM AND ANCILLARY EQUIPMENT	41
SECTION 8	DESIGN OF LEAD SHIPPING CONTAINER	51
SECTION 9	SPECIAL FACILITIES PROVIDED IN THE IRRADIATION CELL	57
SECTION 10	TESTING OF THE SOURCE TRAVEL ASSEMBLY	63
SECTION 11	INSTALLATION OF THE SOURCE CAPSULE	66
SECTION 12	DOSIMETRY AND CALIBRATION OF THE SOURCE	71
PLATES 1 - 9		80
DRAWINGS ANT 8 - 12		81

PAGE

EFFECTS OF RADIATION ON ION EXCHANGE RESINS

SECTION 13	SURVEY OF PREVIOUS WORK	82
SECTION 14	PRELIMINARY INVESTIGATIONS	88
SECTION 15	IRRADIATION OF THE HYDROXIDE FORM OF THE RESIN	101
SECTION 16	THERMAL STABILITY OF THE HYDROXIDE FORM	143
APPENDIX I		149
BIBLIOGRAPHY		155

NOMENCLATURE

C	=	curie
mC	=	millicurie = 10^{-3}C
MC	=	megacurie = 10^{6}C
r	=	rad = 6.24×10^{13} ev/g
mr	=	millirad = 10^{-3}r
Mr	=	megarad = 10^{6}r
Mr/hr	=	megarad per hour
ev	=	electron volt
Mev	=	million electron volt
MW	=	megawatt
g	=	gram
mpl	=	maximum permissible level
mμ	=	millimicron
		where 1 mμ = 10 Angstrom = 10^{-7}cm.

Grades of Stainless Steel

Type	American notation	Remarks
FDP	321	Titanium stabilised
FMB	316	Molybdenum stabilised
FCB	347	Columbium stabilised

D E S I G N O F A C O B A L T
I R R A D I A T I O N C E L L

SECTION 1

I N T R O D U C T I O N

A. CHOICE OF ISOTOPE

B. DESIGN OF COBALT-60 IRRADIATION CELLS

(i) Lead shields containing stationary source, samples moved into position.

(ii) Lead shields where the source is raised or lowered into the irradiation space.

(iii) Shield design using a pit or cavity with lead, concrete and earth as auxiliary shielding material.

(iv) Water shielded sources.

(v) Sources providing a large irradiation space.

(vi) Other methods of irradiating chemical samples.

C. LOCATION OF IRRADIATION CELL AND CHOICE OF DESIGN

A. CHOICE OF ISOTOPE

The use of gamma rays from cobalt-60 for irradiation purposes is very well known (1 - 4). Cobalt sources are widely used for teletherapy (5,6), industrial radiography, radiation chemistry studies and in large-scale irradiation (7 - 10) processes. The source designed in this laboratory was required to give of the order of 10^6 rads per hour dose-rate for studying the radiation chemistry of organic and inorganic compounds, radiation effects on high polymers, and the harmful effects produced by radiation in non-metallic substances, particularly in chemical processing materials.

Cobalt-60 is produced by neutron irradiation of the parent material cobalt-59, in a nuclear reactor (11,12). The properties of cobalt-60 are given in Table I, together with those of caesium-137, which is a less commonly used source of gamma radiation (13). Caesium-137 is formed as a fission product in the fuel of a nuclear reactor, and has been separated in large quantities from the irradiated fuel after a cooling period of several months to allow for decay of short-lived fission products.

Caesium-137, however, is not without its problems when it is to be used as a source of gamma radiation. One of the most serious is the contaminating presence of caesium-134, another beta-gamma emitter of half life

TABLE I

	Cobalt-60	Caesium-137
Half Life Yrs.	5.25	30.00
Type of Radiation (MeV) — Beta	0.306 (100%) 1.48 (0.15%)	(0.52) (92%) 1.17 (8%)
Type of Radiation (MeV) — Gamma	1.17 (100%) 1.33 (100%)	0.662 (82%) Via 2.6 min. Ba-137
K-factor r/mc.hr. at 1 cm.	13.2	3.24
Density g/cm^3	8.90	1.87
Production Process	Co^{59} (n,γ) Co^{60}	Fission Product

2.2 years. This is formed by neutron irradiation of caesium-133 which is produced in about 6 per cent of fissions. Caesium-134 could account for up to 50 per cent or more of the total radiation energy from caesium isotopes, depending on the type of reactor and delay in chemical processing, and could seriously complicate the maintenance of constant source power over a period of years. Caesium-134 also gives a hard gamma component (1.4 MeV) which, though low in abundance, significantly increases shielding requirements. The self-heating of radio-caesium during transport in large quantities, can add to the problem of choosing a stable salt for isolation. Despite these difficulties, which tend to reduce the usefulness of caesium as a gamma source, the separation of caesium-137 from fission product solutions becomes economic only when large quantities are to be produced. One advantage of caesium is that it requires less shielding per curie than cobalt-60. However, the commercial development of this type of source has been less rapid than that of cobalt-60.

Cobalt-60 has a half life of 5.25 years, and therefore a source using this material requires only annual replenishment to maintain its power within $\pm$ 6 per cent. The associated beta radiation (0.3 MeV) is completely absorbed within the sealed capsules normally used to

contain it. The bremsstrahlung (mean energy 0.15 MeV) accounts for less than 1 per cent of the emitted gamma energy. The two gamma photons emitted per disintegration (1.17 and 1.33 MeV) are so nearly equivalent in energy that differential absorption in a target can be neglected. These energies are not sufficiently high to eject photo-neutrons from any element, but are high enough to give useful penetration. During neutron irradiation a small proportion of rather more energetic nuclei is formed, but these decay to cobalt-60 with a half life of about 10 minutes.

Cobalt-~~60~~ may be sealed in stainless steel cans before activation, allowing for leak tests to be performed without the expense of remote handling.

Finally, cobalt-60 can arise as a by-product of power reactors. The necessary absorption of neutrons near the core centre may be attained by insertion of cobalt. During the normal operation of natural uranium thermal reactors, up to 1 MC of cobalt-60 can be produced per 500 MW years of thermal energy. The potential future production of cobalt-60 by this means is very large, considering that 1 C of cobalt-60 is energetically equivalent to about 5 C of caesium-137.

B. DESIGN OF COBALT-60 IRRADIATION CELLS

The design of cobalt-60 irradiation cells depends largely on the type of shielding material used. The more important designs have used water, earth, lead or concrete. The advantage of lead shielding is that only relatively small thicknesses, i.e. up to about 12 in. are required to provide sufficient attenuation of gamma radiation for a kilocurie source. Lead shielding is expensive, and cheaper materials such as ordinary or baryta concrete are often preferred, but shield thicknesses can then be four to five times greater. The cheapness of concrete, however, makes it a widely used shielding material.

Water shielding is also used, but this requires thicknesses up to twelve to fifteen times that of lead for a kilocurie source.

The method of sample irradiation for these various shield designs depends on the size of sample, the homogeneity of the radiation field, and the actual dose rate. Two designs are common, i.e. where the source is brought from storage to irradiate the sample, or where the sample is placed in position near a stationary source capsule.

The shape and design of the source capsule is important in defining the homogeneity of the radiation

field. This is particularly so in multi-capsule source arrangements.

Description of Sources

(i) Lead shields containing stationary source, samples moved into position.

These sources comprise a lead coffin of suitable wall thickness, with the source positioned in a cavity at the centre (14 - 19). Specimens are introduced into the irradiation space by various techniques. Charlesby and Flint (14) describe a 100 curie source of this design, the specimens being attached to the coffin lid, which may be lowered into position in the lead container. Eastwood (15) introduces specimens by means of 0.75 in. I.D. tubes which lead into the centre of eight sources placed in the lead container. The advantage of these source designs is that they are neat and compact, but they lack versatility and severely restrict the size of specimen to be irradiated.

(ii) Lead shields where the source is raised or lowered into the irradiation space.

This type of arrangement affords more versatility in design, and allows the samples to be placed in position prior to the entry of the source capsule. Many compact sources of this type have been described (20 - 25), with some rather more massive structures

incorporating the same principle (26 - 28).

A typical design is that of Hochanadel and Ghormley (20), Greenfield (21), and Blomgren (22). Here, design consists of a lead shielded irradiation volume, often described as the "oven", above which is placed a lead turret containing the source capsule, safely stored. Samples are placed in the "oven", with the source safely stored above, and for irradiation the source is lowered into position. An interlock is incorporated to avoid inadvertent personnel radiation exposure.

Kuhl et al (25) have designed a 1600 curie source which is stored in a lead coffin. An electric motor slowly raises the coffin plug, to which the source is attached, and samples are irradiated above the coffin. An emergency release drops the source back into the coffin.

Breger et al (26), Jones (27), and Colichmann (28) have described larger shields requiring up to 10 tons of lead, where the method of transferring the source capsule to the irradiation chamber is rather more elaborate. In each case the lead shield containing specimens, is transported either beneath or adjacent to the source shield, using a transportable trolley, and the source is transferred for irradiation.

(iii) Shield design using a pit or cavity with lead, concrete, and earth as auxiliary shielding material.

Many workers have made use of an existing pit or cavity in the ground when building cobalt-60 irradiation units (29 - 33). Chapiro (29) used a previously existing cave 50 ft. below the surface, to store a source in the kilocurie range. Samples to be irradiated are placed in marked positions on a table surrounding a central tube in which the source is raised vertically from a shielded container in the pit.

Burton, Ghormley and Hochanadel (30) house a source in a specially prepared 7 ft. hole in the laboratory floor. Samples are lowered down brass tubes to irradiate. A similar design by Aitken (32) differs only in that the source travels up and down a tube set 8 ft. in the ground. The source is raised by compressed air to the irradiation position and falls back to store by its own weight.

(iv) Water shielded sources.

Water shielded sources possess many of the features above, i.e. a well or tank set in the ground, where the source may be raised, or the samples lowered, into position for irradiation (19, 27, 34 - 36). Water as a shielding material has as its main advantage cheapness. Disadvantages of water shielding include corrosion of

equipment, and the necessity, usually, to provide water-tight specimens, unless a sample guide tube is used.

Schwarz and Allen (34) have stored a 120 curie source under water in a pipe buried in the ground under the laboratory floor. Samples for irradiation are placed in a water-tight can and lowered into the hole. Water and earth provide the only shield.

Callinan (35) describes a 2,300 curie source located at the bottom of a well under 12 ft. of water. The water serves as both a shield and coolant for temperature control. Samples are again lowered into position alongside a number of cobalt capsules which make up the source.

All the irradiation assemblies discussed so far, with the exception of some water shielded sources, require that the specimen be of restricted size and shape. For many practical purposes, it is desirable to irradiate larger pieces of equipment, and to have rather freer access to the irradiation space.

(v) Sources providing a large irradiation space and incorporating features of previous designs.

The use of a large irradiation cell has the advantage that there is no restriction on the size of sample, and very many irradiations may be carried out

at the same time. Such irradiation cells usually utilise concrete walls 3 - 5 ft. thick. The source is moved from a storage position into the cell for irradiation (37 - 43).

Obrycki, Ball and Davidson (37) shielded a 25 curie source in a pipe sunk in the ground, with a mineral oil. When in use, the source is raised to the top of the pipe, to a position inside a room completely shielded by concrete walls, accessible through a heavy door. Similarly, Nehemias, Brownell et al (38, 39) describe a ten kilocurie source which is stored under water in a well 16 ft. below the ground. The source is raised into an irradiation cell with 4 ft. thick walls, entered by means of a labyrinth corridor. A safety interlock ensures that the source cannot be raised whilst access to the irradiation cell is possible. Breger and Belynsky (40) have designed a similar unit but they store the source in a lead coffin, inside the irradiation cell, when not in use.

Murray, Dove and Roberts (42) also use a labyrinth corridor leading into a concrete irradiation cell. The source is shielded in a concrete block when in store, and pushed into the irradiation cell by an electrically driven, flexible cable. An interlock prevents the source moving, when access to the

irradiation cell is available.

(vi) Other methods of irradiating chemical samples.

In recent years, spent fuel elements have been used as a source of radiation for irradiating chemical and biological systems. A water shielded spent fuel element pond at Harwell can be used to give dose rates of up to 5 Mr/hr for short periods after reception of new fuel elements, but this dose rate drops to about 1 Mr/hr.

Reactors have also been used as sources of gamma radiation, but they suffer from the disadvantage of making many materials radioactive due to neutron capture.

C. LOCATION OF IRRADIATION CELL AND CHOICE OF DESIGN

After a consideration of the various types of irradiation units described above, it was decided to construct an irradiation cell based on the design of Murray, Dove and Roberts (42).

A kilocurie source of cobalt-60 would provide dose rates of up to 1 Mr/hr, which was sufficient for a wide range of investigations in radiation chemistry. The irradiation cell was to be built on the site of the Nuclear Technology Laboratories (Drawing NT6).

Economy of space was most important in designing the irradiation cell and in many ways determined the final design of the concrete shield shown in the above drawing.

SECTION 2

D E S C R I P T I O N O F
S O U R C E T R A V E L

DESCRIPTION OF SOURCE TRAVEL

In an irradiation cell of the type under consideration, elaborate arrangements must be made so that the source can be withdrawn to a safe position when apparatus or samples are being assembled within the irradiation space.

It was, therefore, essential to design a safe and efficient method for transporting the source capsule between the "safe" and "exposed" position, through a metal guide tube running through the concrete shield.

Various methods have been considered for moving the source, and early designs had the source mounted at the end of a steel bar, which could be pushed along a metal tube cast in the concrete. The disadvantage of this type of arrangement was that the movement of the source was strictly limited, and rigidly maintained only along a straight line which was the projection of the guide tube. This leads to the problem of shielding from radiation directed down the guide tube.

A far more satisfactory arrangement is to use a curved tube rather than a straight one. Scattered radiation is prevented from reaching either end. This means that the source can be moved between two points which need not be strictly in the same plane, and this leads to more flexibility in design. The disadvantage

of a bent guide tube is that it is impossible to use a rigid mechanism for pushing the source into the irradiation position. Other methods, such as pneumatic movement, are not advisable because of the danger of the source sticking between the "safe" and "exposed" position. A positive method of moving the source can be achieved by using a flexible cable, of the type known commercially as "TELEFLEX" cable. This is widely used to provide push-pull actions in aeronautical engineering. The flexible cable is made from a multi-strand high tensile steel wire core, over which additional layers of wire are wound, so that a continuous helical worm or thread is formed. This engages a special form of gear wheel, and a direct and positive pull-push action can be transmitted to the cable.

The source capsule can therefore be attached to "Teleflex" cable and moved along an S-shaped guide tube in such a way that the source movement cannot slip relative to the cable. This, as will be seen, is essential for the design of the source interlocking mechanism.

Careful consideration had to be given to dimensions chosen both for the source capsule and for the bends in the guide tube. The dimensions of the source capsule are chosen so that it can travel freely along the guide tube and that there is no possibility of the [illegible] of dimensions in

source sticking due to irregularities or constrictions in the internal surface. The dimensions of the internal diameter of the guide tube, the radius of the bends, and the diameter and length of the source capsule are, therefore, critical.

Drawing (NT3) shows the layout of the concrete shield, and the position of the guide tube. The guide tube is S-shaped (ANT 11) and the source capsule moves 18 ft. from the "safe" to "exposed" position. The "Teleflex" cable is driven along this guide tube by means of a gear wheel. For accurate dosimetry it is necessary that the source be removed from the irradiation position as quickly as possible. A 4 in. drive wheel will transmit a 12.67 in. travel along the "Teleflex" cable, which means that the source can be moved the total 18 ft. by 17 revolutions of a hand-wheel. This means that the total travel can be achieved in 20 - 30 seconds.

By incorporating an electric drive, it was considered that the source could be removed more rapidly and at a constant rate. A removal rate of 12 - 18 in. per second would be sufficiently rapid for most needs.

A most important feature in the design of the source travel mechanism, was to achieve a completely reliable source interlocking device. This required

that the source could under no circumstances be moved into the irradiation cell until the labyrinth corridor gate was securely locked. This meant that an interlocking system between the source travel mechanism and the corridor gate had to be devised. Drawings (NT4) and (NT5) show the source interlock and the corridor gate in detail.

The requirements of the interlock are as follows:-

(i) When the source is in the irradiation position the gate is rigidly locked and cannot be opened.

(ii) The corridor gate can only be opened when the source has been withdrawn to the "safe" position.

(iii) Once access to the irradiation cell has been achieved, it is impossible to move the source into the irradiation position.

The operation can most simply be achieved by having one key which operates two locks, one on the gate, the other on the lock to the source travel mechanism. The complete interlock design is described in Section 7 (d).

The final design of the source travel mechanism may therefore be summarised as follows:

An electric operator pushes the source capsule into the cell in approximately 14 seconds. The drive motor is coupled to an interlocking disc, which moves in strict synchronisation with the source capsule, and

this disc can be locked in the safe position, thereby locking the source travel mechanism. A reliable interlock is obtained between this disc and the corridor gate. Limit switches in the electric operator ensure that the source travels between the same two points, and a physical stop on the free end of the "Teleflex" cable prevents the source capsule from travelling beyond the exact exposed position. The incorporation of a slipping clutch device in the drive motor ensures that the source capsule and the electric motor cannot be damaged should the source become jammed in the guide tube.

SECTION 3

C O N C R E T E

F O R R A D I A T I O N S H I E L D I N G

A. DISCUSSION

(i) Homogeneity of shield material.

(ii) Constructional problems.

(iii) Space requirements.

B. CALCULATION OF SHIELD THICKNESSES

(i) Goldstein and Wilkins' Method.

(ii) Callan's Method.

C. COMPARISON OF RESULTS

A. DISCUSSION

The choice of a particular shielding material is based primarily on its property to reduce the radiation level to a safe level, i.e. density is an important factor in choosing a shield material. Secondary to this are economic and mechanical factors, which are interrelated to a very large extent. Although water is a good neutron shield, it requires excessive thicknesses for shielding gamma radiation. Lead shields require the minimum thicknesses for gamma radiation, but lead lacks mechanical strength for large structures and is extremely expensive. Concrete, which is cheap and has adequate mechanical strength, is an excellent shielding material for large permanent shields. Only moderate thicknesses of concrete are required, i.e. between 4 and 5 ft. Ordinary concrete in sufficient thicknesses will provide a satisfactory shield, but the use of various heavy concretes made from special aggregates have also been used (44 - 51). High density concrete is often preferred, due to smaller shield thicknesses, but is more expensive and may lead to certain mechanical problems. Important factors in choosing a concrete shield are:

(i) Homogeneity.

Weaknesses and voids in the concrete structure

must be avoided. If pockets are formed in the concrete shield, or segregation occurs, the effective concrete thickness is lessened and the radiation passing through such sections is greater than the calculated value.

(ii) Constructional problems.

Concrete shields including a labyrinth corridor need extensive formwork and careful placement of concrete to avoid segregation. Vibration of the concrete is essential, but can be difficult with high density concretes. Shrinkage characteristics of high water content concretes are severe, and cracking must be avoided.

(iii) Space requirements.

High density concretes may only require half the thicknesses that would be needed with ordinary concrete. An economic balance must be struck between valuable floor space lost and relative costs of high and ordinary density concrete. Previous sources have used interlocking concrete bricks in the building of the shield. Concrete bricks, usually of a high density (3.0 - 4.0 g/cm^3), have been fabricated and assembled with use of mortar. The bricks are arranged so that there are no straight gaps through the shield, i.e. bricks are staggered in two dimensions, broadly termed manhole bonding. Such concrete blocks are very expensive and

assembling them is difficult and time-consuming. It was felt that both on economical grounds and also for quickness it would be satisfactory to use pre-mixed, poured concrete in building the concrete shield in this laboratory. Poured vibrated concrete of density (2.2 - 2.4 g/cm^3) was specified in the design of the concrete shield.

B. CALCULATION OF SHIELD THICKNESSES

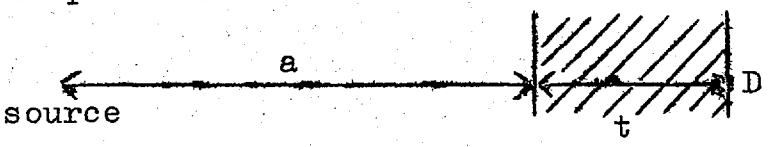
Several methods for calculating shield thickness are available (44, 50, 52 - 55). The most useful methods are those discussed by Goldstein and Wilkins (53) using Taylor's (55) dose build-up data, and the half thickness method described by Callan (44).

(i) Goldstein and Wilkins' Method.

Making the general assumption that the source is a point source of 1,400 curies, that shielding data for aluminium (density 2.7 g/cm^3) can be used for concrete (density 2.2 - 2.6 g/cm^3) and that the constants derived for aluminium can be used without appreciable error; then the general expression for dose-rate (D) through a concrete shield is given by

$$D = \frac{S \times 3.7 \times 10^{10} \times e^{-\mu ot} \times B(\mu ot)}{4\pi \times (a + t)^2 \beta} \text{ m.p.l.}$$

Consider the particular case:



where s = source strength (curies)

μ_o = linear absorption coefficient (cm^{-1})

t = thickness of shield (cm)

$B(\mu_o t)$ = dose build-up factor

β = conversion factor from photon energy to flux (dis./cm^2/sec.)

a = source to shield distance (cm)

1 mpl = 2.5 mr/hr. (56)

The gamma radiation from a cobalt-60 source includes emission of two photons of energy 1.17 and 1.33 MeV, respectively.

Assuming a = t = 2ft., then a table may be set up as follows:

MeV	a	t	r	β	μ_o	$\mu_o r$	$\mu_o t$	$e^{-\mu_o t}$	$B(\mu_o t)$
1.17	61	61	122	3.65×10^{3}	0.1575	19.2	9.6	6.8×10^{-5}	44.25
1.33	61	61	122	3.19×10^{3}	0.1430	17.5	8.72	1.6×10^{-4}	33.50

$$\therefore D = \frac{1.4\times3.7\times10^{13}}{4\,(1.22)^2\times10^{4}}\left[\frac{6.8\times10^{-5}\times44.25}{3.65\times10^{3}} + \frac{1.6\times10^{-4}\times33.50}{3.19\times10^{7}}\right] \text{ mpl}$$

$$= 0.276\times10^{6}\left[82.5\times10^{-5} + 16.8\times10^{-4}\right] \text{ mpl}$$

$$= 692 \text{ mpl}$$

$$= \underline{1.73 \times 10^{3} \text{ mr/hr}}$$

(ii) Callan's Method.

Half thicknesses for various types of concrete are as follows:

Type of concrete	Density g/cm^3	Half thickness (ins.)
Ordinary	2.2 - 2.4	2.82
Limonite	2.6	2.38
Magnetite	3.0 - 3.8	1.65

Considering the same example as above, the source intensity at the point D is given by the equation

$$I = \frac{7\ c\ E}{(a+t)^2}$$

where C = source strength (curies)

E = total energy of gamma energy in MeV/disintegration

i.e. $I = \frac{7 \times 1400 \times (1.17 + 1.33)}{16}$

$= \underline{1530\ r/hr}$

The number of half-thicknesses required for a shield is obtained from the expression

$$N = 3.32 \log R$$

where R is the attenuation coefficient.

$\therefore$ No. of half thicknesses required $= \frac{\text{shield thickness}}{\text{half thickness}}$

$= \frac{24}{2.82}$

For ordinary concrete (density 140 lb/ft^3 or 2.2 g/cm^3)

$$N = 8.52$$

$$8.52 = 3.32 \log R$$

$$\log R = 2.57$$

$$\underline{R = 3.72 \times 10^2}$$

The total dose rate received at D is given by

$$D = I/_R$$

$$= \frac{1530}{3.72 \times 10^2}$$

$$= \underline{4.12 \text{ r/hr or } 4.12 \times 10^3 \text{ mr/hr}}$$

C. COMPARISON OF RESULTS

Method	Shield Thickness Ft.	Dose Rate mr/hr.
Goldstein and Wilkins	2	1.73×10^3
Callan	2	4.12×10^3

These two methods give a comparable result but the method by Callan is simple and quick to apply. It therefore provides a very useful and rapid method for the calculation of the dose rate around the concrete shield. This dose rate must be kept below the I.C.R.P. recommended maximum permissible-level (56), i.e. 100 mr/40 hour week. Shielding thicknesses were calculated to give a dose rate not greater than

2.5 mr/hr at any point around the shield. A specimen calculation follows. Consider a point 10 ft. away from a 1,400 curie source shielded by 4.5 ft. of ordinary concrete (density 140 lb/ft^3).

The intensity at 10 ft. is given by

$$I = 7cE/_{a^2}$$

$$= \frac{7 \times 1400 \times 2.5}{100}$$

$$= \underline{245 \text{ r/hr}}$$

Thickness of shield = 54 in.

Thus, no. of half thicknesses required $N = \frac{54}{2.82}$

but $N = 3.32 \log R$

$$\log R = \frac{54}{2.82 \times 3.32}$$

$$\underline{R = 5.37 \times 10^5}$$

Dose rate outside shield $= \frac{2.45 \times 10^5}{5.37 \times 10^5}$ mr/hr

$$= \underline{0.45 \text{ mr/hr}}$$

This is well within safe limits and an average concrete thickness of 4.5 - 5 ft. can be specified in the design of the shield for a 1,400 curie cobalt source.

The cobalt source is to be stored in a concrete block when not in the exposed position. The dose

rate may be calculated when the source is placed at the centre of a concrete cube of 10 ft. side, i.e. the source is shielded by at least 5 ft. concrete in any direction.

Intensity of source at 5 ft. is given by

$$I = \frac{7 \times 1400 \times 2.5}{25}$$

$$= \underline{980 \text{ r/hr}}$$

No. of half thicknesses = $\frac{60}{2.82}$

∴ Attenuation Coefficient is given by

$$\log R = \frac{60}{2.82 \times 3.32}$$

$$\text{and } R = \underline{2.5 \times 10^6}$$

$$\text{Dose rate outside the shield} = \frac{9.8 \times 10^5}{2.5 \times 10^6} \text{ mr/hr}$$

$$= \underline{0.40 \text{ mr/hr}}$$

It was therefore satisfactory to shield the source by 5 ft. concrete in the store position.

A shield thickness of 5 ft. was provided above the irradiation cell, to act as a ceiling. This was sufficient shielding to maintain the radiation level at points above the source chamber at levels below those required in areas frequented by non radiation workers (56).

SECTION 4

D E S I G N O F C O N C R E T E S H I E L D

A. DESIGN OF CONCRETE SHIELD

B. CALCULATED DOSE RATES AROUND THE SHIELD

A. DESIGN OF CONCRETE SHIELD

The location of the irradiation cell within the Nuclear Technology Laboratories is shown in Drawing (NT6). It was designed to occupy the minimum amount of floor space in the laboratory. A detailed drawing of the concrete shield is given in Drawing (NT3).

The source chamber has overall dimensions of 6 x 8 x 7 ft. high. The source in its exposed position is located at a point 3 ft. from three inner walls as shown. A labyrinth corridor is essential in order to avoid scattered radiation from the source reaching the control position. Accordingly the design provides for four right angle bends in the labyrinth corridor. The width of this corridor was determined primarily by the size and shape of the lead shipping container, which would be used to bring the source capsule into the irradiation cell. Furthermore, the corridor must be wide enough to allow apparatus of appreciable size to be taken into the source chamber. It was for this reason that corners were shaped as shown on Drawing (NT3), i.e. to allow for manoeuvrability in the corridor.

A wooden framework was fabricated, the dimensions of which corresponded to the floor space occupied by the lead shipping container, i.e. 40 x 30 in. This

was pushed round the proposed shield layout on the actual site. A 3 - 3.5 ft. corridor width was specified, guaranteeing that the shipping container would have ample space to be moved into position.

The shielding calculations show that an average thickness of 4.5 ft. concrete of density no less than 140 lb/ft^3 is necessary in all directions, from any point in the line of source travel.

The side elevation view of the shield design shows that a 5 ft. thick ceiling was provided. Extra shielding was specified because of office and lecture room facilities to be built above the irradiation cell.

The 17 ft. high concrete tower outside the building was required to accommodate the S-shaped source guide tube. Preliminary design considerations indicated that it was preferable to have direct access to the "Teleflex" cable at a point close to the source storage position, i.e. near to the top of the concrete tower. This would have been difficult if the guide tube had bent downwards, and the "store" position had been below ground level.

For this reason it was decided to move the source upwards after leaving the source chamber. The "store" position was positioned in the centre of a concrete

block in the shape of a cube having 10 ft. sides. The simplest way to place this concrete block in the required position was to support it on concrete, i.e. the upper section of the concrete tower comprised the source store, and the lower section served as extra shielding, but chiefly as a support. This method of using concrete as the support was as cheap, if not cheaper, than other methods of supporting the upper concrete block. In order to avoid subsidence and possible collapse of the walls of an underground passage which runs close to the laboratory, it was necessary to take the foundations for the concrete tower down to a depth of 7 ft. below ground level.

A 6 in. diameter cast iron pipe (item 6) was set into the brickwork portion of the shield. The reason for this was that, should subsidence of the tower occur, then the guide tube was free to move, relative to the block. The guide tube could, therefore, not be bent or distorted in shape.

Other facilities provided in the source chamber are:

(i) a 4 in. diameter cast iron pipe leading from the source chamber to the control face. This can be used to provide extra facilities in the source chamber, which need operation from outside.

(ii) a 6 x 6 x 8 in. provision for a lead glass window.

(iii) a 4 ft. duct 6 x 3 in. in cross-section, used for extracting air from the cell.

B. CALCULATED DOSE RATES AROUND THE CONCRETE SHIELD

Dose rate calculations were made around the concrete shield assuming the source strength to be 1.400 curies. Values for the dose rates calculated were as follows. Refer to Drawing (NT6).

Position	Dose Rate mr/hr	
	Calculated	Murray (57)
A	0.38	0.15
B	0.38	—
C	1.5×10^{-4}	2×10^{-5}
D	3.8	2.4
E	96.0	100 Direct 100 Scattered
F	1.9	—
G	0.7	—

The concrete shield, as designed, provided adequate shielding and reduced the radiation level to a satisfactory minimum.

SECTION 5

B U I L D I N G O F
T H E C O N C R E T E S H I E L D

BUILDING OF THE CONCRETE SHIELD

Wooden formwork was erected to the design shown in Drawing (NT3). The formwork was hardboard faced, to give a smooth surface to the concrete walls. Preliminary work was also carried out to prepare the foundations, 7 ft. deep, for the concrete tower.

It was possible to erect the source shielding walls directly from ground level because the existing floor had been designed to take very heavy loads.

The concrete shield was erected from poured "Ready-Mix" concrete. The operation was carried out in three lifts, i.e. the first 5 ft. height of the shielding was poured and allowed to set. A further 6 ft. high section was then poured on top of this, allowed to set, and the final 6 ft. high section poured. Continual vibration of the concrete was carried out to prevent formation of air pockets or voids in the shield structure. The total curing time for the concrete was twenty-eight days, and during this time the formwork was kept in position. During pouring, great care was taken to ensure that the guide tube remained rigidly located in position.

The ceiling to the source chamber was built up from 6 in. thick pre-stressed concrete planks, which were supported above the source chamber and control

TABLE 2

Test No.	1	2	3	4	5	6	7	8	9	10	11	12
Age at Time of Test (Days)	28	28	28	28	28	28	28	28	28	28	8	8
Weight of Concrete (lbs/ft^3)	145½	147	146½	147½	147½	146	147	146½	147	146	145½	146
Cross Sectional Area (in^2)	36.0	36.4	36.4	36.0	36.0	36.0	36.4	36.0	36.07	36.0	36.0	36.0
Maximum Load (tons)	45.63	47.20	50.26	40.38	46.41	29.26	56.01	42.49	45.67	55.59	22.96	28.38
Maximum Stress ($tons/ft^2$)	183	187	199	162	186	117	222	170	183	222	92	113
(lbs/in^2)	2840	2900	3090	2510	2890	1820	3450	2640	2840	3460	1430	1770

face. The remaining concrete shielding was poured on top of the supporting planks.

To guarantee a minimum concrete density of 140 lb/ft^3, specimen 6 in. cubes were formed from each batch of the concrete mix and sent for testing. The results of the concrete tests are given in Table 2 This shows that the concrete was of a consistent density between 144 - 146 lb/ft^3 and that the properties of the concrete were such that no weaknesses could occur in the final shield design.

SECTION 6

S O U R C E C A P S U L E D E S I G N

A. AVAILABILITY OF COBALT-60 IN THE UNITED KINGDOM AND ELSEWHERE

B. DETAILS OF CHALK RIVER SOURCE

C. FEATURES OF SOURCE CAPSULES AT WANTAGE

D. SPECIFIED SOURCE DESIGN

A. AVAILABILITY OF COBALT-60 IN THE UNITED KINGDOM AND ELSEWHERE

In the Autumn of 1958, enquiries were made with the Isotope Division of the United Kingdom Atomic Energy Authority, about the supply of 1,000 curies of high specific activity cobalt. Only about 500 curies of cobalt, at 1 - 5 curies/gm in the form of standard 10 cm. rods or 12 x 12 mm cylinders were available at that time. In addition, a limited number of 6 in. source rods could be obtained. These had been prematurely discharged from one of the Windscale reactors, and had specific activity of the order of 0.5 curies/gm.

Low specific activity cobalt of this type would require a very large volume of material (up to 200 cm^3), to provide a kilocurie source. This would lead to a source of appreciable dimensions, i.e. a solid cylinder 2 in. diameter by 6 in. A less homogeneous radiation and a lower dose rate might be expected. It would further complicate the design when considering the actual movement and flexibility of the source travel.

Atomic Energy of Canada Limited offered rapid delivery of cobalt, of specific activity about 40 curies/gm., and at a price of $3.50/curie. This is to be compared with the United Kingdom price of £2/curie

at that time.

B. DETAILS OF CHALK RIVER SOURCE

A.E.C.L. offered to supply three cold-welded capsules containing about 1,300 curies of cobalt as follows:

Capsule No.	No. of curies	Specific Activity (curies/gm)
1	450	35
2	450	29
3	450	27

The cobalt was in the form of cylindrical pellets 1 mm diameter by 1 mm length, encapsulated in containers shown in Drawing (ANT8). The dimensions were approximately 0.875 in. diameter, 1.875 in. total length for each individual capsule. Placed one above the other to provide one complete capsule, this would measure 0.875 in. diameter, 5.625 in. total length.

C. FEATURES OF SOURCE CAPSULES DESIGNED AT WANTAGE

Much work on the design of cobalt sources has been carried out at the Wantage Radiation Laboratories, and it was therefore considered that the Nuclear Technology source capsule design should be based on the recognised designs approved by experience at

Wantage. Eastwood et al (12) and Murray et al (42) have described various designs of cobalt source capsules. Important features in designing a source of this type are:

(i) the source is cylindrical, for uniform radiation flux,

(ii) the diameter of the capsule is a minimum, as this is the critical dimension in choosing the diameter of the guide tube,

(iii) the cobalt is doubly-encapsulated to avoid the risk of leakage of activity from the containers,

(iv) the containers are made of a metal compatible with that of the guide tube; stainless steel is usually preferred,

(v) the source is attached to 12 - 18 in. stainless steel rope. This is a handling facility discussed in Section 8.

D. SPECIFIED SOURCE DESIGN

A.E.C.L. re-encapsulated the three separate sources to form one capsule to the design shown in Drawing (ANT9).

The initial source design specified a 6 in. cylinder, 0.565 in. diameter, incorporating hemispherical ridges to give an overall diameter of 0.715 in.

The ridges were introduced to provide riding surfaces for the capsule. The cobalt would be doubly encapsulated, the inner container having a volume of 9 cm^3 to be fabricated from standard (0.395 in. I.D. 0.445 in. O.D.) F.M.B. grade stainless steel tubing. The stainless steel rope could be swaged into the 0.272 in. diameter hole provided.

A later modification required that the hemispherical ridges be removed in order that the overall dimensions of the capsule could be reduced. In their place a slight rounding at either end of the capsule was considered adequate (58).

The final outer source capsule, Drawing (ANT 10), has overall dimensions, 0.565 in. diameter by 6 in. length. The end fitting for the stainless steel rope is modified to provide plug welding in preference to swaging. The retaining dish plugs are cold-welded into position and the source appears as a solid cylinder, with rounded ends. The total overall length of the source capsule and stainless steel rope is 26.375 in. (Plate 1).

SECTION 7

DESIGN OF SOURCE TRAVEL MECHANISM AND ANCILLARY EQUIPMENT

A. DESIGN OF GUIDE TUBE

B. DESIGN OF GUIDE TUBE END-PIECE AND COUPLING

C. DESIGN OF "TELEFLEX" ELECTRIC OPERATOR

D. DESIGN OF INTERLOCK

E. DESIGN OF CORRIDOR GATE

A. DESIGN OF THE GUIDE TUBE

In fabricating the guide tube to the dimensions of Drawing (ANT 11) it was important to ensure precise values for the radii of the two 90° bends. The critical dimension was the 2 ft. 3 in. bend. There should be no possibility of the source capsule jamming in this bend.

Early in the design programme a dummy source capsule was manufactured Drawing (ANT 9), and pushed through a 1 in. diameter guide tube in one of the irradiation cells at the Wantage Laboratories. It was found that this source capsule would slide round a 2 ft. radius, 90° bend in a 1 in. diameter guide tube.

Stainless steel tubing 1 in. O.D. 16 SWG, was specified for the guide tube for the Nuclear Technology source, Drawing (ANT 11).

The total guide tube length, i.e. 23 ft., could not be obtained in one complete length, and was, therefore, fabricated from:

(i) 2 x 14 ft. lengths stainless steel tube 1 in. O.D. 16 SWG FDP quality (titanium stabilised).

(ii) 8 in. 1¼ in. O.D. 10 SWG stainless steel tube to provide the joining collar.

The guide tube was bent by Messrs. Universal

Radiators to the required specification, and the two component pieces joined in the Chemical Engineering Workshops at Imperial College. Care was taken to ensure that there was no lip on the inside surface of the tube, which might interfere with the travel of the source capsule.

A 6 in. collar was silver brazed over the join. Penetration of between ¼ - ½ in. was obtained in the brazing process. The tube, throughout the joining process, was secured to a specially prepared jig.

B. DESIGN OF GUIDE TUBE END-PIECE AND COUPLING

Drawing (ANT 12) shows in rather more detail the source guide tube end-piece which comprises the last 20 in. of the guide tube at the exposed position.

This end-piece ensures that the source can be accurately located at the end of its travel and retained within the minimum shielding thickness of stainless steel. Standard stainless steel tubing FDP quality ⅝ in. OD x 25 SWG was most suitable for this purpose.

A standard ERMETO stainless steel reducing coupling connected this end-piece to the guide tube. A collar was silver brazed to the end-piece, 1¾ in. length to increase the outside diameter of the tube to ¾ in., i.e. wall thickness of 0.145 in. to prevent

collapse of the tube on compression fitting. A standard 1 in. OD - ¾ in. OD reducing coupling could now be used.

A modification to the Ermeto coupling was made in order to remove the sharp break in the internal diameter. The coupling barrel was machined in such a way that a funnel shape was introduced, and this served to introduce the source capsule smoothly into the end-piece.

C. DESIGN OF THE TELEFLEX ELECTRIC OPERATOR

The Teleflex electric operator is shown in Drawing (NT 7). This electric operator was fabricated by Teleflex Limited, and is a modification of their standard window operation driving gear. This particular operator was built in their workshops to meet the specifications given below. By using a 4 in. dia. drive gear wheel, the Teleflex cable moves 12.67 in. in either direction. This 4 in. dia. driving wheel forms the basis of the cable drive mechanism in the electric operator. The cable drive wheel is coupled, through a reduction gear box, to the electric motor. It was required to give an output of 70 RPM on the cable drive wheel, and this was accomplished by using a 2,800 RPM 3 phase reversing

electric motor, through a 40:1 worm gear reduction gearbox onto the output drive shaft.

Drawing (NT 7) shows that the output shaft is coupled to a slipping clutch arrangement, which incorporates a Ferodo type clutch plate to engage the 4 in. dia. cable drive wheel.

This, as previously mentioned, is a safety precaution, should the source capsule become jammed. In such an event, the drive wheel can run freely relative to the motor, and so avoid damage to the source capsule, and serious damage to the electric motor.

The pressure on the drive plate can be increased by compressing the disc spring onto the clutch plate. The drive plate incorporates a running cam device, the cam travelling between two preset Burgess micro-switches at the exposed and safe position.

The starter for the electric operator, containing forward, reverse and stop buttons, is connected to the limit switches through an isolator, stopping the motor automatically at the exposed position. As an extra safety precaution a physical stop is provided. The Teleflex cable contains a metal stop attached to the spent travel end, which arrests the cable and prevents any further movement of the drive wheel.

Plate 2. shows the electric operator mounted in position.

D. DESIGN OF INTERLOCK

The electric operator is situated on the outside wall of the concrete shield, position J, Drawing (NT 6), in a position most suitable to accommodate the whole length of Teleflex cable (i.e. 75 ft.) and, in particular, the 18 ft. of spent travel. Before reaching the operator, the cable passes over a 4 in. dia. drive wheel which is situated at the end of the 1 in. dia. duct which passes through to the control face (Plate 2). This 4 in. dia. drive wheel is coupled to a 10 ft. extension shaft which passes through to the control face. A 1:1 bevel gearbox connects this extension shaft to the interlock mechanism and is shown in Drawing (NT 4).

When the motor is actuated, it drives the cable wheel which in turn rotates the extension shaft and directly couples the source movement to the interlocking device.

Detail of Interlock

The source interlock is coupled directly to the cable movement. The cable moves 12.67 in per revolution of the drive wheel. Therefore, to travel

the total 18 ft. we require $\frac{18}{38} \times 3 \times 12$ revolutions

$= \underline{17 \text{ revolutions}}$ of the drive wheel

Cable speed = 70 RPM

Time taken to travel 18 ft. $= \frac{17}{70} \times 60$ sec.

$= \underline{14.5 \text{ sec.}}$

Drawing (NT 4) shows the source interlocking device, which operates as follows:

(i) the source travel is transmitted by 1:1 gearing to the upper spindle of the T-drive bevel box (Item 4), (ii) the bevel box is coupled to the output shaft of a 25:1 Crofts worm gear reduction gearbox (Item 3), (iii) an 8 in. diameter brass interlocking disc (Item 2) is keyed to the output shaft of the gearbox, (iv) a Castell bolt lock (Item 1) is used to lock this disc in position.

The 25:1 reduction on the output shaft of the Crofts gearbox provides that the interlocking disc will travel $^{17}/_{25}$ revolutions in relation to the total travel of the source from the safe to the exposed position, i.e. the disc moves almost ¾ of a complete revolution as the source travels the complete 18 ft.

The disc may be locked in position by throwing the bolt as shown in the drawing. At the same time

a micro-switch is opened, so cutting the electricity supply to the starter switch of the electric operator. The source capsule is now in the safe position. The key C1 may now be removed from the lock, and used to operate the corridor gate lock shown in Drawing (NT 5). On inserting key C1 into the gate lock and turning, this frees key C2 which can now be used to open the corridor gate. When the corridor gate is open key C2 may be removed, but key C1 remains trapped in the gate lock, and so the source travel mechanism cannot be operated. At this point it is safe to enter the irradiation chamber.

After leaving the source chamber and locking the corridor gate (i.e. with key C2), key C1 may be removed from the gate lock, and returned to the source interlock position. Key C2 is now trapped in the gate lock and cannot be turned independently to open the gate.

Using key C1, the locking disc can now be released and the electric operator actuated. As the source capsule moves to the exposed position the locking disc rotates ¾ of a revolution. At the exposed position the locking disc comes to rest in such a position that the bolt cannot be thrown, i.e. key C1 cannot be turned, and remains trapped in the

lock. With the source capsule exposed, it is impossible to remove key C1, and therefore impossible to open the corridor gate and gain access to the irradiation chamber.

Plate 3. shows the completed source interlock with cover. An auxiliary handle may be used to operate the source travel mechanism manually.

Manual operation may be required if the electricity supply fails, and was in fact necessary on original loading of the source capsule. By releasing the slipping clutch, the cable and drive wheel assembly can be moved slowly by hand.

The source interlock still operates under manual conditions and it is important to note that the interlocking device can only fail-safe, i.e. it is impossible to enter the irradiation chamber until the source capsule is in the safe position.

E. DESIGN OF THE CORRIDOR GATE

The corridor gate serves to provide a barrier at the entrance to the irradiation chamber. Drawing (NT 5) shows fabrication details for the corridor gate, with particular emphasis to the double Castell gate lock. After setting the gate lugs into the concrete, the gate was placed in position. The lock

was fixed to the precise dimensions shown in the drawing. It was necessary to obtain a precise fitting so that the gate catch and the lock operated correctly.

The corridor gate also operates a switch on closing, which automatically switches off the lights in the labyrinth corridor and irradiation chamber. This serves as a warning should anyone remain in the irradiation cell.

SECTION 8

D E S I G N O F L E A D S H I P P I N G C O N T A I N E R

A. DESCRIPTION OF SOURCE CONTAINER

B. SUGGESTED METHODS FOR UNLOADING THE SOURCE CONTAINER

C. DESIGN OF THE MODIFIED LEAD PLUG

A. DESCRIPTION OF SOURCE CONTAINER

The source shipping container was constructed of lead encased in steel, weighing approximately 6,500 pounds, and overall dimensions of 40 in. long, 30 in. wide and 44 in. high. A detailed drawing of the container is given in Drawing (NT 1). This shows that an average thickness of 10 in lead shielded the source capsule in all directions, sufficient to maintain the radiation level on the outside of the container within the accepted permissible levels for handling, (i.e. 2.5 mr/hr). This container was used to transfer the source from Chalk River to the Imperial College site.

The disadvantage of the shipping container (lead coffin) shown in Drawing (NT 1) is that no provision is made for unloading the source. For the purposes of this design, it was therefore necessary to modify the shipping container, in order that the source capsule could be withdrawn directly on removing the lead plug, without using elaborate remote handling equipment.

B. SUGGESTED METHODS FOR UNLOADING THE SOURCE CAPSULE

The source capsule, attached to a 0.272 in. dia. stainless steel rope, is retained in the special

cavity provided in the lead container (Plate 4). In the manufacturing process the Teleflex cable is quenched in a hydrocarbon oil after heat treatment. The purpose of the stainless steel rope, which provides an 18 in. separation between the Teleflex cable and the source capsule, is to protect the lubricant of the cable if the source capsule were to be used in a closed system at high and low temperatures, and also to protect the lubricant against radiation effects. Experience with this type of design has shown that no detrimental effects are observed in the Teleflex cable after five years of operation (59).

Unloading of the lead container was to be performed as follows:

(i) the end of the stainless steel guide tube in the exposed position would be provided with an inverted cone arrangement to facilitate entry of the source capsule into the tube,

(ii) the coffin to be placed in the source chamber under the guide tube,

(iii) the stainless steel rope, attached to the source capsule, passes through the upper lead plug of the coffin, and the free end is available for direct manual attachment to the Teleflex cable,

(iv) the lead plug would be raised by means of a

hoist set up in the source chamber, and lifted clear of the guide tube. Operation of the hoist would take place from the control face,

(v) the capsule would be withdrawn into the guide tube and storage position by retracting the Teleflex cable manually. The coffin may then be removed from the source chamber.

In this way, unloading of the source capsule could be achieved both quickly and safely, providing the lead plug could be modified so that the stainless steel rope is brought outside the coffin lid, without causing any radiation hazard. Three ways of doing this were considered:

(i) by providing a slot down the whole length of the lead plug,

(ii) by providing a slot in the neck of the coffin and alongside the lead plug. This was undesirable because it meant modification of the coffin itself,

(iii) the lead plug should be split and slotted, so that when it is raised it falls apart and frees the stainless steel rope.

The stainless steel rope is reasonably flexible and can be bent to a minimum radius of about 2 - 3 in. but care must be taken in the design, to avoid the rope becoming rigidly clamped, e.g. it may set in

position, so preventing ready access to the guide tube.

C. DESIGN OF THE MODIFIED LEAD PLUG

The most satisfactory way of modifying the lead plug was to provide a slot arrangement whereby the stainless steel rope can be fed round the lead plug, allowing the connector to be freely accessible above the lid.

Drawing (NT 2) shows the modified plug in detail. The plug is made up in three sections, the lower section remaining in the container, the source being drawn out through a hollow tube in the centre. The centre plug is machined to provide an outlet for the rope. The plug has an overall diameter of 10 in. and is 7¾ in. deep. A section of the plug is cut away in order to form a 0.5 in. path alongside the plug, the top and bottom being chamfered at 45°, so that the rope may pass round the plug easily without being trapped in position. A funnel arrangement leads the cable into a 0.5 in. groove and up alongside the plug.

The total length of the source capsule and stainless steel rope is 26.375 in. A 4 in. high spacer was used in the coffin to position the source in

such a way that 5 in. of rope and the connector protruded when the centre plug was in position. The rope can now be connected to the Teleflex cable, without danger from radiation exposure, and the source capsule unloaded as outlined above and described in detail in Section 11.

SECTION 9

SPECIAL FACILITIES PROVIDED IN THE IRRADIATION CELL

A. GAMMA WARNING ALARM

B. WATER

C. ELECTRICITY

D. FIRE EXTINGUISHER

E. AIR EXTRACTION SYSTEM

F. LEAD GLASS VIEWING WINDOW

A. GAMMA WARNING ALARM

The principal hazard in this type of irradiation cell is from direct gamma radiation. An automatic radiation monitor is therefore located in the cell, to give warning of an unsafe radiation level in the source chamber when the source capsule is in the store position. This could arise if the capsule is damaged and the guide tube becomes contaminated with cobalt.

The monitor consists of a high current Geiger counter tube (halogen quenched) situated in the source chamber and operating an alarm unit at the control face (60, 61). Should the radiation level in the source chamber exceed 100 mr/hr (40 mpl), the current from the Geiger tube operates a red warning light and a warning bell.

The Geiger counter tube in the source chamber has a limited radiation lifetime, and, therefore, the operating voltage is automatically switched off as the source capsule moves to the exposed position. A micro-switch is operated at the interlock, by a catch fitted to the interlocking disc. This switch opens as the source capsule moves to the exposed position, and is closed just before the source capsule returns to the safe position, i.e. supplying the

voltage to the Geiger tube. A test button is provided on the instrument, in order that the alarm signal and light can be tested when the source is in the exposed position. The co-axial cable connecting the Geiger tube to the alarm unit passes through the 4 in. dia. duct shown in Drawing (NT3 - item 2).

B. WATER

As a water supply is occasionally required within the source chamber, a cold water supply point and drain leading out through the shielding to waste, is provided. The water flow may also be controlled in case of emergency by a master tap at the control face.

C. ELECTRICITY

Three power points are provided in the source chamber, and these can be isolated by a master switch at the control face.

D. FIRE EXTINGUISHERS

An automatic carbon dioxide blanket fire extinguishing system is provided in the source chamber. This consists of a CO_2 cylinder, placed in the corridor approach just behind the corridor gate,

linked to two CO_2 ejection nozzles in the source chamber. The alarm and extinguisher mechanism is triggered by a pick-up in the source chamber, which operates by differential temperature rise in the cell. Should there be a sudden rise in temperature, e.g. as in a fire or explosion, the CO_2 is automatically released at a pressure of 80 lb/in^2, and an 8 in. dia. fire alarm bell sounded. Sufficient CO_2 is released to blanket the complete cell and half of the labyrinth corridor.

E. AIR EXTRACTION SYSTEM

For many practical experiments it is necessary to maintain the source capsule in the exposed position for many days or even weeks. A kilocurie source, confined in a small space, can give rise to appreciable concentrations of ozone by ionisation of the air, and also of oxides of nitrogen. This could prove serious unless an adequate air extraction system is provided. It is also not uncommon for other toxic vapours to accumulate in the source chamber from experiments.

Drawing (NT 3) shows the position of a duct, 6in. x 3in. x 4ft., which passes through the concrete shield. Ten complete air changes per hour were con-

sidered necessary to remove trace quantities of toxic vapours from the source chamber and half of the labyrinth corridor, i.e. for a volume of approximately 500 ft^3. A rotary vane extraction fan was fitted on the outside face of the ventilation duct, giving 1,000 RPM.

When the source was in the exposed position for long periods, it was later found that the air ventilation was not sufficient and that ozone could be detected at the control face. This was considered to be due partially to back suction of air from the source chamber to the control face by the main laboratory ventilation plant which extracts air from the adjoining laboratory. The original fan was therefore replaced by a second fan of the same type, rating 1,500 RPM, which gave satisfactory ventilation. Under normal working conditions, the fan is kept operating continuously.

F. LEAD GLASS VIEWING WINDOW

A small viewing window is provided in the concrete shield. Using one mirror, placed in the corridor H, Drawing (NT 6), samples and source tube can be seen from the control face without actually entering and interupting an experiment in the irradiation cell.

It is not necessary to use radiation stabilised glass for the window as the radiation dose rate on the inner face of the wall, i.e. position E, Drawing (NT 6), is only of the order of 200 - 300 mr/hr. The complete window, therefore, consists of two unstabilised glass blocks of density 2.5 g/cm^3 and dimensions 5.75 x 5.75 x 8.75 in. thick. These blocks were held in position in the iron frame (set in the shield) by means of rammed lead wool. There is a gasket at the 0.5 in. gap between the blocks and this gap is provided with a dessicant to prevent condensation.

SECTION 10

T E S T I N G O F T H E
S O U R C E T R A V E L A S S E M B L Y

TESTING OF THE SOURCE TRAVEL ASSEMBLY

After construction of the irradiation cell and assembly of the source travel mechanism, and before the actual loading of the active cobalt capsule, the complete unit was tested.

A dummy capsule, identical in every detail to the active source capsule, was attached to the Teleflex cable as follows:
A stainless steel rod end (0.312 in. dia. 1.5 in. length) swaged to the Teleflex cable was fitted into the coupling on the stainless steel rope attached to the source capsule. This coupling was also fabricated from stainless steel, and was 3 in. overall length by 0.437 in. dia. The rod end was pushed into the connector and held in position by two grub screws. This was only a temporary arrangement for the dummy capsule, and was disconnected after the test period.

The limit switch on the electric operator was then set at the exposed position by moving the dummy capsule until it just touched the end of the guide tube end-piece. The capsule was retracted 18 ft., measured on the spent travel, to the store position, and the other limit switch adjusted. The two limit switches now governed the exact distance of travel. The slipping clutch was then tightened until there

was no free movement relative to the interlocking disc.

During the test period of one month, the dummy source capsule was moved from the store to exposed position and back about 300 times. The interlock, the limit switches and the time of travel (14 sec.) were frequently checked. During this time it was expected that the Teleflex cable might stretch 0.5 - 1.0 in. and it was in fact found necessary to readjust the limit switches after the test period.

Lubrication of the entire cable is usually advised by the manufacturers, but it was considered that this might lead to deposition of grease in the end piece of the irradiation tube. If so, there might be some hardening of the grease by radiation, which might in turn lead to jamming of the source. Zinc oxide based grease was, however, applied to the spent travel end of the cable, i.e. where it passes over the electric operator drive.

During the test period, the CO_2 fire extinguisher system was also checked.

SECTION 11

INSTALLATION OF THE SOURCE CAPSULE

A. PREPARATION FOR UNLOADING

B. UNLOADING

A. PREPARATION FOR UNLOADING

Immediately after arrival on the College site, the lead transport container was monitered by the Health Physicist. Radiation levels around the container were low, and within the maximum permissible levels, i.e. (2.5 mr/hr). The top plug was then removed, exposing the protruding stainless steel rope and connector, and the centre plug. The dose rate immediately above the channel in the centre plug, which leads down to the source capsule, was approximately 40 mr/hr.

The top plug was replaced and the lead container was moved on rollers into the source chamber.

The total height of the container, including top plug, was 45.5 in., whilst the end of the guide tube was 47.5 in. from floor level. The container could not be placed directly under the guide tube (centre to centre), and was therefore positioned 5 in. off centre (Plates 5, 6 and 7). The centre plug (10 in. dia. by 9 in. total depth) could now be lifted clear.

A small funnel-shaped end piece was attached to the end of the guide tube to provide a smooth entry for the source capsule (page 53).

A 2 in. dia. eye-bolt, required for hoisting

the centre plug, was set in the ceiling, directly above the centre of the container (Plate 6). A second 2 in. dia. eye-bolt was screwed into the centre plug and a "Haltrac" nylon hoist, capable of lifting 1,000 lb., was suspended between these two eye-bolts. As the guide tube was positioned 5 in. off centre, it was therefore possible to raise the plug (weighing 220 lbs.) until the hoist was choc-a-block.

To avoid jamming the source capsule on removal from the locating tube in the coffin, it is essential first to raise it 6 in. by a vertical pull. This can be achieved by (i) pulling the raised centre plug to one side, by means of a wire passing through the 4 in. duct to the control face, and then (ii) pulling the guide tube, by a second wire, into a position directly over the centre of the locating tube. This operation was tested prior to unloading. Plate 6 shows the hoist and pulling wires in the cell.

The complete unloading operation can be carried out from the control face and observed through mirrors placed at each corner of the labyrinth corridor.

B. UNLOADING

The unloading schedule was as follows:

(i) the source capsule was attached to the Teleflex cable (Plate 7). The coupling was secured by driving two slotted and tapered metal pins through two holes drilled at right angles through it. This method of connecting ensured that the coupling could not slacken or break apart on continual operation of the source,

(ii) the Teleflex cable and coupling were pulled into the guide tube by manual operation of the source travel mechanism,

(iii) the lead plug was raised slowly, pulling from the control face. Dose rates around the coffin did not exceed 100 mr/hr until the plug was raised free from the coffin,

(iv) once the plug was completely raised (Plate 8) it was pulled to one side,

(v) the guide tube was now pulled directly over the centre of the coffin,

(vi) the source capsule was raised slowly into the guide tube and drawn back to the store position. Dose rates in corridor H, Drawing (NT 6), were approximately 300 mr/hr when the source was freely exposed before entering the guide tube. Plate 9

shows the capsule at this point in the operation, (vii) the interlocking disc was locked in position, and it was safe to enter the source chamber.

The lead coffin was removed from the cell, and the guide tube end piece placed in position. The electric operator was carefully reset, the slipping clutch tightened, the source travel and interlock control were tested and found to function satisfactorily.

The complete unloading operation was performed in 60 minutes. All personnel engaged in the unloading were subject to Health Physics supervision. No person received a dose greater than 20 mr.

SECTION 12

D O S I M E T R Y A N D C A L I B R A T I O N O F T H E S O U R C E

A. INTRODUCTION

B. EXPERIMENTAL DOSIMETRY

C. THE INTENSITY OF GAMMA RADIATION EMITTED BY CYLINDRICAL SOURCES

A. INTRODUCTION

A number of methods are available for the dosimetry of high intensity gamma ray sources, e.g. calorimetry, and solid state and chemical dosimeters.

Properties of the ideal dosimeter are that it should be independent of dose rate, of total dose, of radiation energy, of small temperature and pressure changes and furthermore should be simple and convenient to use.

Fricke and Morse (62) first suggested that the oxidation of ferrous sulphate solutions could be used as a dosimeter for high energy gamma radiation. The use of ferrous sulphate as a dosimeter has been widely discussed (63 - 66), particularly the effect of organic impurities on the rate of oxidation. Dewhurst (64) demonstrated that the presence of chloride ions would inhibit the oxidation of ferrous ions by organic impurities.

Hochanadel and Ghormley (67) obtained the yield for gamma ray oxidation of ferrous sulphate in air saturated 0.4 M sulphuric acid solution. The value was based on a calorimetric measurement of gamma ray absorption in water, and gave the G value as 15.6 ± 0.3 ferrous ions oxidised per 100 eV absorbed. This result compares satisfactorily with similar work

carried out by Lazo et al (68) who also measured the oxidation of ferrous sulphate by calorimetry and obtained a G value of 15.8 ± 0.3. A valuable contribution to ferrous sulphate dosimetry came when it was suggested that irradiated solutions of ferrous sulphate could be analysed for ferric ion concentration by direct spectrophotometric measurement of the absorbancy at a wavelength of 305 mμ (69, 70). This method is now widely used and is a quick and reproducible means of measuring gamma ray energies (71 - 73). More recent papers (74, 75) have dealt with the various mechanisms of the oxidation of ferrous sulphate solutions and the development of the method to high energy gamma radiation and fast electrons. Ceric sulphate is a useful chemical dosimeter in the range 10^5 - 10^7 rads, and has the advantage of not being oxygen dependent as is the ferrous-ferric system. Ferrous-ferric oxidation only gives satisfactory results when used in the range 4,000 - 40,000 rads, i.e. until all the available oxygen is used up. Saturation of the system with oxygen extends the useful range five-fold. A number of solid state dosimeters have been described for calibrating high intensity gamma ray sources. Thus poly vinyl

chloride films and various glass dosimeters can be used at high doses (79 - 81), i.e. in the range from 10^4 to 2 x 10^6 rads.

B. EXPERIMENTAL DOSIMETRY OF THE SOURCE

Approximately 10^{-3} M ferrous sulphate solution was prepared by dissolving the following reagents in 1l of distilled water.

$(NH_4)_2 \cdot SO_4 \cdot FeSO_4, 6H_2O$	A.R.	0.40 g
NaCl	A.R.	0.06 g
H_2SO_4	A.R.	3.00 mls.

5 ml. aliquots of this solution were transferred to stoppered test tubes of diameter 12mm. The test tubes were placed near the cobalt source and distances were measured from the centre of the source to the centres of the test tubes. The solution in each case was irradiated to receive 10,000 - 30,000 rads. The optical densities of each sample were measured at 304 mμ in a Unicam S.P. 500 spectrophotometer, using unirradiated solutions as a blank.

Calculation of Results

The results obtained on three independent determinations are shown in Table 3. The dose rate

was determined as follows, assuming the G value for ferrous ion = 15.50 molecules per 100 eV (73).

Optical density O.D. = E x c x l

where E = extinction coefficient

c = concentration of solution (moles/l.)

l = thickness of solution

For 10mm optical measuring cells $l = 1$

$$c = \frac{O.D.}{E}$$

$$\therefore \quad c = \frac{O.D.}{E} \times 6.025 \times 10^{23} \text{ molecules/l.}$$

$$= \frac{O.D.}{E} \times \frac{6.025}{15.5} \times 10^{23} \times \frac{100}{1000} \text{ eV/g in water}$$

$$1 \text{ rad} = 6.24 \times 10^{13} \text{ eV/g}$$

$$\therefore \quad \text{dose} = \frac{O.D.}{E} \times \frac{6.025 \times 10^{22}}{15.5 \times 6.24 \times 10^{13}} \text{ rads}$$

Optical density varies 0.7% per degree above 20°C (73).

$$\therefore \quad O.D._{20^\circ C} = O.D._{T^\circ C} (1 - 0.007\,t)$$

where $t = T - 20$

and T = temperature of sample

$$\therefore \text{ dose} = O.D. \frac{(1 - 0.007t)}{E} \times \frac{6.025 \times 10^{22}}{15.5 \times 6.24 \times 10^{13}} \text{ rads}$$

Using values reported by Haybittle, Saunders and Swallow (73)

Concentration of Sulphuric Acid	Temperature	E
0.1N	20°C	2115
0.8N	20°C	2094

Substituting E = 2115 for 0.1N H_2SC_4

$$\text{Dose} = \underline{2.94 \times 10^4 (1 - 0.007t) \times \text{O.D.}} \text{ rads}$$

Results in Table 3 were calculated using the above equation and a calibration curve of dose rate plotted against distance was prepared (Fig. 5). The dose rate is proportional to the distance according to the inverse square law, and Fig. 5 shows that a ~~semi-~~log. plot gives a straight line of slope approximately -2. However, at points closer than 6 cm., the geometry of the source is less uniform and the points deviate from the straight line. At points 15 cm. or further away, the dose distribution becomes more uniform. Assuming, therefore, that the source can be treated as a point source at distances of the order of 100 cms., the specific source strength may be obtained from dose rates measured at this distance.

k factor for Co^{60} = 13.5 r/hr/mc at 1 cm. (56)

$\therefore$ Dose at 100 cm = 13.5×10^{-4} r/hr/mc.

TABLE 3

DOSE RATE MEASURED IN NOVEMBER 1959

Dist. (cms.)	Time	O.D. (304mμ)	Total Dose rads x 10^4	Dose Rate M rads/hr	T. °C
1.5	30 sec	1.43	1.08	1.30	23.0
1.5	30 sec	1.43	1.03	1.24	25.0
1.7	40 sec	0.61	1.76	1.58	22.5
1.7	30 sec	0.37	1.07	1.28	22.5
3.0	2 min	0.46	1.34	0.40	22.5
3.0	2 min	0.89	2.54	0.76	23.5
3.0	1 min	0.33	0.95	0.57	22.5
4.5	2 min	0.41	1.18	0.35	23.0
4.5	2 min	0.47	1.25	0.37	23.5
6.0	4 min	0.25	1.24	0.19	22.5
6.0	8 min	0.54	1.56	0.23	23.5
8.0	7 min	0.57	1.65	0.14	22.5
10.0	15 min	2.00	1.42	0.06	25.0
10.0	15 min	0.86	2.45	0.10	23.5
10.0	10 min	0.58	1.66	0.10	22.5
12.0	18 min	0.72	2.10	0.07	22.5
15.0	25 min	0.67	1.92	0.05	22.5
18.0	25 min	0.48	1.37	0.03	23.5
20.0	30 min	0.93	1.38	0.03	25.0
100.0	17.83 hrs	0.73	2.10	0.01	23.5
100.0	17.08 hrs	0.72	2.08	0.01	23.0

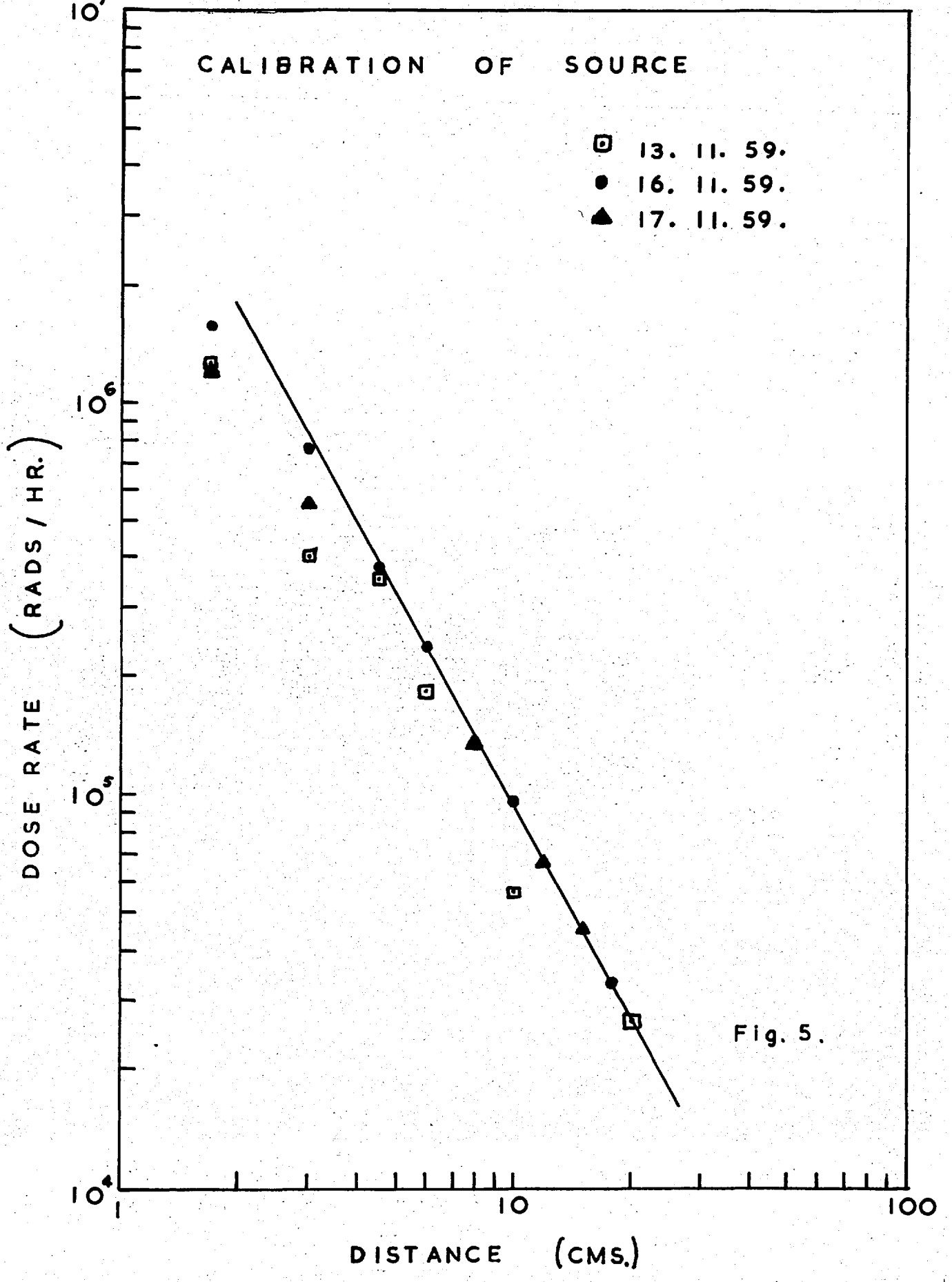

CALIBRATION OF SOURCE
13. 11. 59.
16. 11. 59.
17. 11. 59.
DOSE RATE (RADS / HR.)
10^7
10^6
10^5
10^4
1
10
100
DISTANCE (CMS.)

Fig. 5.

Experimental Dose at 100 cm = 1.22×10^3 rads

Specific source strength = $\frac{1.22 \times 10^3}{13.5 \times 10^{-4}}$ mc.

= 936 curies

This calibration dcos not take into account losses due to self absorption in the source capsule or self shielding in the source tube.

C. THE INTENSITY OF GAMMA RADIATION EMITTED BY A CYCLINDRICAL SOURCE

Very few attempts have been made to calculate the dose rate emitted by a solid cylindrical source of cobalt-60. Several workers have developed equations to calculate the intensity of radiation at the centre of a hollow cylindrical source (82 - 85) in order to plot the distribution of radiation dose i.e. plot of isodose curves. Elementary calculations of dose rates from cobalt sources are usually based on the assumption that the source may be considered as a point. However, for a solid cylindrical source of finite size, the geometry of the dose distribution at points close to the axis of the source becomes critical and cannot be treated by point-source calculations. Magat and Reinisch have considered various source shapes and calculated

the approximate dose-distance relationships to be expected. A rather more fundamental treatment is given by Kovalev (87) who has considered the dose rate at a given point along the axis of a solid cylindrical source. An analytical expression involving only tabulated functions is presented, which may be used when neglecting self absorption of the source. A self absorption factor has also been tabulated in this work, for sources with various absorption coefficients and for cylindrical sources of different height:diameter ratios.

Assuming an active source length of 0.395 in. diameter by 4.5 in. long, then according to Kovalev, the self-absorption coefficient (Table 4) may be calculated as follows:

μ_o = linear absorption coefficient for cobalt (density 8.9 g/cc)

= 0.22 cm^{-1}

$\frac{H}{D} > 2.5$ i.e. ∞

D = 0.395 in. = 1.0 cm.

$\mu_o D$ = 0.22

From Table 4, self absorption coefficient = 0.8

$\therefore$ Specific source strength = $\frac{936}{0.8}$

= $\underline{1170 \pm 5\% \text{ curies}}$

According to A.E.C.L., 1,200 curies of cobalt-60 were supplied and this would have decayed to 1,170 at the time the dosimetry was carried out.

TABLE 4

SELF ABSORPTION COEFFICIENTS (87)

μD \ H/D	0.50	1.0	1.5	2.0	2.5	∞
0	1.000	1.000	1.000	1.000	1.000	1.000
0.1	0.967	0.958	0.952	0.947	0.942	0.853
0.2	0.931	0.920	0.912	0.904	0.896	0.797
0.3	0.903	0.884	0.871	0.863	0.852	0.753
0.4	0.880	0.856	0.838	0.826	0.812	0.713
0.5	0.852	0.825	0.808	0.793	0.780	0.676
0.6	0.832	0.800	0.777	0.762	0.744	0.640
0.7	0.811	0.773	0.750	0.730	0.714	0.609
0.8	0.790	0.750	0.723	0.700	0.686	0.578
0.9	0.771	0.730	0.698	0.673	0.656	0.552
1.0	0.752	0.704	0.676	0.648	0.631	0.528

H = height of source (cms.)

D = diameter of source (cms.)

P L A T E S 1 - 9

SOURCE CAPSULE SHOWING

STAINLESS STEEL ROPE

AND COUPLING

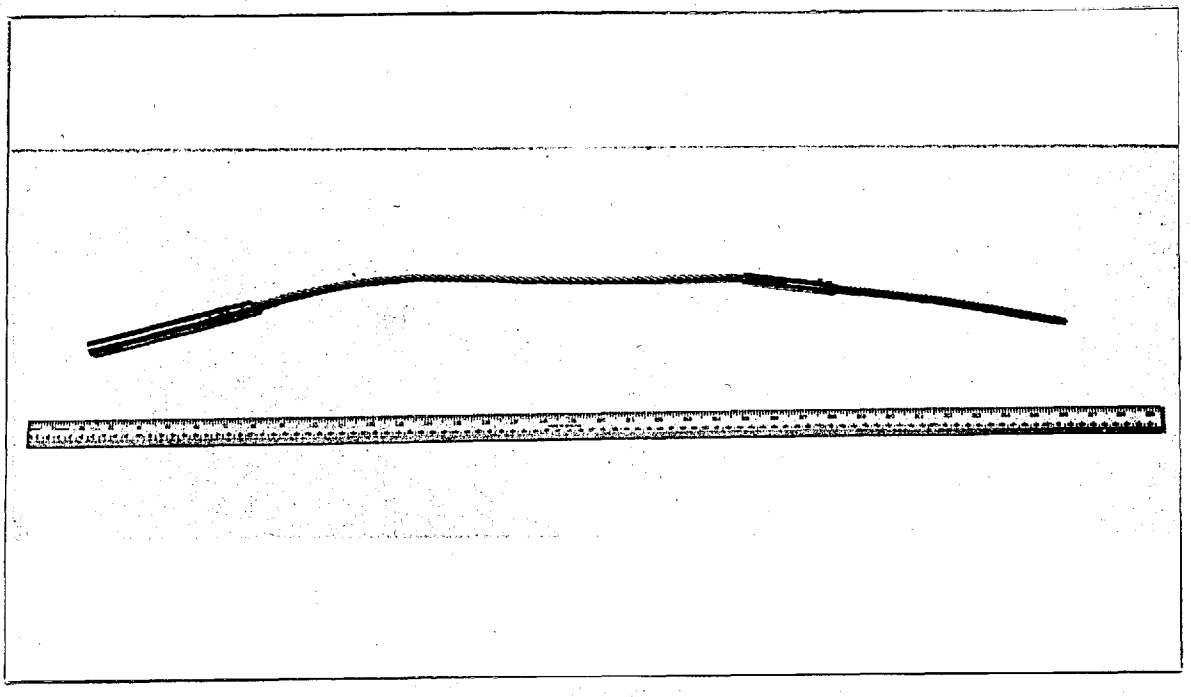


PLATE 1

"TELEFLEX" ELECTRIC DRIVE

MOTOR

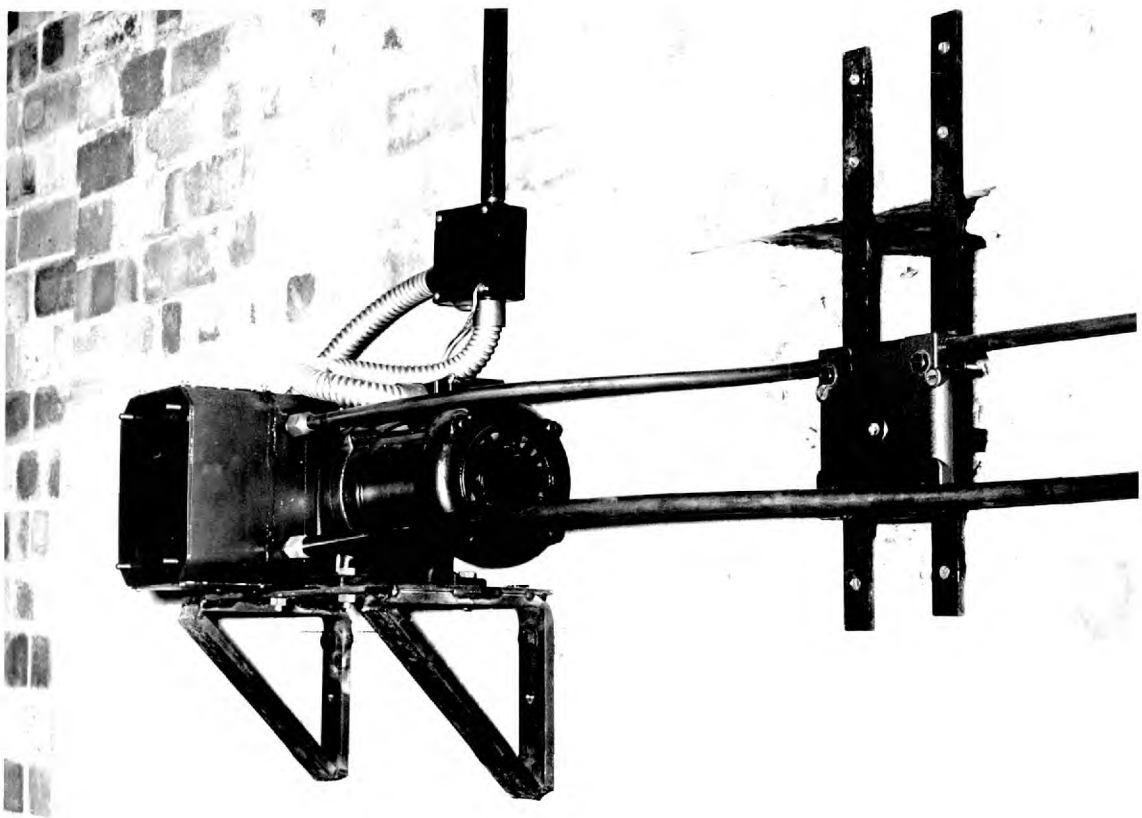


PLATE 2

SOURCE INTERLOCK

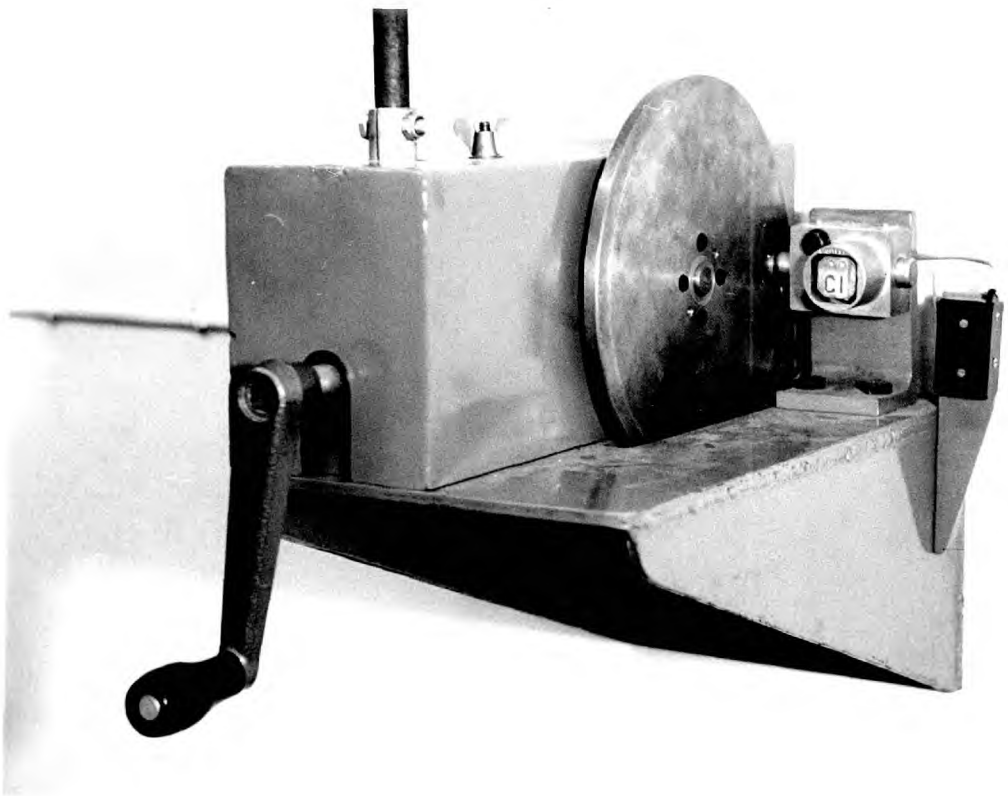


PLATE 3

LEAD SHIPPING CONTAINER

WITH PLUG REMOVED

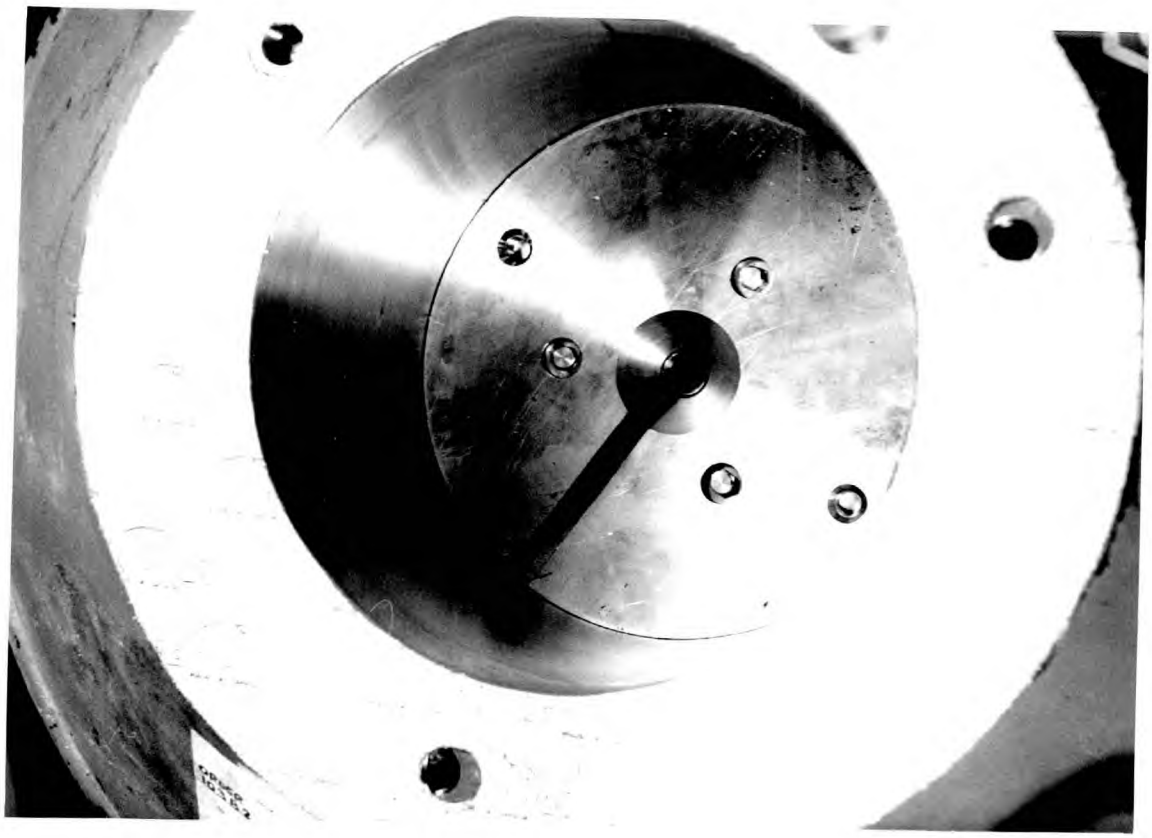


PLATE 4

LEAD SHIPPING CONTAINER

IN POSITION IN THE

IRRADIATION CELL



PLATE 5

UNLOADING ASSEMBLY

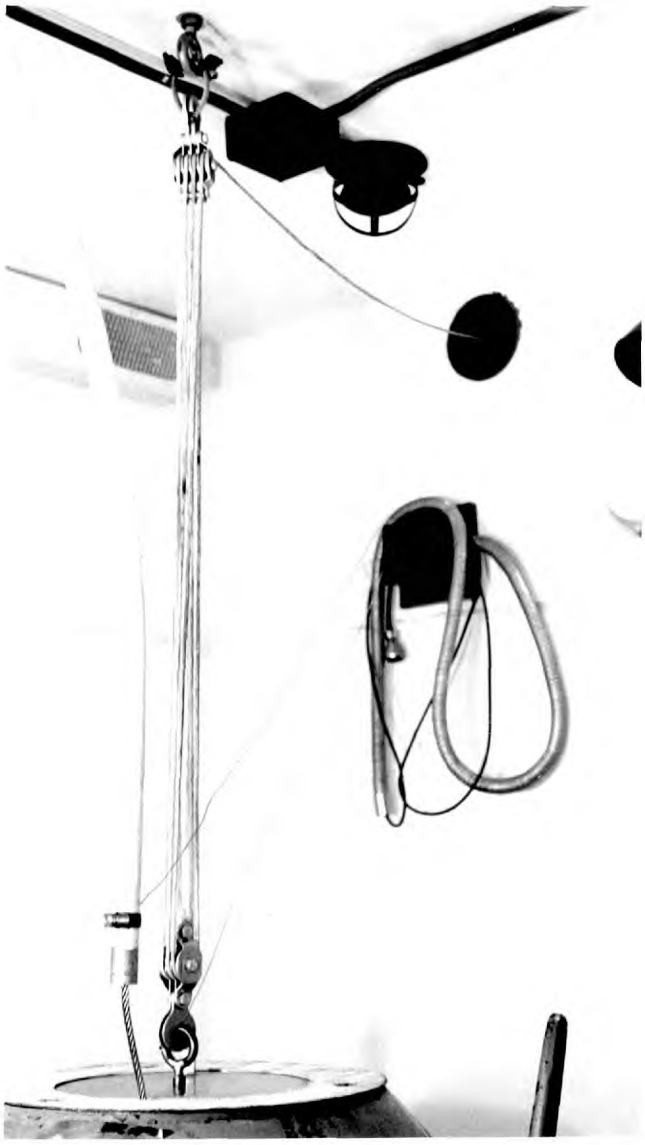


PLATE 6

COUPLING BETWEEN STAINLESS STEEL ROPE

AND "TELEFLEX" CABLE

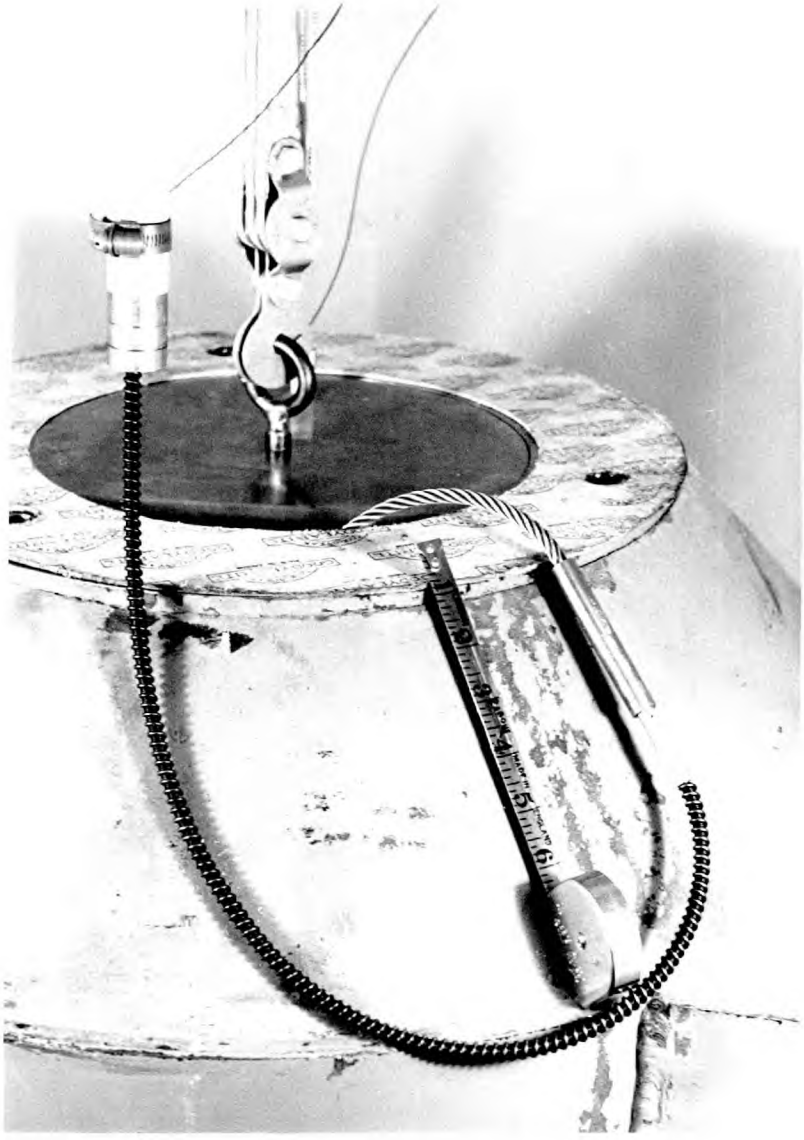


PLATE 7

LEAD PLUG IN RAISED

POSITION

(photographed through one mirror)



PLATE 8

ACTIVE SOURCE ENTERING

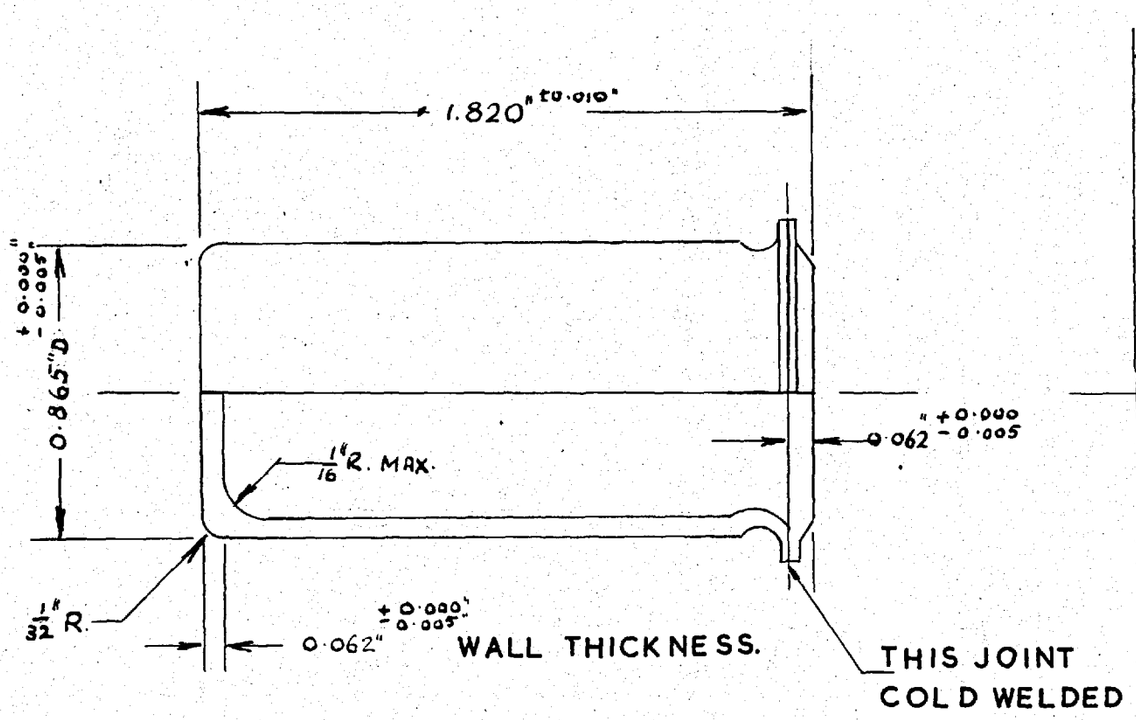
GUIDE TUBE

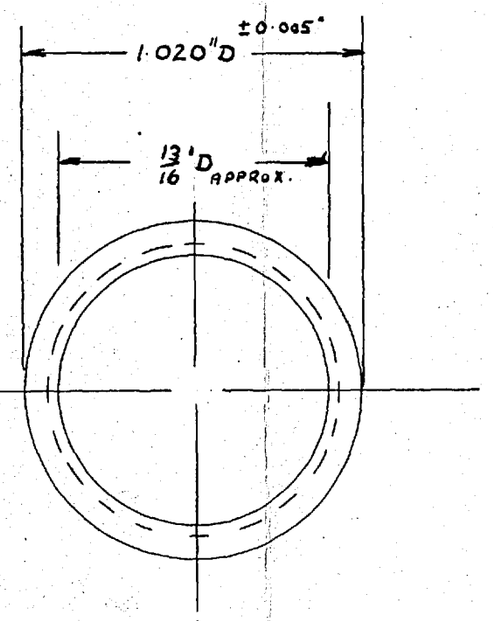
(photographed through two mirrors)



PLATE 9

D R A W I N G S ANT 8 - 12





PART No.	No. OFF	RAW MATL AND REMARKS

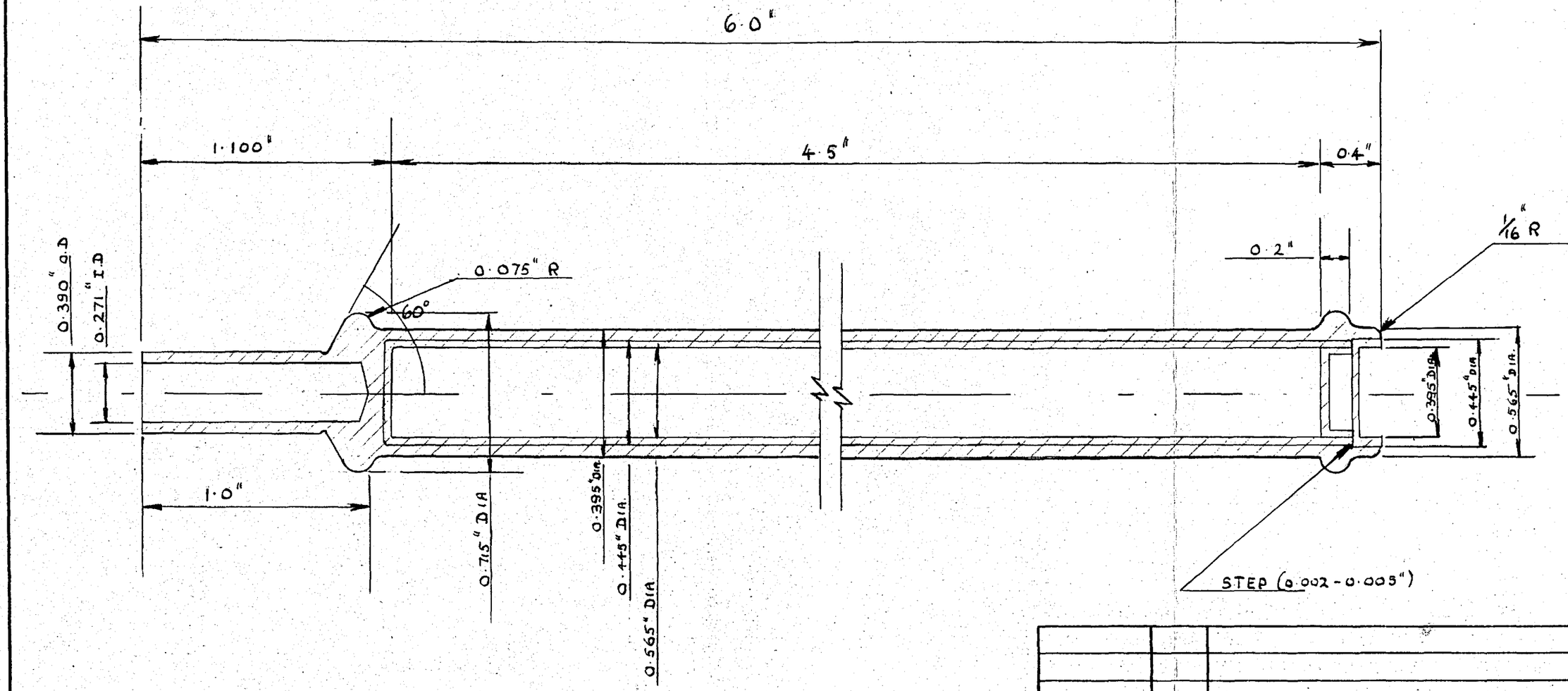
SCHEDULE FOR

IMPERIAL COLLEGE, LONDON S.W.7.

CHEMICAL ENGINEERING DEPARTMENT

PART NAME **A.E.C.L. CAPSULE**

SCALE 2/1	DRAWN BY M. Streat.	DATE
JOB No.	~~PART~~ No. ANT. 8.	



PART No.	No. OFF	RAW MATL AND REMARKS

SCHEDULE FOR

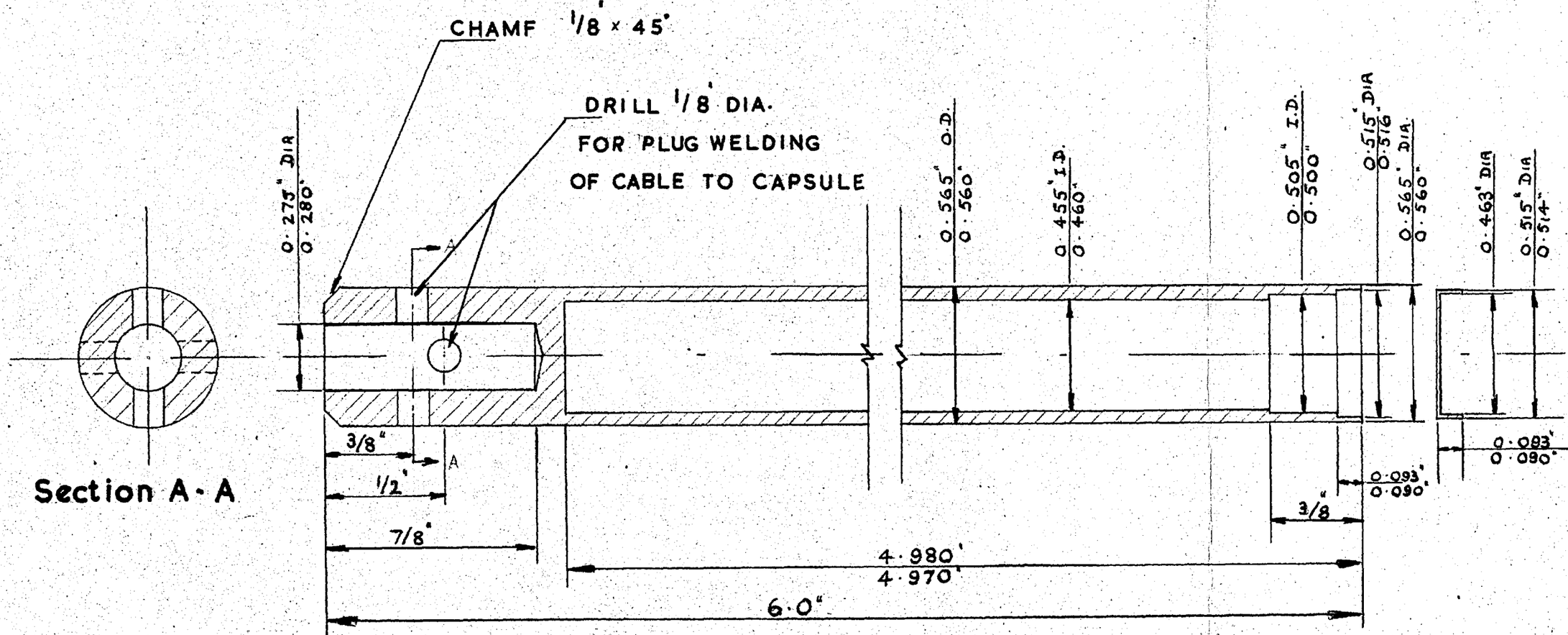
IMPERIAL COLLEGE, LONDON S.W.7.

CHEMICAL ENGINEERING DEPARTMENT

PART NAME **A.E.R.E. TYPE CAPSULE**

SCALE	DRAWN BY M. Sheak	DATE
JOB No.	~~PART~~ No. ANT. 9.	

H.M.L.D.

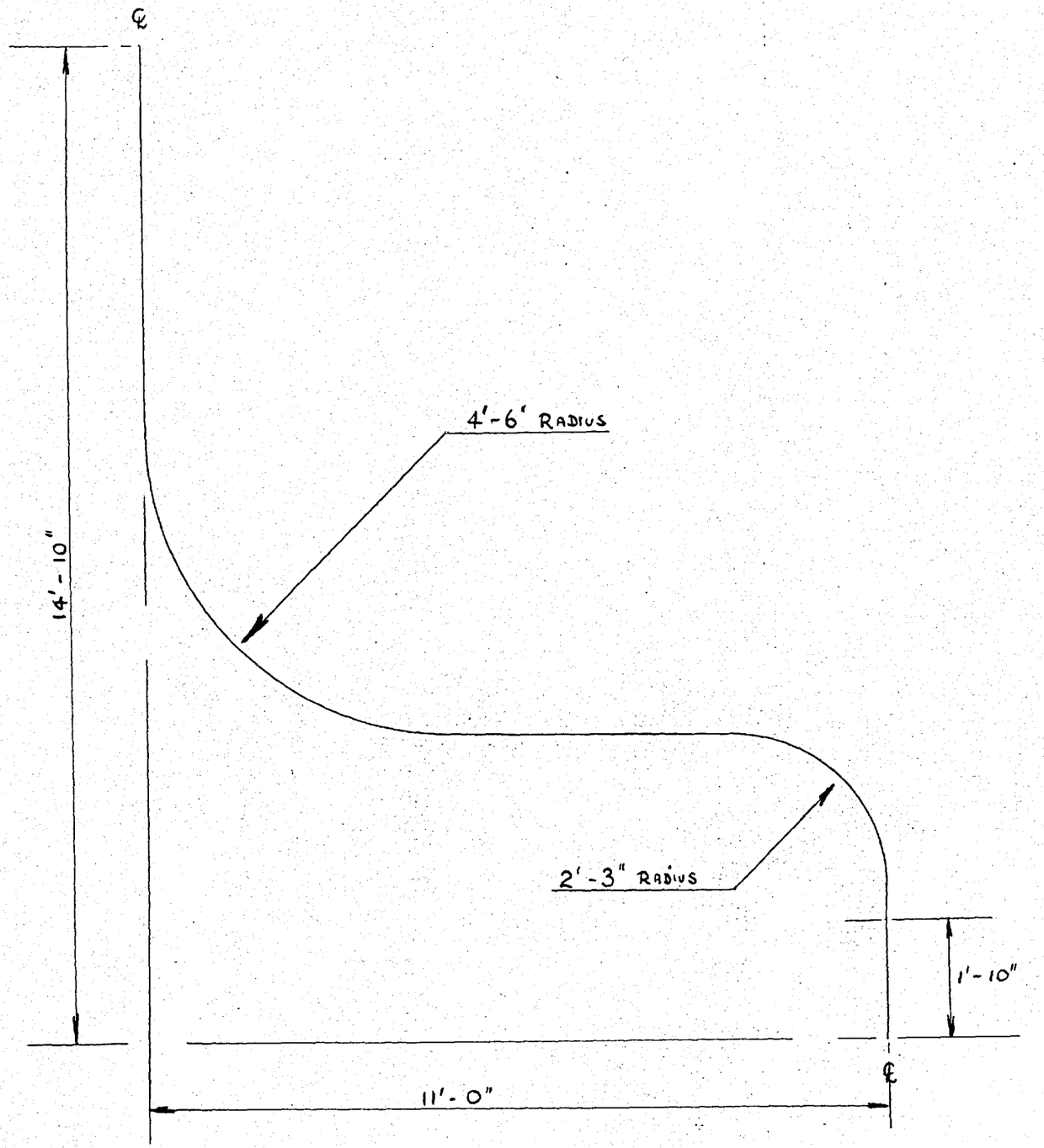


Section A-A

A 2FT LONG 0·27" DIA.
STAINLESS STEEL ROPE TO
BE WELDED TO CAPSULE AFTER
INSERTION IN 0·272" HOLE
0·275"

BOND MUST BE GUARANTEED

		TYPE 316 STAINLESS STEEL
PART No.	No. OFF	RAW MATL AND REMARKS
SCHEDULE FOR		
IMPERIAL COLLEGE, LONDON S.W.7. CHEMICAL ENGINEERING DEPARTMENT		
PART NAME OUTER CAPSULE		
SCALE 2 / 1	DRAWN BY M. Streat.	DATE
JOB No.	PART No. A N T. 10.	



		1" O.D. STAINLESS STEEL
		TUBE 16 S.W.G. BST 55
		TOTAL LENGTH 23 FT.
PART No.	No. OFF	RAW MATL AND REMARKS

SCHEDULE FOR

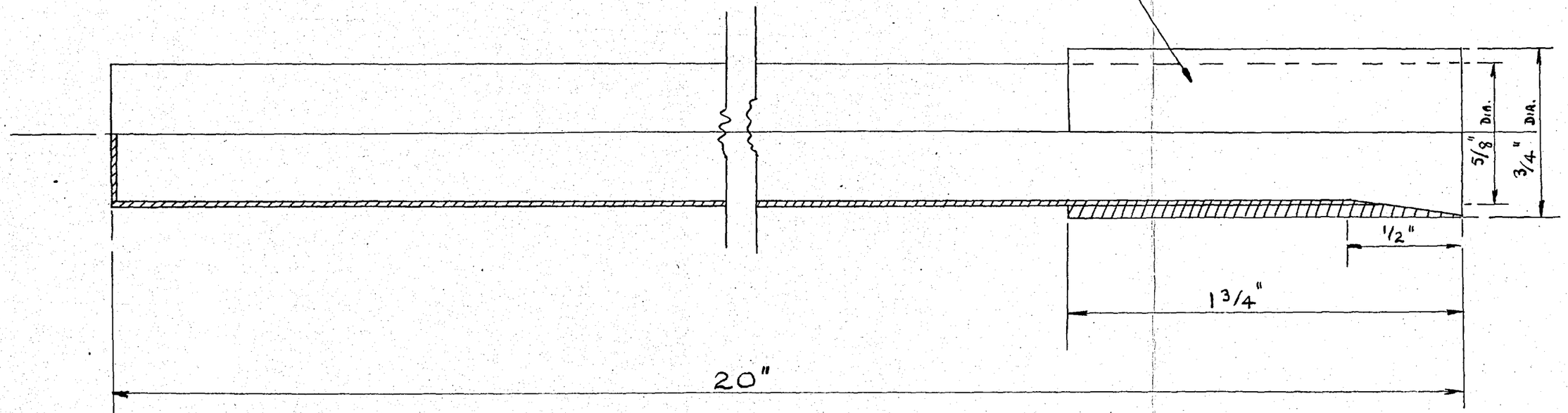
IMPERIAL COLLEGE, LONDON S.W.7.

CHEMICAL ENGINEERING DEPARTMENT

PART NAME S-SHAPED GUIDE TUBE

SCALE 1/2" TO 1 FT.	DRAWN BY M. Street	DATE 12.9.60.
JOB No.	PART No. ANT. 11.	

H.H. Ltd



		5/8" O.D. STAINLESS STEEL
		TUBE 25 S.W.G.
		0·585" I.D.
PART No.	No. OFF	RAW MATL AND REMARKS

SCHEDULE FOR

IMPERIAL COLLEGE, LONDON S.W.7.

CHEMICAL ENGINEERING DEPARTMENT

PART NAME SOURCE END PIECE

SCALE 2 / 1	DRAWN BY M. Streat	DATE 12.9.60.
JOB No.	~~PART~~ No. ANT. 12.	

E F F E C T S O F R A D I A T I O N
O N
I O N E X C H A N G E R E S I N S

SECTION 13

S U R V E Y O F P R E V I O U S W O R K

Ion exchange finds a limited application in the chemical reprocessing of spent reactor fuel elements, of aqueous homogeneous reactor fuel (88) and in the recovery and concentration of plutonium from waste solutions (89). Mixed bed demineralisation is also used to purify water in water-cooled reactors.

Cathers (90) and Hammond (91) have outlined the major problems associated with the use of process reagents under high energy ionising radiation. The magnitude of the chemical changes produced by the irradiation of organic materials such as ion exchange resins, may be sufficient to render them useless for chemical processing.

Many workers have studied the properties of irradiated ion exchangers (92 - 107). Resins have been exposed to cobalt-60 gamma radiation, X-rays, beta radiation by radio-isotopes adsorbed on the functional groups and also by nuclear reactor irradiation.

Higgins (92) showed that the capacity loss of the strong acid (sulphonated polystyrene) resin Dowex 50, when irradiated by cobalt-60 gamma radiation and also by beta radiation from Ce^{144} - Pr^{144} adsorbed on the resin, was of the

order of 10-20% per watt.hr. g. of energy absorbed. The capacity loss calculated from titration of the resin, agreed with the sulphate ion concentration released on irradiation. Variations were attributed to experimental error. Higgins postulated that the bond holding the active sulphonate group to the polystyrene skeleton is broken. It was also found that Dowex 50, with uranyl ion adsorbed, lost 8% capacity per watt. hr. g. of radiation absorbed. No physical degradation effects were observed. Dowex-1, a quaternary ammonium polystyrene resin, lost 40% capacity per watt.hr.g. The colour of the resin changed from pale yellow to reddish brown and the odour of amines was observed.

An extensive study by Fisher (93), showed radiation degradation effects in a variety of sulphonic acid based resins, also strong and weak base anion exchangers. Capacity losses of the order of 12% per watt.hr.g. were observed with the strong acid exchangers, and attempts were made to explain the results by means of a satisfactory mechanism. Strong base quaternary ammonium resins were found to decompose liberating nitrogenous products in the leach solutions. Irradiation causes a loss of strong base capacity at a greater rate than the

total anion exchange capacity. Fisher suggests a step-wise mechanism, involving first the loss of a methyl group from the quaternary structure and then the entire loss of the functional group. Sufficient experimental evidence to justify such a mechanism was not obtained.

Wedemeyer (94) irradiated a series of ion exchange resins, using a 60 kV X-ray machine, and obtained a penetration of 1.3 mm. in air-dried resin specimens. Owing to the low penetration of these X-rays, water slurries of the resins could not be studied. Wedemeyer's work showed that resin samples were more stable to radiation, the greater the degree of crosslinking. The effect of heat, particle size and solubility were found to be negligible. Semi-quantitative analyses of the degradation products, of irradiated Dowex 50 resin, showed no weakly acidic or neutral organic fragments. The overall capacity loss could be approximately accounted for by the amount of sulphur released from the resin, two-thirds appearing as free sulphate ion, or as water-soluble acid fragments, the remainder as higher molecular weight water insoluble sulphonic acid material. No attempt to isolate degradation products of basic exchangers

TABLE 5

RADIATION STABILITY OF ION EXCHANGE RESINS

Type of Resin	Loss in Exchange Capacity (%)					
	Wedemeyer (94)	Fisher (93)	Higgins (92)	Nikashina (95)	Nater (102)	Shigematsu (101)
Strong Acid:						
Dowex 50 (sulphonated polystyrene)	23	-	20	5	5	8
Amberlite IRA-112) 120) (nuclear sulphonic acid)	-	12	-	-	-	-
Dowex 30 Amberlite-105 (sulphonated phenolic resin)	-	-	1 1	-	-	-
Weak Acid:						
Amberlite IRC 50 Permutit H Duolite CS 101 (carboxylic acid)	100			16		0

Continued.

Table 5 (continued)

Type of Resin	Loss in Exchange Capacity (%)					
	Wedemeyer (94)	Fisher (93)	Higgins (92)	Nikashina (95)	Nater (102)	Shigematsu (101)
Strong Base:						
Dowex 1	44	-	40			28
Amberlite IRA-400	42	84			30	
Amberlite IRA-410	40	40				
Imac S4 (quaternary ammonium polystyrene resin)					40	
Stamex S (trianisole-sulphonium formaldehyde)					100	
Weak Base:						
Amberlite IR-4B (phenol formaldehyde amine resin)	13	34				
Amberlite IR-45 (styrene base amine resin)	53	24				
Dowex 3 (styrene base amine resin)	19					16

Results show the capacity loss for a total dose of 1 watt.hr.g. radiation energy absorbed, i.e. 3.8×10^8 rads.

Results of Shigematsu for a total dose of 3.7×10^7 rads.

was made.

Strong acid resins have also been irradiated by Nikashina et al (95). Costachel et al (97 - 100) using X-ray, beta and gamma radiation have shown that irradiation of bifunctional resins of the phenolsulphonic-formaldehyde type produces a change in the exchange capacity and in the aqueous swelling properties. The production of sulphate ions in leach solutions has been found to account for 65 - 75 per cent of the loss in sulphonate capacity. It is suggested that the discrepancy may be explained by formation of bridges in the macromolecular lattice and interaction between functional groups. Nater (102) has irradiated strong acid and strong base resins in a nuclear reactor, but the interpretation of the results is complicated by neutron effects.

The results of the foregoing work (Table 5) show that strong acid exchangers are approximately twice as stable to radiation as strong base quaternary ammonium resins. Carboxylic weak acid resins are the least stable to radiation, whereas sulphonated phenolic strong acid resins are the most resistant. The poor chemical stability of the phenolic resins, however, would tend to offset the favourable

radiation stability.

A great deal of the work that has been published up to the present has been concerned with the properties of cation exchangers. These have been used for separation of individual fission products, e.g. caesium-137 and strontium-90, where the stability of the resin to radiation is important.

Anion exchangers have also been suggested for the chemical separation of individual fission products (108), and have been used for separation, concentration and purification of plutonium (89). Further work is required to obtain a more complete knowledge of the radiation stability, chemical decomposition and reaction mechanisms involved when these resins are subjected to high radiation doses.

SECTION 14

P R E L I M I N A R Y I N V E S T I G A T I O N S

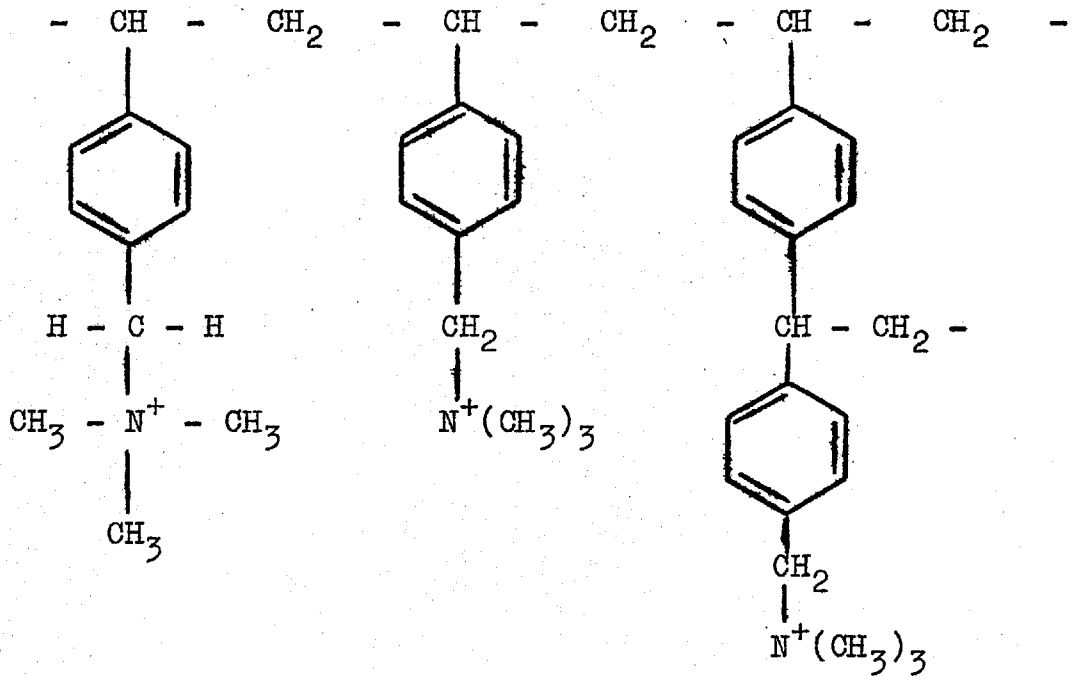
A. INTRODUCTION

B. EXPERIMENTAL AND RESULTS

C. DISCUSSION

A. INTRODUCTION

The anion exchange resin chosen for study was one of the commercially available Permutit resins, of the strong base quaternary ammonium polystyrene type, i.e. Deacidite FF. The structure of this resin is as follows.



This consists of a quaternary methyl amino group attached to a polystyrene skeleton which is cross-linked with divinyl benzene. The resin under investigation had the following properties.

(i) 7 - 9% cross-linking

(ii) 0.6 - 1.0 water regain, i.e. 0.6 - 1.0 g. of water associated with 1.0 g. dry resin in the chloride form

(iii) particle size 100 - 200 mesh.

The structure of the resin will henceforth be designated as $\underline{R - CH_2 - \overset{+}{N}(CH_3)_3}$. Deacidite FF resin may be compared with other resins shown in Table 6.

TABLE 6

Duolite	A - 42 A - 101 A - 40 A - 102	Dowex - 1 - 21K - 2
Amberlite	IRA - 400 IRA - 401 IRA - 402 IRA - 410 IRA - 411	Lewatit M 11 or (MN) Wolfatit L

The properties of strong base resins of this type are well known (109 – 112) and typical reactions are as follows:

(i) $$2\,R - CH_2 - \overset{+}{N}(CH_3)_3\,\overset{-}{Cl} + SO_4^{=} \longrightarrow \left[R - CH_2 - \overset{+}{N}(CH_3)_3\right]_2 SO_4^{=} + 2Cl^{-}$$

(ii) $R - CH_2 - \overset{+}{N}(CH_3)_3\ \overset{-}{OH} + NaCl \longrightarrow R - CH_2 - \overset{+}{N}(CH_3)_3\ \overset{-}{Cl} + NaOH$

(iii) $2\ R - CH_2 - \overset{+}{N}(CH_3)_3\ \overset{-}{NO_3} + \left[Pu(NO_3)_6\right]^{=} \longrightarrow \left[R - CH_2 - N(CH_3)_3\right]_2 Pu(NO_3)_6 + 2NO_3^-$

The affinity of anions for the resin largely depends on the charge and radius of the ion, its concentration and the pH of the solution. The affinity of some important anions is in the order

$$SO_4^{=} > NO_3^- > Cl^- > OH^-$$

the ion to the left is able to replace an ion to the right more easily. The hydroxide ion is the least strongly attached to the functional group.

The resin, which is supplied in bead form, is stable to organic solvents, to strong mineral acids and alkalis, and at temperatures up to 60°C both in non-aqueous and in aqueous media.

B. EXPERIMENTAL AND RESULTS

(i) Preparation of Hydroxide Form of Resin and Measurement of Capacity

Deacidite FF resin is usually supplied in the chloride form, and may contain small amounts of

soluble coloured side-products, which are removed before regeneration. Impurities are washed out with deionised water and methanol at 40 - 50°C.

It is recommended by the manufacturers that the resin be regenerated by passing a 3% solution of sodium hydroxide through a resin bed, two column volumes being sufficient to give an optimum working capacity of 3.5 m.equ/g. Using this procedure, it was found only possible to achieve a capacity of 1.4 - 1.8 m.equ/g with respect to hydroxide ion. Other workers (94) have experienced difficulty in converting the resin to the hydroxide form, i.e. until no further chloride ions remained attached to the functional groups.

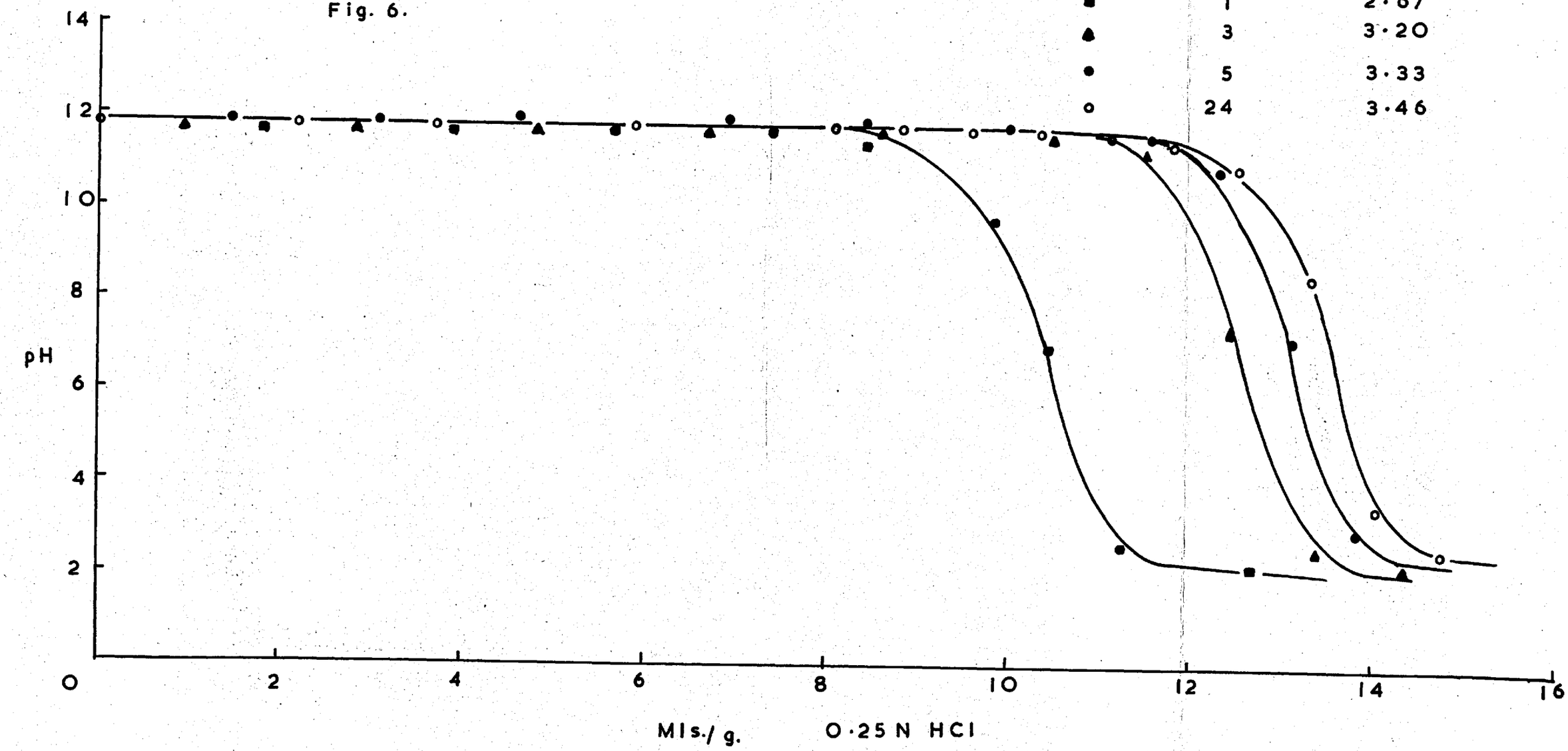
By passing 250 ml. of 4% sodium hydroxide solution (i.e. about 25 column volumes) through a resin bed, over a period of 24 hrs., it is found that gradual replacement of chloride ions takes place, and the hydroxide capacity approaches 3.5 m.equ/g.

Hydroxide capacity measurement

Approximately 1.0 g. of moist resin in the hydroxide form is transferred to a 50 ml. beaker. 20 mls. of 0.1N sodium chloride solution is added. The resin slurry is titrated against standard

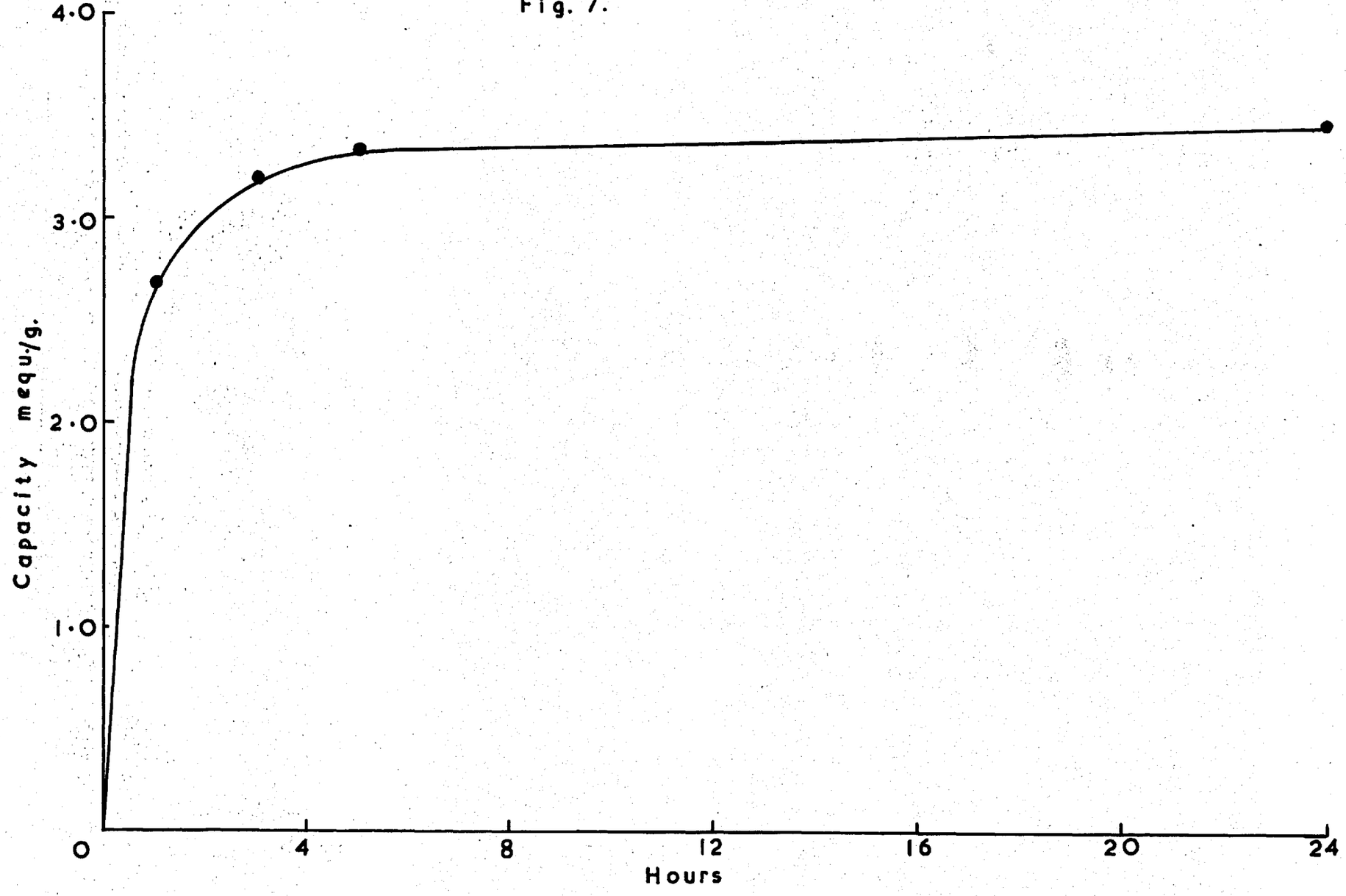
REGENERATION OF HYDROXIDE FORM

Fig. 6.



INCREASE IN HYDROXIDE CAPACITY WITH TIME

Fig. 7.



0.25 N hydrochloric acid using a glass electrode and calomel reference electrode with an automatic reading pH meter. A pH titration curve is plotted, and the end-point determined.

Previous work had shown that if the hydroxide form is titrated against standard acid, in the presence of water, the rate of reaction is slow, and the end-point is reached only with difficulty. Sodium chloride rapidly releases into the solution the OH ions attached to the functional groups, and a straight acid - base titration follows, i.e.

$$R - CH_2 - \overset{+}{N}(CH_3)_3\ \overset{-}{OH} + NaCl \longrightarrow R - CH_2 - \overset{+}{N}(CH_3)_3\ \overset{-}{Cl} + NaOH$$

$$NaOH + HCl \longrightarrow H_2O + NaCl$$

Thus, equilibrium is reached rapidly and the titration end-point, i.e. capacity, may be obtained. Typical strong acid - strong base titration curves, with end points at pH7, are obtained in the hydroxide capacity determinations (Fig.6). The capacity increases as the resin remains in contact with the sodium hydroxide solution until a limiting capacity of 3.5 m.equ/g. is reached after 24 hrs. (Fig.7).

Resin samples are dried at 100°C for 20 hours,

IRRADIATION OF ION EXCHANGE

RESINS

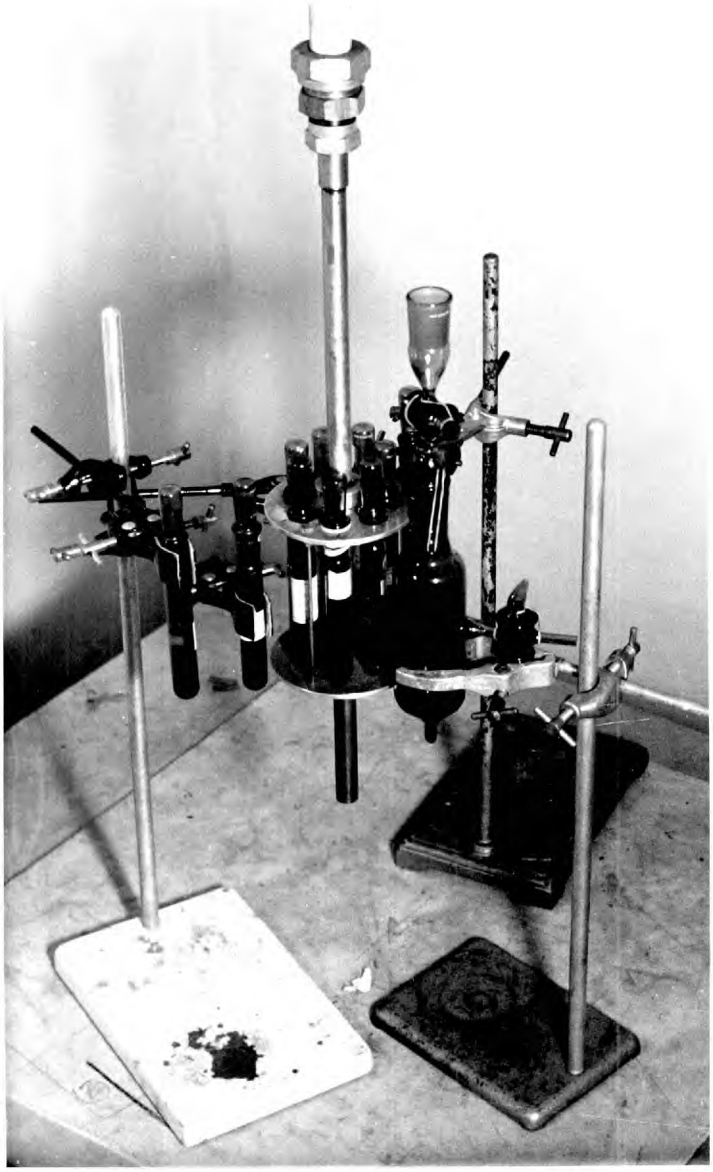


PLATE 10

and weighed in the chloride form, and the capacity expressed as milliequivalents per dry gram (weighed in chloride form).

Chloride capacity

Resin samples are converted completely to the chloride form by leaching with 4% hydrochloric acid. Excess chloride ions are removed by washing with distilled water. The resin samples are placed in a filter funnel and washed with 4% sodium sulphate solution, the filtrate being collected in a 100 ml. standard flask.

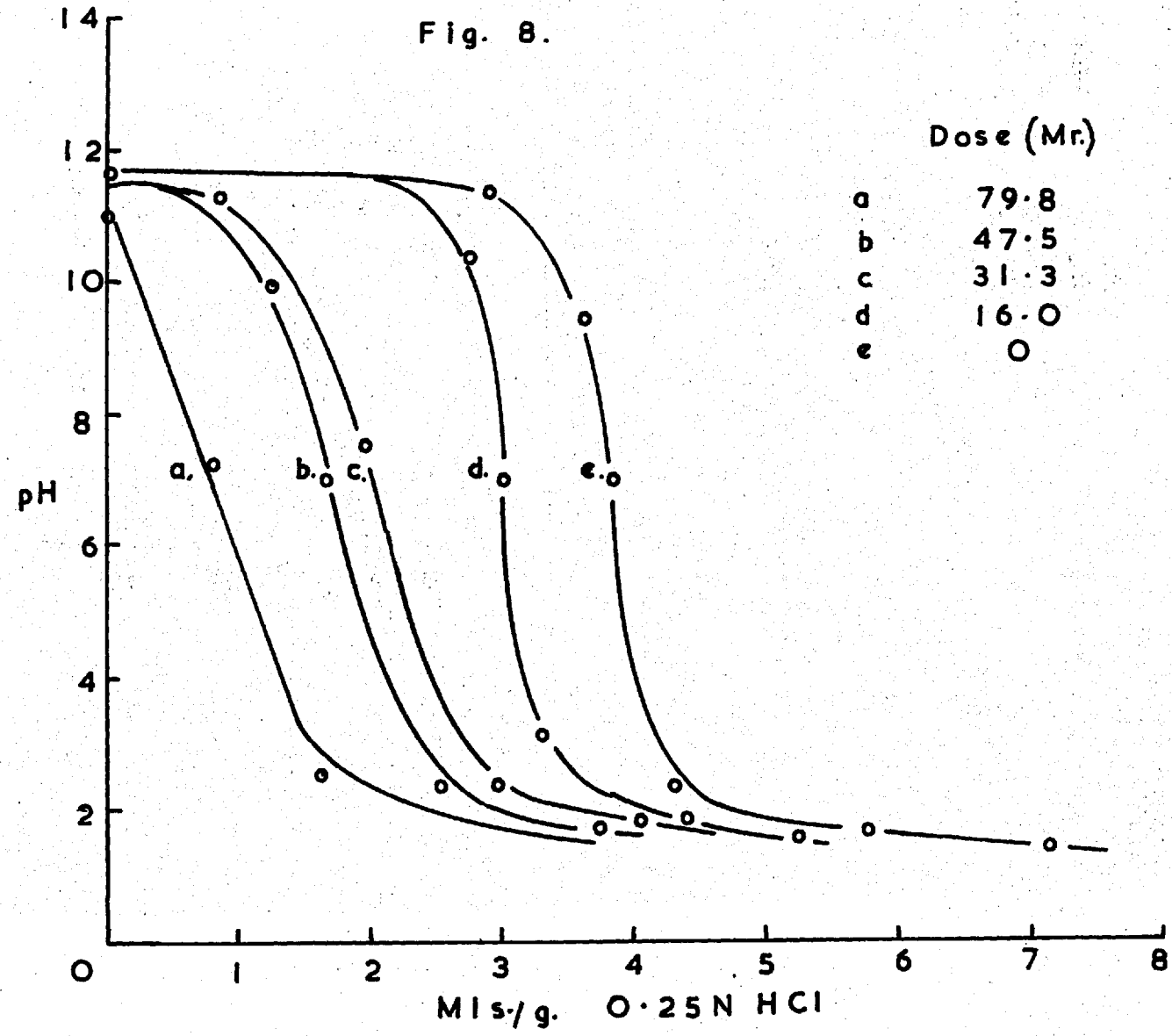
The filtrate is analysed for chloride ions, by taking a 10 ml. aliquot, and titrating against standard silver nitrate solution using potassium chromate as indicator. Resin samples are dried at 100°C and weighed in the sulphate form. Capacity is expressed with respect to chloride ion, as milli-equivalents per dry gram.

(ii) Irradiation of Resin Samples

Resin samples in the hydroxide and chloride form have been irradiated. Approximately 1 - 2 g (5 ml.) of moist resin are placed in glass stoppered test tubes (approximate volume 12 ml.) and irradiated at 3 cms. from the kilocurie source, the test tubes being located in a specially designed holder (Plate 10).

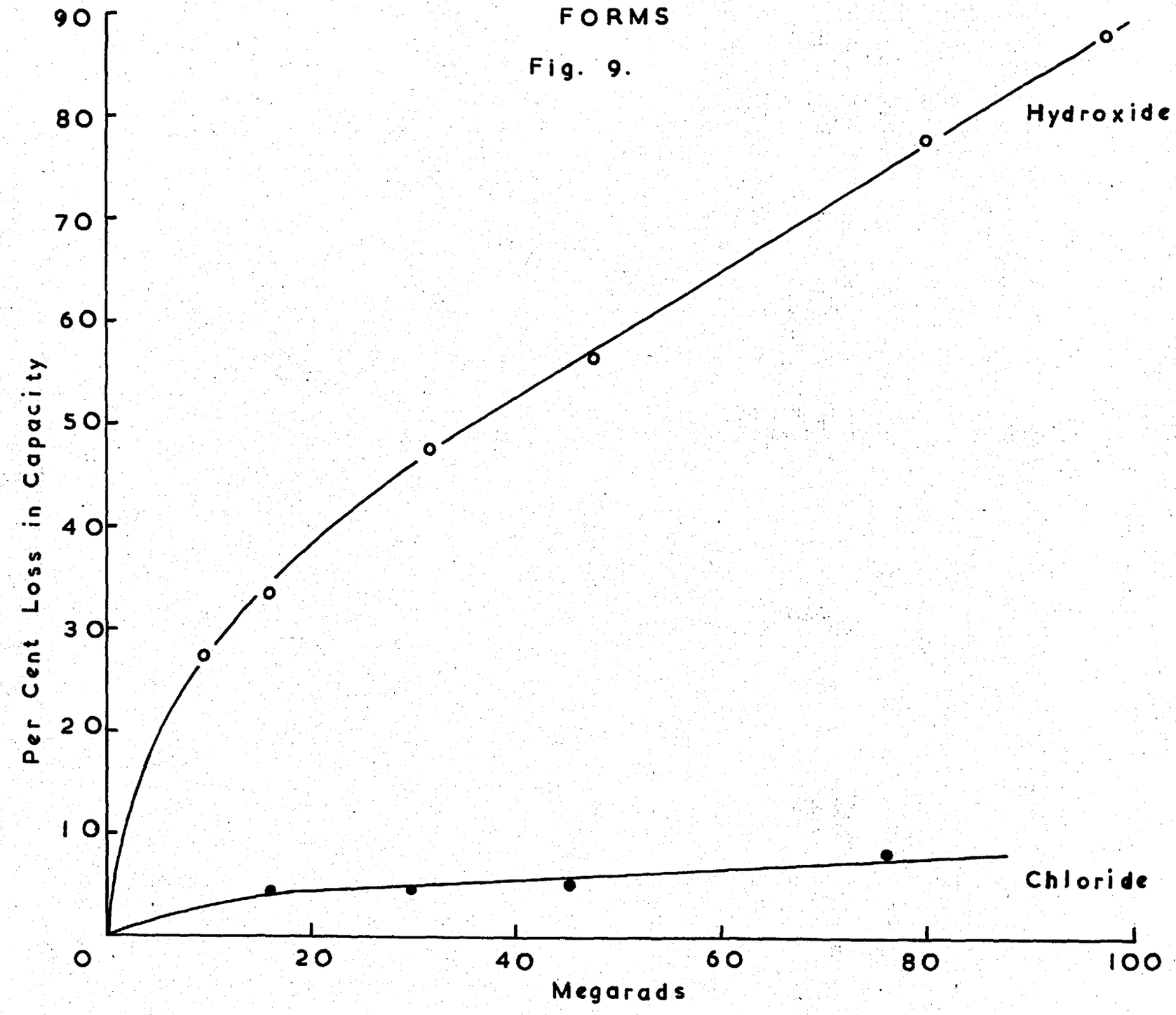
LOSS OF CAPACITY ON IRRADIATION

Fig. 8.



RELATIVE STABILITIES OF HYDROXIDE AND CHLORIDE FORMS

Fig. 9.



Dose rates of 0.7 - 0.8 Mr/hr. were obtained in similar test tubes placed at 3 cm. from the source, by ferrous-ferric dosimetry.

The hydroxide capacity of irradiated samples was obtained by the procedure described above. Fig. 8 shows the pH titration curves of resins after irradiation at doses up to 80 Mr. and Fig. 9 compares the loss in capacity for both chloride and hydroxide forms of the resin for doses up to 100 Mr.

(iii) Detection of Degradiation Products

Irradiation of the hydroxide form brought about a colour change from pale yellow to reddish brown, and the characteristic odour of amines was observed.

Aqueous slurries of resins irradiated in the hydroxide form were washed and the aqueous leach collected. This solution was titrated against centinormal standard acid, and titration curves (Fig.10) showed that basic products had been liberated. The basic products accounted for up to 80% of the loss in hydroxide capacity.

Qualitative spot tests were performed to establish the nature of the basic products released (113, 114). Aliphatic amines, e.g. trimethylamine, would be the most likely products, considering the

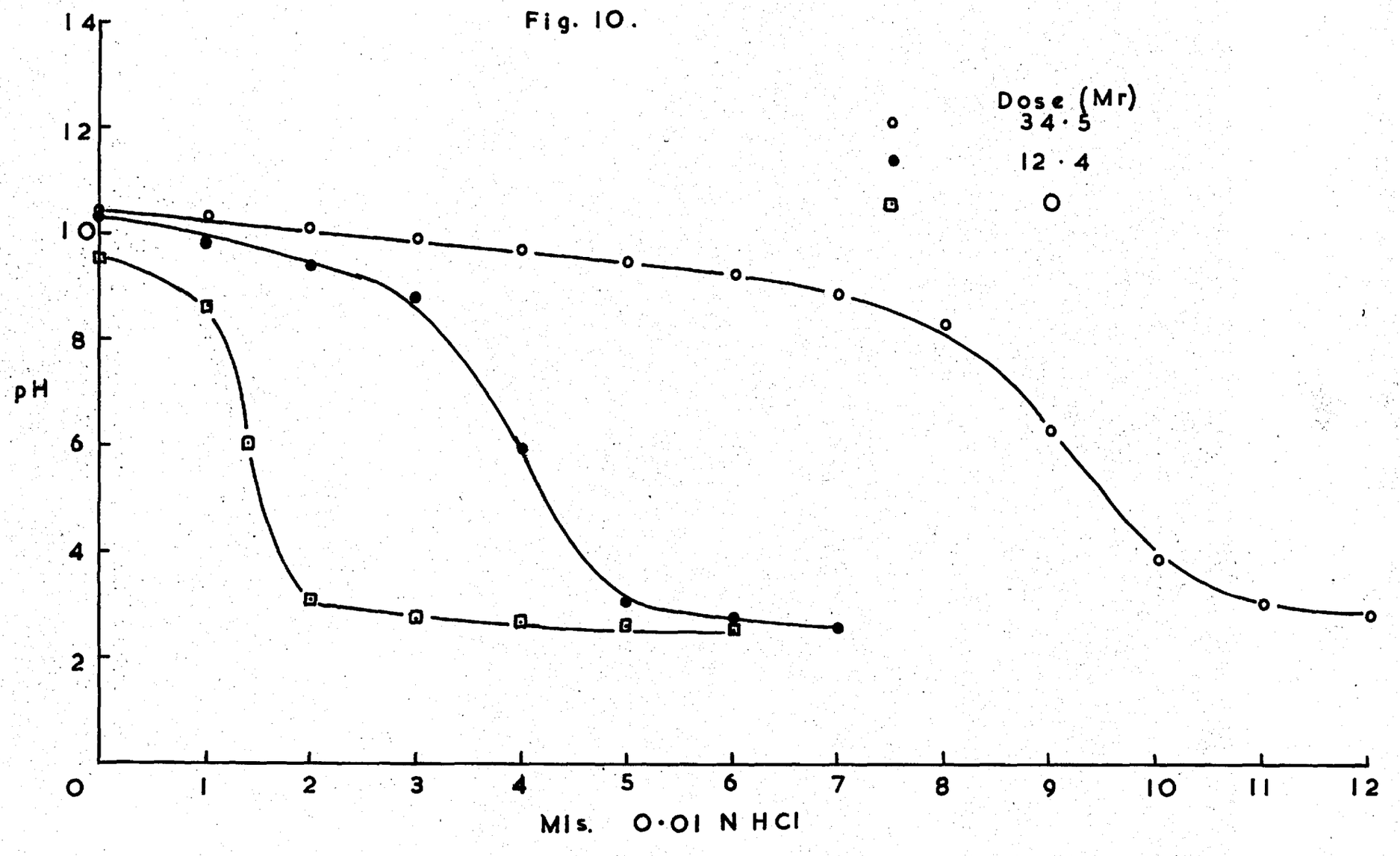
TABLE 7

RESULTS OF SPOT TESTS

FUNCTIONAL GROUP	REACTION INVOLVED	STANDARD	S µg/drop	RESULT
Secondary Amine	Reaction with sodium nitro prusside and acetaldehyde in sodium carbonate soln. gives blue colour (115)	Dimethylamine	5	Test positive at doses greater than 20 Mr.
Primary Amine	Reaction with sodium nitro prusside and acetone in neutral soln. gives red colour (116)	Methylamine	-	Test negative
Peroxide	Reaction with acidified potassium iodide in starch solution gives blue colour	Hydrogen peroxide	5	Test negative
Nitrite	Diazotisation of sulphanilic acid and coupling with N-I-naphthyl-ethylene-diamine gives pink colour	Sodium nitrite	5	Test negative
Methyl Alcohol	Oxidise with $KMnO_4$ decolourise with sodium bisulphite and develop colour with chromotropic acid in cone H_2SO4	Methyl	5	Test negative

NEUTRALISATION OF BASIC PRODUCTS IN THE LEACH

Fig. 10.



structure of the resin, i.e. $R - CH_2 - N(CH_3)_3$. A spot test to determine the presence of tertiary amines in a mixture of amines was not developed. Secondary and primary amines, peroxides and nitrites were tested for as shown in Table 7.

(iv) Decomposition of the Resin

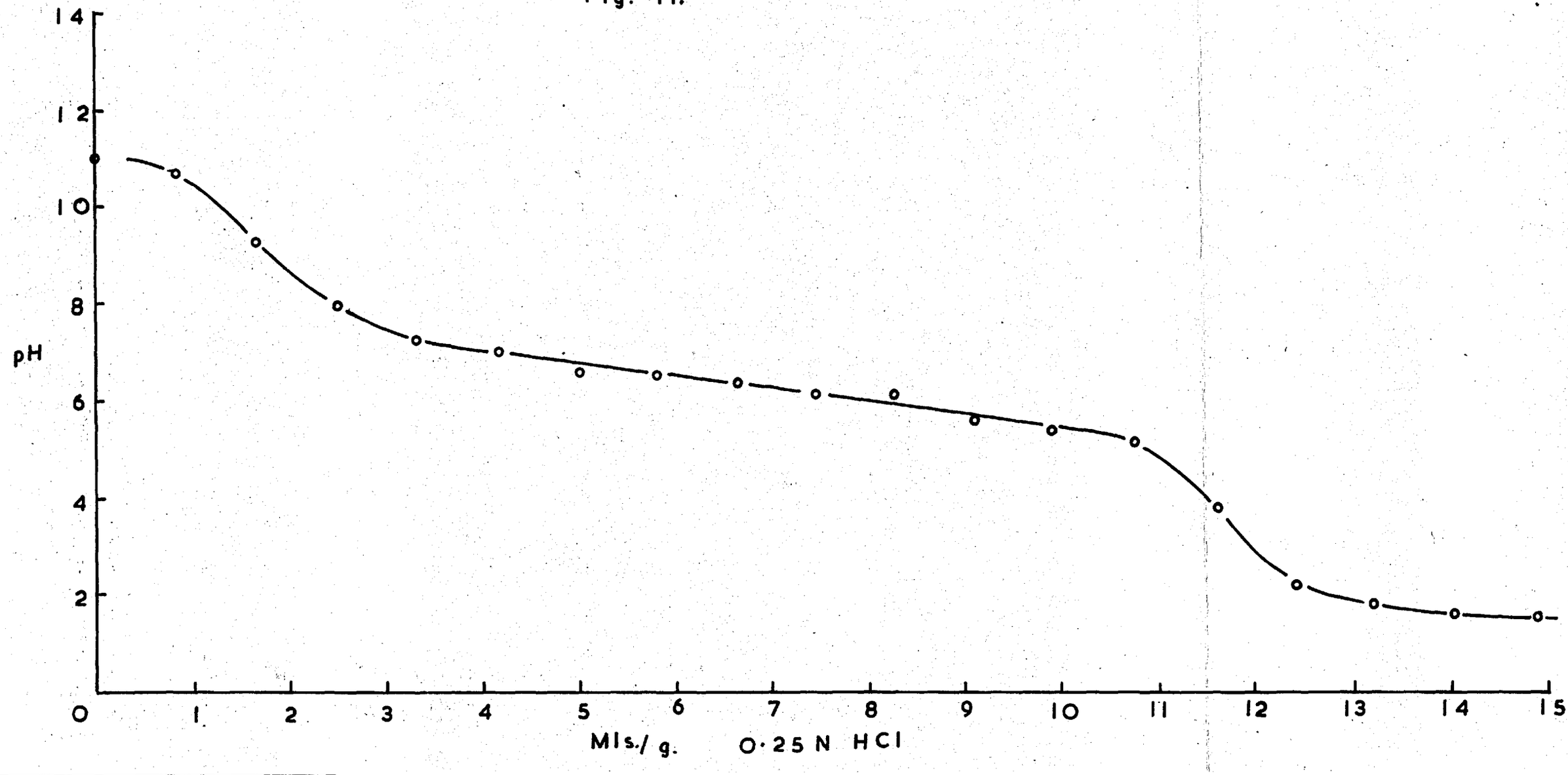
The nature of the pH titration curves of the irradiated resin (Fig. 8) indicated that there was no change in strong base properties. The formation of weak base groups might be expected to produce a change in the pattern of the titration curve.

A resin sample containing both quaternary and tertiary methyl amino groups (Deacidite H), prepared in the hydroxide form gave neutralisation curves as shown in Fig. 11 when titrated under the identical conditions to Deacidite FF resin. Two distinct end-points are observed, corresponding to the strong and weak base end-points. Further, it is found that in the presence of 0.1 N sodium chloride solution the rate of exchange is slow, and the end-points less distinct, (cf. Deacidite FF).

Evidence so far did not indicate the formation of weak base groups.

NEUTRALISATION OF DEACIDITE H RESIN IN THE HYDROXIDE FORM

Fig. 11.



(v) Effect of Carbon Dioxide on the Hydroxide Form of the Resin

Resins in the hydroxide form are known to take up carbon dioxide from the atmosphere, resulting in carbonate ions exchanging with hydroxide on the resin functional groups. This decreases the effective

$$2\left[R - CH_2 - \overset{+}{N}(CH_3)_3\ \overset{-}{OH}\right] + CO_2 \longrightarrow \left[R - CH_2\overset{+}{N}(CH_3)_3\right]_2\ CO_3^{=} + H_2O$$

hydroxide capacity of samples, and may result in appreciable error. The extent to which carbon dioxide reacts with air-dried speciments, has been studied.

Procedure

Samples of moist hydroxide resin were allowed to dry in contact with the atmosphere for one week, and the capacity measurements were compared with those from blank samples, retained under water in stoppered test tubes to prevent diffusion of carbon dioxide.

A 4% solution of sodium sulphate was passed through a resin bed, and collected in a 100 ml. measuring flask. Sodium sulphate replaces carbonate, chloride and hydroxide ions from the functional

groups.

An aliquot of the leach solution is titrated against standard acid using methyl orange indicator. The end-point indicates neutralisation of the total base, i.e. carbonate and hydroxide. A further aliquot is taken and titrated against standard acid using phenolphthalein indicator. The end-point indicates neutralisation of hydroxide only. A final aliquot titrated against silver nitrate gives the total chloride ions released. Hydroxide, Carbonate and Chloride capacity can therefore be calculated separately. The resin is washed, dried and weighed in the sulphate form.

Results and Discussion

Ionic Form	Resin in contact with CO_2		Blank	
	m.equ/g	% W/W	m.equ/g	% W/W
Hydroxide	1.84	42.8	2.10	48.4
Chloride	2.10	49.0	2.17	49.8
Carbonate	0.35	8.2	0.08	1.8
Total	4.29	100.0	4.35	100.0

The results above show that carbon dioxide can account

for up to 8 - 10% loss in hydroxide capacity, when resins are exposed to the atmosphere for long periods. By maintaining resin samples in the hydroxide form as water slurries, carbon dioxide adsorption is small and within the limits of experimental error.

C. DISCUSSION

Preliminary investigations have shown that the hydroxide form of the resin is less stable to radiation than the chloride form. This result agrees with the observations of Shigematsu (101) and with the evidence quoted by other workers (99), that the salt form of the resin is more stable than the free base form. Wedemeyer (94), however, on the basis of one result concludes that the hydroxide and chloride forms are equally unstable to radiation.

Decomposition takes place by loss of capacity and the liberation of basic products in the aqueous leach. The concentration of the products obtained by titration can account for up to 80% of the total capacity loss. Aliphatic amines appear to be produced, i.e. tertiary and secondary amines, being the most likely.

The resin does not appear to lose strength on

irradiation, because the pH neutralisation curves do not indicate that weakly basic groups are being formed. The degradation reactions may be explained by (1) a functional group being severed from the polymer skeleton resulting in (2) the production of tertiary amine as a main product, and secondary amine by further reaction.

e.g. $R - CH_2 - N(CH_3)_3 OH \longrightarrow R - CH_2OH + N(CH_3)_3$

$$N(CH_3)_3 + \tfrac{1}{2}O_2 \longrightarrow NH(CH_3)_2 + CH_2O$$

The C - N bond between the polymer skeleton and the functional group breaks on irradiation.

The adsorption of carbon dioxide on the functional groups from the atmosphere can account for a change in the hydroxide capacity of up to 10% under the worst conditions of exposure. Further resin samples will be irradiated in aqueous solution for the following reasons:

(i) to minimise carbon dioxide adsorption,

(ii) so that water-soluble aliphatic amines may dissolve and be trapped in the leach,

(iii) aqueous slurries represent more closely industrial process conditions.

SECTION 15

IRRADIATION OF THE HYDROXIDE FORM IN AQUEOUS SOLUTION

A. INTRODUCTION

B. EXPERIMENTAL

C. RESULTS

D. DISCUSSION

A. INTRODUCTION

The instability of the hydroxide form of the resin, and a qualitative estimation of the degradation products have been described in the preceding section. A systematic study is necessary to give a quantitative analysis of the nature of decomposition of the resin and the total degradation products.

Measurements so far have not clearly established a change from strong base to weak base capacity, i.e. a loss of a methyl group from the quaternary ammonium functional group, or a change in total capacity. The proportion of strong and weak base groups must be obtained by analysis to establish the mechanism of the decomposition.

Rather more elaborate procedures are required to relate the total nitrogenous products liberated on irradiation, with the resultant loss in capacity. Quantitative analysis of tertiary, secondary, primary amines and ammonia, in the presence of each other must be developed.

A systematic irradiation of resin samples in the hydroxide form has been performed at total doses of up to 500 Mr, with a fixed dose rate of 0.61 Mr/hr.

B. EXPERIMENTAL

(i) Measurement of Capacity

pH Titration Curves

It has been shown that a resin sample containing up to 90% weak base groups (Deacidite H) gives a characteristic titration curve (Fig. 11) containing two distinct end-points. Both strong base and weak base capacity may be calculated independently from such a graph.

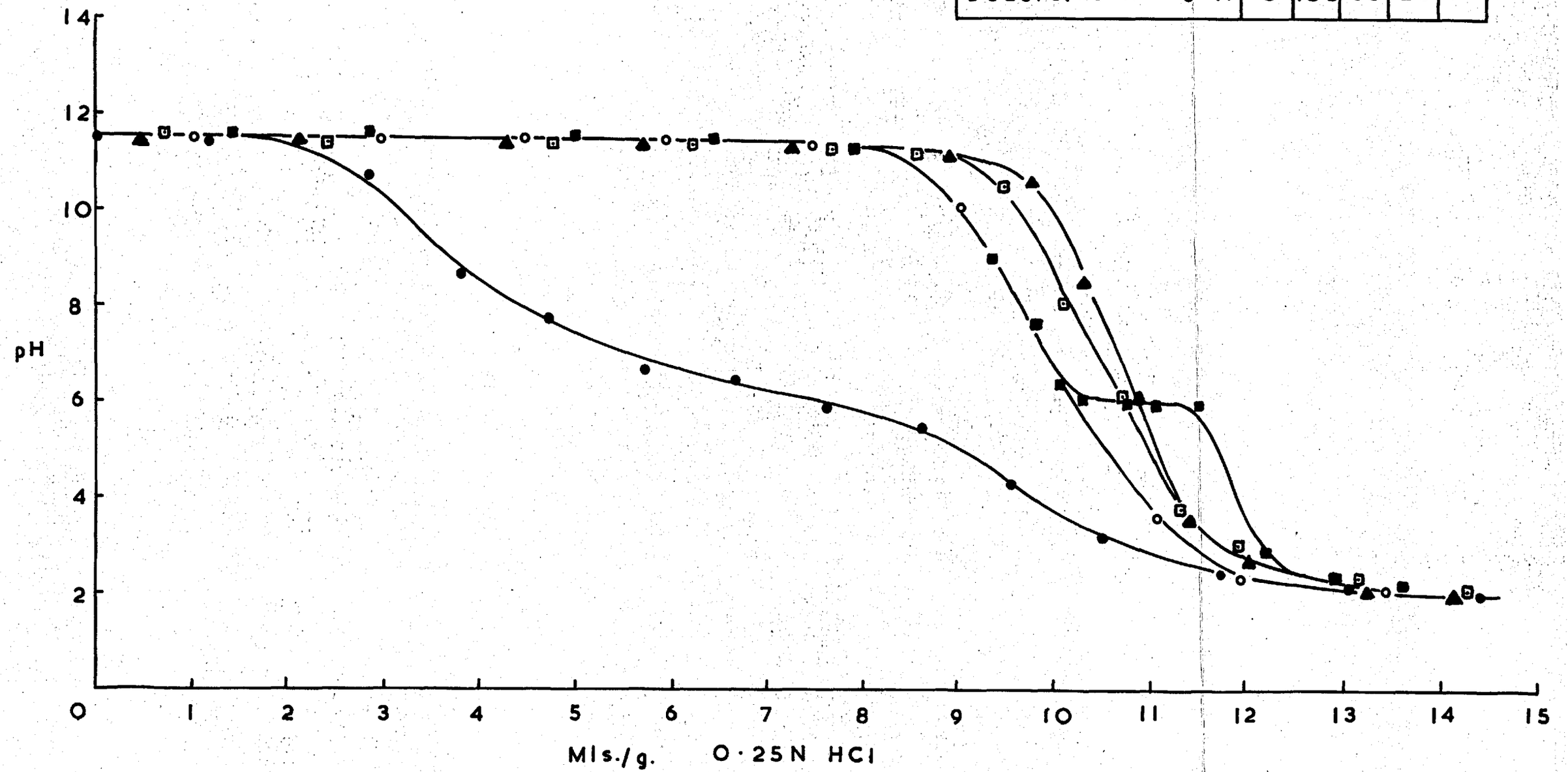
The sensitivity of this procedure to detect small changes from strong base to weak base was examined by mixing known volumes of Deacidite H and Deacidite FF in the hydroxide form. Samples were prepared, so that the weak base capacity increased from zero to 100% (represented by Deacidite H resin). The prepared samples (1 - 2 g) were mixed intimately, without exposing them to the atmosphere, and titrated against 0.25 N hydrochloric acid, after addition of 20ml. 0.1 N sodium chloride solution.

The resulting pH neutralisation curves are shown in Fig. 12. Strong base Deacidite FF resin reproduces the characteristic neutralisation curve seen in Fig. 6. The end-point is distinct at pH = 7. Neutralisation of Deacidite H resin alone gives two clear end-points at pH = 9 and pH = 3.5

NEUTRALISATION CURVES OF RESIN SAMPLES CONTAINING TERTIARY AND QUATERNARY GROUPS

Fig. 12.

	○	●	■	⊡	▲
Deacidite FF % v/v	100	0	70	80	90
Deacidite H % v/v	0	100	30	20	10



A break in the titration curve at pH = 6 is observed when the ratio of strong base to weak base resin is 2:1. As the proportion of strong base increases, however, the break in the titration curve can no longer be seen, and a smooth curve is obtained.

The pH titration method cannot be applied to distinguish between strong and weak base capacity, unless the proportion of weak base groups represents 30% or more of the total capacity.

Modified Capacity Measurement

A method of measuring both total capacity, i.e. sum of weak and strong base capacity, and quaternary capacity, i.e. strong base capacity, has been described by Fisher and Kunin (117). In their method the exchange capacity is measured with respect to the chloride ion.

Resin samples are converted completely to the chloride form by passing excess hydrochloric acid, and washed free of chloride ions using alcohol. This avoids hydrolysis of the weak base groups. Leaching with dilute ammonia solution hydrolyses the weak base groups, the strong base groups remaining unaffected.

$$R - CH_2 - N(CH_3)_2 : HCl + NH_4OH \longrightarrow R - CH_2 - N(CH_3)_2 + NH_4Cl + H_2O$$

Capacity of the weak base groups is obtained by measuring the concentration of chloride released.

Further leaching with sodium sulphate solution, replaces the chloride ions attached to the strong base quaternary groups.

$$2\left[R - CH_2 - \overset{+}{N}(CH_3)_3\ \overset{-}{Cl}\right] + Na_2SO_4$$

$$\left[R - CH_2 - \overset{+}{N}(CH_3)_3\right]_2\ SO_4^{=} + 2\ NaCl$$

Strong base capacity may be obtained by measuring the chloride ions released on sulphate leaching. The total anion exchange capacity is the sum of strong base and weak base capacity.

The titration of chloride ions in the leach solutions was performed by Volhard's procedure. The Mohr titration, using potassium chromate indicator, could not be applied in alkaline solutions, because of the precipitation of silver hydroxide masking the silver chromate end-point. The Mohr method is only applicable in solutions within the pH range 6.5 - 9.

Procedure

The resin sample is transferred to a small column containing a sintered glass disc, and thoroughly washed with distilled water. A 4%

solution of sodium chloride (50 ml.) is passed through the resin bed, and collected in a 50 ml. volumetric flask. This solution contains the hydroxide ions released, and may be titrated against decinormal hydrochloric acid, using methyl orange indicator, to give the hydroxide capacity.

Excess 4% hydrochloric acid (50 ml.) is then passed slowly through the resin bed (i.e. 2 mls/min) to convert the resin sample completely to the chloride form. Excess chloride is washed from the resin bed, i.e. until the leach is negative to the silver nitrate test, using pure methanol.

0.15 molar ammonium hydroxide (50 ml.) is passed slowly through the bed and the leach is collected in a 50 ml. volumetric flask, until no further chloride is released. A further 50 ml. of 4% sodium sulphate is passed through the bed and the leach collected in a separate volumetric flask.

Estimation of Chloride in the Leach by the Volhard Method

A 10 ml. aliquot is taken from the leach solution, and to this is added 5 ml. of 6 N nitric acid. A further 10 ml. of standard 0.1 N silver nitrate solution is added, to precipitate the chloride, and 1 ml. of ferric indicator solution is added,

i.e. saturated ferric ammonium sulphate (approximately 40%) in water. 2 - 3 ml. of nitrobenzene is added, and shaken to coagulate the precipitate. The excess silver nitrate is back titrated against standard 0.1 N ammonium thiocyanate solution. The end-point is approached dropwise and indicated by the formation of a distinct reddish-brown colouration, which is not removed on further shaking.

Resin specimens are filtered, dried at 100°C for 20 hours and weighed in the sulphate form.

Results and Discussion

Sample No.	Strong base capacity (m.equ/g)	Weak base capacity (m.equ/g)	Total (m.equ/g)
1	4.02	0.21	4.23
2	3.86	0.22	4.08
3	4.22	0.18	4.40
4	4.18	0.19	4.37

A sample capacity determination is shown in Appendix I

The results show that Deacidite FF resin (un-irradiated) contains approximately 5% of weak base groups. The strong base capacity varies from 3.8 - 4.2 m.equ/g, and this may be explained by non-homogeneous quaternisation of the polymer

skeleton on manufacture. Mean values for the total capacity of the resin with respect to chloride ions are

Strong base = 4.00 m.equ/g.

Weak base = 0.20 m.equ/g.

(ii) Quantitative Estimation of Water-Soluble Degradation Products

After irradiation, the resin sample is transferred to a column and thoroughly washed with distilled water, washings being collected in a 50 ml. volumetric flask.

Total volatile base products have been obtained for this solution, and the total amount of free nitrogen estimated by Kjeldahl distillation. The concentrations of individual aliphatic amines are measured, and related to the total nitrogen in the leach.

a) Estimation of Total Nitrogen in the Leach Volatile Amines and Ammonia

A suitable aliquot (usually 1 - 5 ml.) containing 0.01 - 0.05 m.equ. of basic product is transferred to the distillation flask of a semi-micro Kjeldahl distillation apparatus. 1 ml. of concentrated sulphuric acid is carefully added, whilst cooling the flask. The apparatus is assembled,

and 10 ml. 50% sodium hydroxide solution is slowly allowed to enter the digestion flask. The mixture is steam distilled and collected in a flask containing 25 ml. standard 0.1 N hydrochloric acid. This is then back-titrated against standard 0.1 N sodium carbonate solution using methyl red indicator.

The total volatile base is expressed in terms of m.equ/g. dry resin.

Total Nitrogen by Kjeldahl Digestion

The aqueous leach solution may contain high molecular weight aromatic amines, produced by breakdown of the cross-linked polystyrene skeleton. Such amines may not be steam volatile, and it is necessary to digest with concentrated sulphuric acid in the presence of a catalyst to liberate volatile ammonia for analysis.

An aliquot containing 0.01 - 0.05 m.equ. basic product is transferred to a Kjeldahl digestion flask, and 1 ml. concentrated sulphuric acid added. Approximately 10 mg. of selenium is added as a catalyst and the solution is heated and allowed to digest for 20 minutes. On cooling the concentrate is diluted with about 5 - 10 ml. of distilled water, and connected to the Kjeldahl distillation apparatus Approximately 20 mls. of 50% sodium hydroxide is

added to the distillation flask, and the contents steam distilled into 25 ml. standard 0.1 N hydrochloric acid. This is back-titrated with 0.1 N sodium carbonate solution using methyl red indicator.

The total nitrogen in the leach is calculated as in the specimen calculation in Appendix I.

b) Quantitative Analysis of Tertiary Amine

Most of the methods available for the determination of tertiary aliphatic amines in the presence of other amines, depend on the isolation of the tertiary amine after reaction of the primary and secondary amine components with nitrous acid, and subsequent titration of the unreacted tertiary base (118, 119). Other methods which include gravimetric analysis (120), and acetylation of a mixture of amines followed by titration against perchloric acid (121), have been found insensitive when applied to millimolar concentrations.

The method selected here for the determination of tertiary amine is based on the method of Dyer (122), who modified the picrate method used by Richter, Lee and Hill (123). Dyer's method, developed for the estimation of trimethylamine produced in the deterioration of fish, is based on measurement of the yellow colour of amine-picrates,

e.g. with trimethylamine, dimethylamine, methylamine and other compounds such as indole and histamine.

Irradiated leach solutions have been shown by the spot tests to contain practically no primary amine, but measurable amounts of secondary amine.

The contribution of secondary and primary amine, to the measured concentration of tertiary amine was examined at the peak absorbance at 410 mμ. The independent concentration of secondary and primary amines can be obtained by specific analysis (pages 113 - 118) and the actual concentration of tertiary amine by subtraction.

Procedure

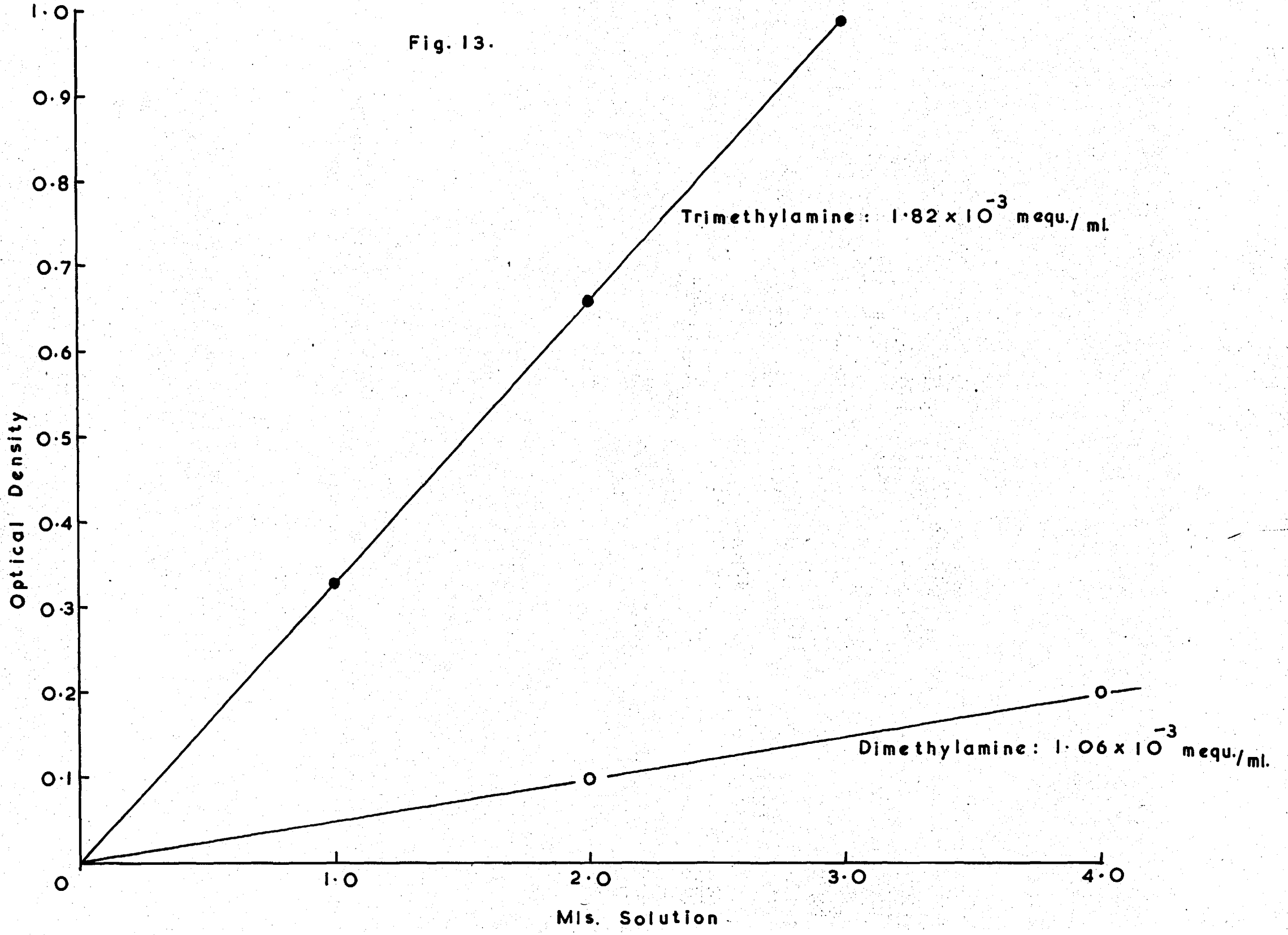
Dilute an aliquot sample (containing 0.002 - 0.005 m.equ. tertiary amine) to 4 ml. Shake commercial 37% formaldehyde solution with $MgCO_3$, filter and dilute with three volumes of water. Add 1 ml. of this solution to the amine solution, followed by 10 ml. toluene (A.R. grade) and 3 ml. 50% potassium carbonate solution. Stopper and shake vigorously 30 - 40 times to transfer the amines to the toluene layer. Shake a 5 ml. aliquot of the solvent layer with 0.3 - 0.4 g of anhydrous sodium sulphate and decant into 5 ml. of 0.02% picric acid in dry toluene. The yellow

TABLE 8 - SENSITIVITY OF THE PICRATE METHOD FOR TERTIARY AMINES

	Trimethylamine 1.82×10^{-3} m.equ/ml.	Dimethylamine 1.06×10^{-3} m.equ/ml.	Methylamine 0.64×10^{-3} m.equ/ml.
Volume of solution (ml)	3	3	4
Concentration (m.equ)	5.46×10^{-3}	3.18×10^{-3}	2.56×10^{-3}
Measured Optical Density	1.0	0.15	0.025
Calculated Optical Density of solutions of 5.46×10^{-3} m.equ concentration	1.0	0.26	0.053

CALIBRATION CURVE FOR AMINE PICRATE COMPLEX IN TOLUENE (410mμ)

Fig. 13.



amine-picrate colour is produced and the optical density of this solution at 410 mμ is measured against a reagent blank in a Unicam SP 500 spectrophotometer. The colour is stable for up to one month, if free from ammonia.

A calibration curve (Fig. 13) has been obtained for this method, and found to be reproducible within 2%. Standard millimolar solutions of trimethylamine and dimethylamine were prepared by titration against standard acid using methyl red indicator. All titratable nitrogen was assumed to be amines. The values agreed with Kjeldahl estimations. Results show that the calibration curve obeys Beer's Law and that the method is sensitive to solutions of millimolar concentration of tertiary amine. The sensitivity of the method to secondary and primary amines, in relation to tertiary amines has been tested.

Table 8 shows that the sensitivity of the picrate method to tertiary, secondary and primary amine is in the ratio 20:4:1. It is necessary to determine the concentrations of primary and secondary amines individually, in order to correct for the contribution to the overall optical density at 410 mμ of their picrates. In most cases the contribution of primary amine is small enough to be neglected. A specimen calculation is given in Appendix I.

c) Quantitative Analysis of Secondary Amine

Secondary amines are usually determined by difference (118, 119). Such methods are unsuitable for the estimation of small quantities of secondary amines in the presence of large amounts of other amines. A method has been described, in which the nitrosamine is formed by the action of nitrous acid. The optical density of the nitrosamine can be accurately measured without initial separation (124). A modification to this procedure (125) was found to give unreliable results in the presence of related bases. A modification of an already known colour reaction (115), involving the interaction of secondary amines with sodium intropruside to give a violet blue compound has been used to estimate secondary amine quantitatively, (126). This method was tested and found to be cumbersome to apply, and difficulty was experienced in obtaining reproducible results.

A rapid and reproducible method has been used in this work, based on the procedure of Stanley, Baun and Gove (127). Secondary amines are reacted with carbon disulphide and ammonia to form the dialkylthiocarbamate, and the colour intensity of the copper complex, extracted into an organic

phase (benzene), is measured.

The reaction is:

$$(CH_3)_2NH + CS_2 + NH_3 \longrightarrow (CH_3)_2N.\ \underset{\underset{S}{\|}}{CSNH_4}$$

$$2(CH_3)_2\ N.\ \underset{\underset{S}{\|}}{CSNH_4} + Cu^{++} \longrightarrow \left[(CH_3)_2\ N\underset{\underset{S}{\|}}{CS}\right]_2 Cu + 2NH_4^{+}$$

The stability of the yellow colour developed is increased by complete removal of ammonia from the benzene layer. Trimethylamine does not react and therefore does not interfere in the estimation. Methylamine gives a similar colour reaction, which decreases as the alkalinity of the aqueous phase is increased. The interference of monomethylamine is negligible when present in low concentrations, i.e. equal or less than the concentration of dimethylamine. This is due to

i) the relative insolubility of the cupric monomethyldithiocarbamate,.

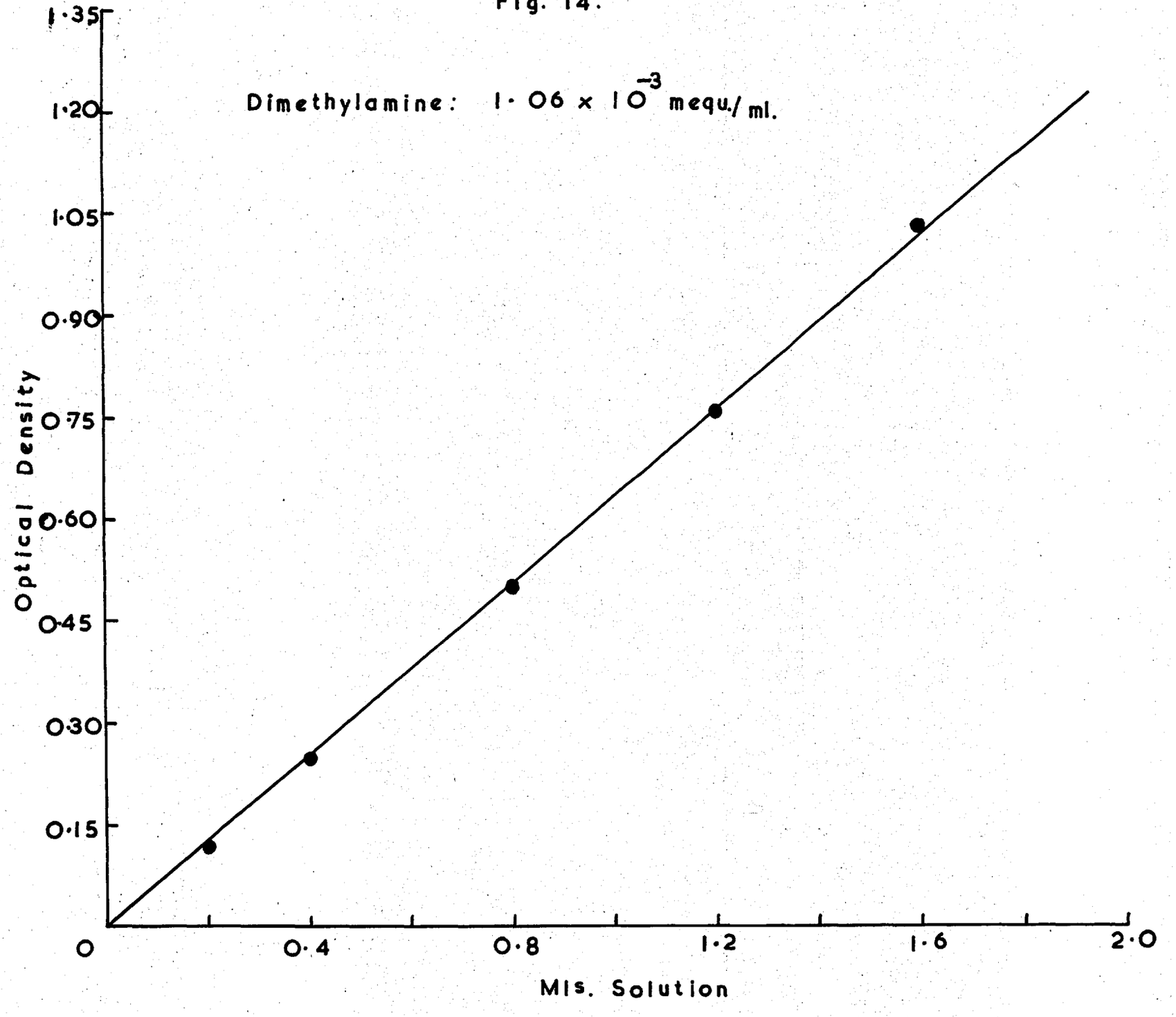
ii) the absorption peak of this complex is in the region of 360 mμ .

Cupric dimethyldithiocarbamate has a peak absorbance at 434 mμ .

Ammonia and methanol in concentrations equal to dimethylamine also do not interfere.

CALIBRATION CURVE FOR SECONDARY AMINE BY COPPER DITHIOCARBAMATE COMPLEX (434 mμ)

Fig. 14.



Procedure

Prepare a reagent solution by dissolving 20 g. ammonium acetate and 0.2 g. copper sulphate in 30 ml. of water. Add 10 g. sodium hydroxide in 25 ml. water, and 20 mls. of concentrated ammonia, and dilute to 100 ml. with water.

To 10 ml. of sample solution (containing 0.0006 - 0.015 mg. of dimethylamine/ml.) add 1 ml. of reagent solution and 10 ml. of 5% carbon disulphide in benzene. Warm to 43 - 48°C for 3 minutes, stopper and shake vigorously for 30 seconds. Add 1 ml. of 30% acetic acid and shake again for 30 seconds. Cool and centrifuge to separate the solvent layer. Measure the absorbance at 434 mμ, within an hour, against a reagent blank. The calibration curve, using dimethylamine as standard, obeys Beer's Law over the range studied (Fig. 14). The method is sensitive to solutions of millimolar concentration and reproducible within 2%.

A specimen calculation to obtain concentrations of dimethylamine is given in Appendix I.

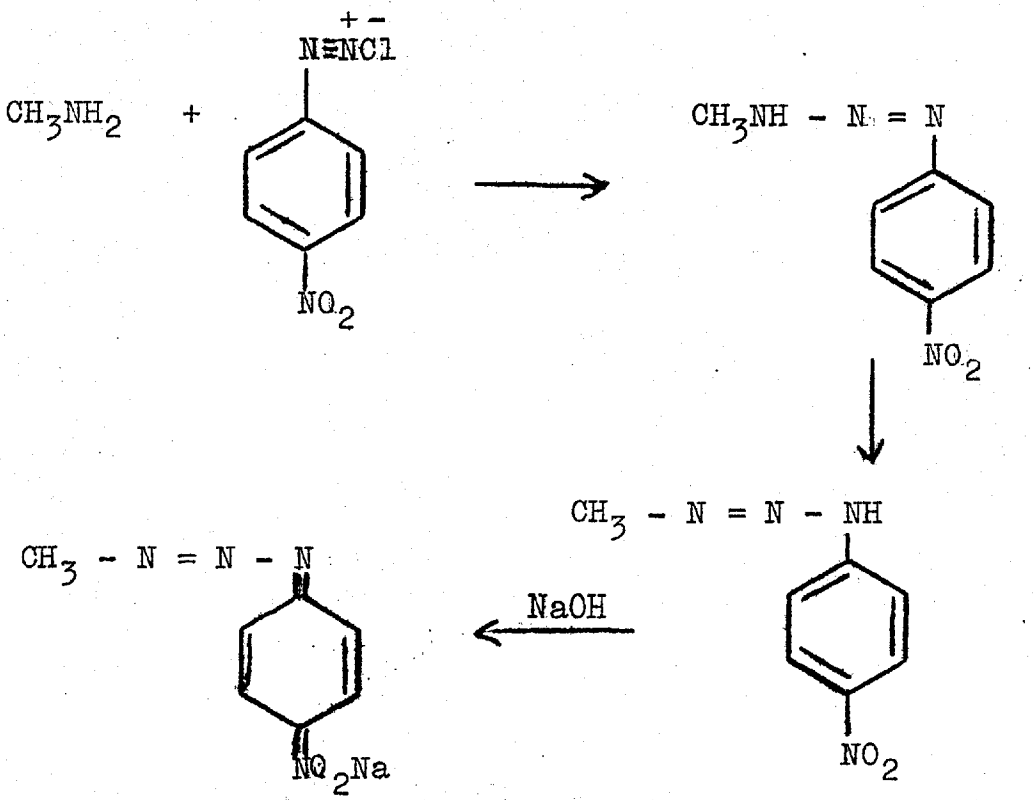
d) Quantitative Analysis of Primary Amine

Primary amines have been determined colorimetrically with an aqueous reagent containing cupric chloride, salicylaldehyde and triethanolamine

(128). This method is however not applicable in the presence of ammonia. A further method, in which the intensity of the colour due to the Schiff base resulting from the reaction of primary amine with salicylaldehyde is measured at 410 mμ (129), has been tested and found insensitive in solutions of 10^{-3} molar concentration.

The diazonium salt formed when p-nitroaniline reacts with acidified sodium nitrite will couple with primary aliphatic amines (130). The colour intensity of the product may be used to estimate the concentration of primary amine present.

The reaction taking place has been suggested by Persez and Poirier (130) as



They also found that secondary amines did not interfere at all concentrations, but formed an insoluble yellow precipitate. Waddington (114) has also shown that tertiary and secondary amines do not interfere and ammonia at concentrations up to and equal to the concentration of primary amine also does not interfere.

Procedure

Dissolve 0.5 g of p-nitroaniline in 100 ml. 1N hydrochloric acid, and cool to 0°C. Add a further 10 ml. of 3% sodium nitrite also cooled in ice. Store this solution in a dark place for 30 minutes before required and use within three hours of preparation.

Prepare a buffer solution by dissolving 4.08 g of potassium dihydrogen phosphate, 1.6 g borax in 80 ml. water, and adding 13 ml. of 10% sodium hydroxide, and making up to 100 ml.

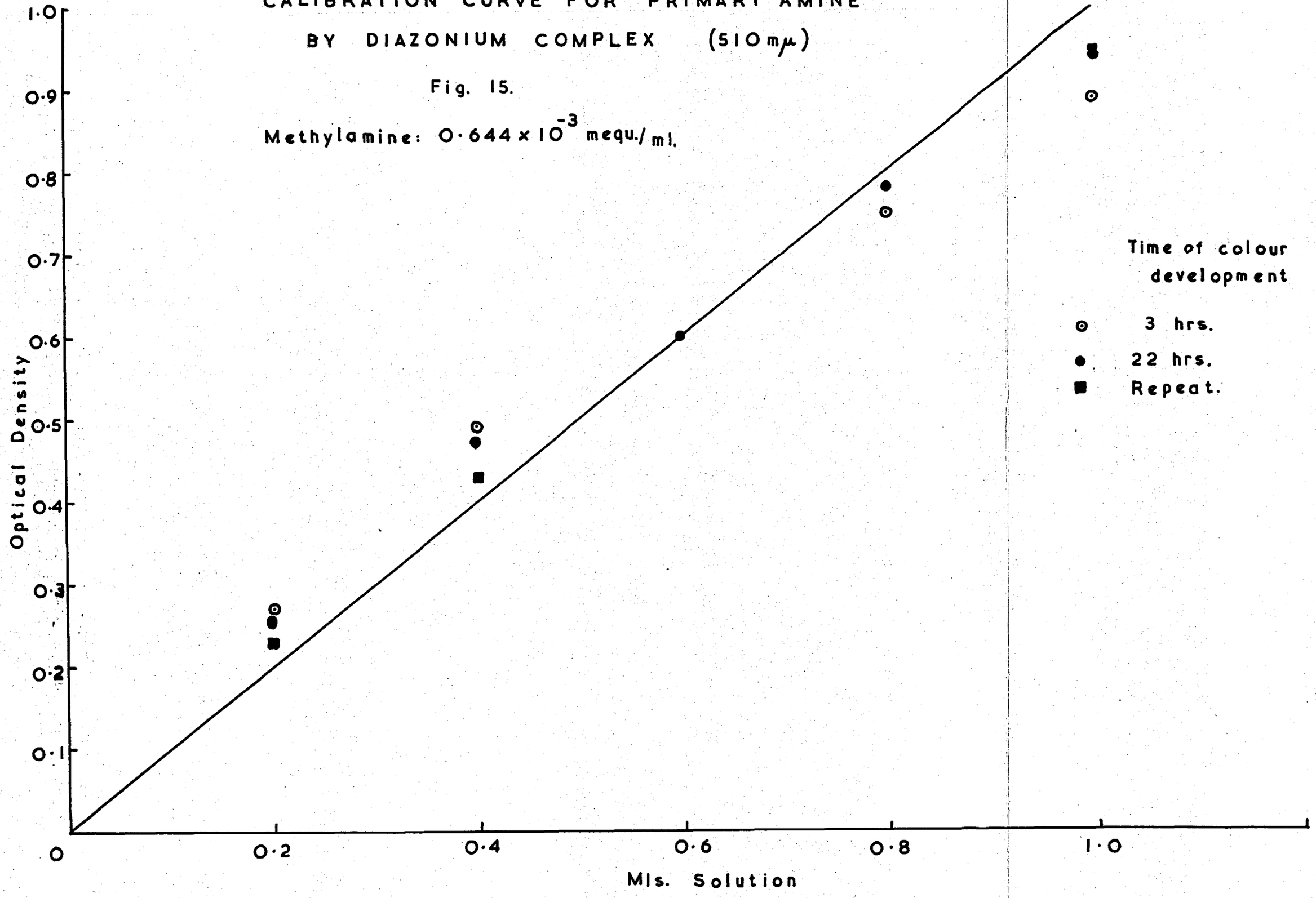
To 1 ml. of neutral or slightly acidic amine solution (containing 0.0002 - 0.0006 m.equ), is added 10 ml. of buffer solution. Shake and cool in ice for 10 minutes, before adding 1 ml. of reagent solution. After a further 20 minutes, 2 ml. of 10% sodium hydroxide, previously cooled in ice, is added dropwise.

The red colour develops slowly and the optical

CALIBRATION CURVE FOR PRIMARY AMINE
BY DIAZONIUM COMPLEX (510 mμ)

Fig. 15.

Methylamine: $0 \cdot 644 \times 10^{-3}$ mequ./ml.



density at 510 mμ is measured against a reagent blank after a period of 22 - 24 hours.

The calibration curve shows variation of optical density with concentration. There is some spread of the calibration values around the straight line, but the method is considered reproducible to approximately ± 10% providing spectrophotometric readings are taken 22 hours after colour development.

e) Quantative Analysis of Ammonia

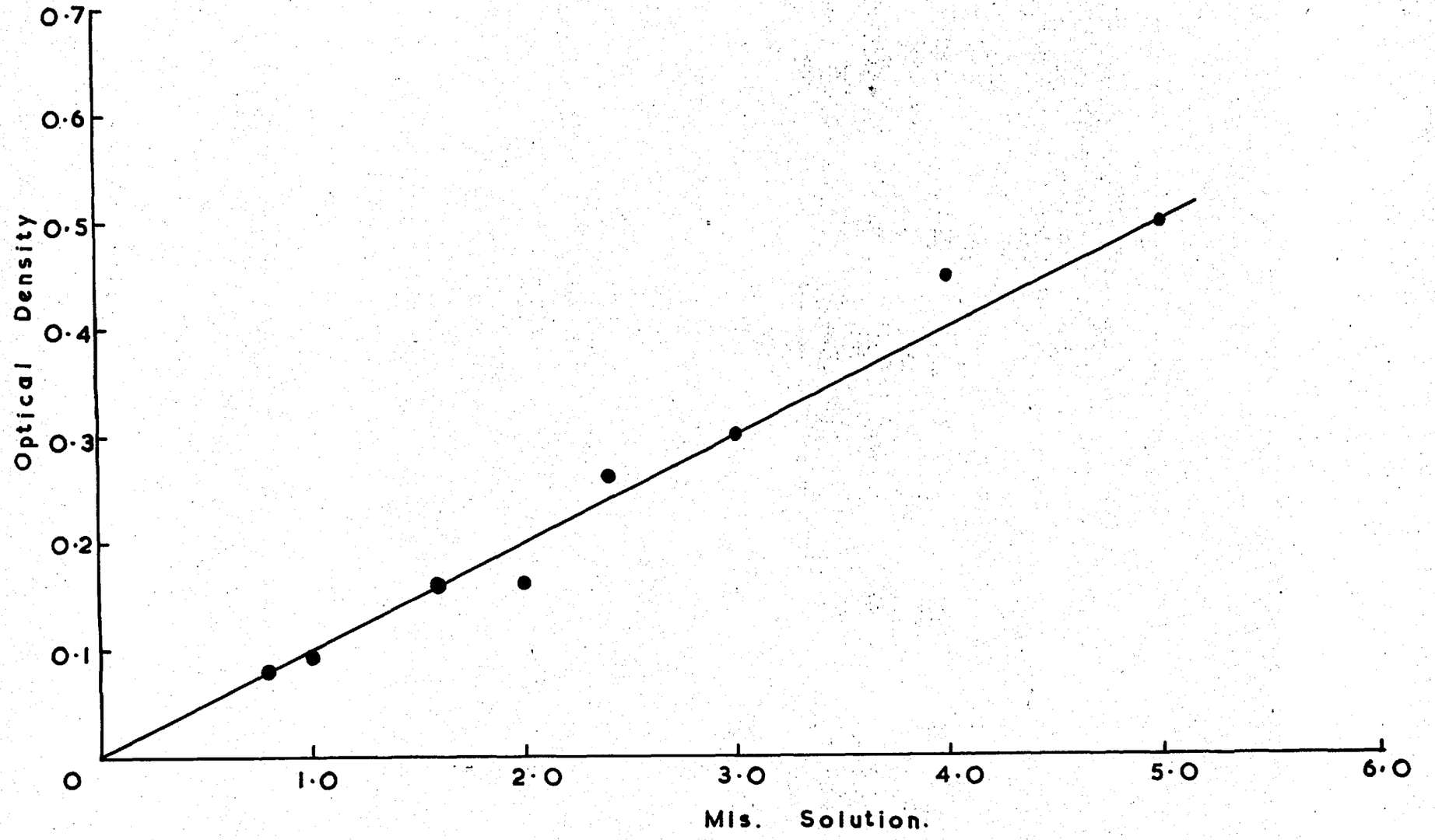
The estimation of small quantities of ammonia in the presence of aliphatic amines is difficult. Nessler's reagent, may be used to determine ammonia at low concentrations (131), but it has been found in this work that interference of secondary amines renders the solutions cloudy and makes the method inapplicable. It has also been suggested that certain brands of yellow mercuric oxide will absorb traces of ammonia, in the presence of related bases (132). The ammonia may be regenerated by dissolving the complex in potassium iodide. Attempts to use this method showed that commercially available brands of mercuric oxide did not absorb ammonia preferentially to other amines present.

Colorimetric determination with phenol-sodium hypochlorite reagent may be used to estimate ammonia

CALIBRATION CURVE FOR AMMONIA ANALYSIS

BY INDOPHENOL METHOD (625 mμ) Fig. 16.

Ammonium Chloride Solution: 10^{-3} m equ./ ml.



in the presence of tertiary and secondary amines, but primary amines in large amounts interfere (133). Bolleter, Bushman and Tidwell (134) have recently modified this method by using freshly prepared chlorine water in place of sodium hypochlorite. Using the procedure described below it has been found that primary amine interference is negligible, i.e. primary amines being 32 times less sensitive than ammonia:-

0.161 m.equ. methylamine gives an optical density = 0.50

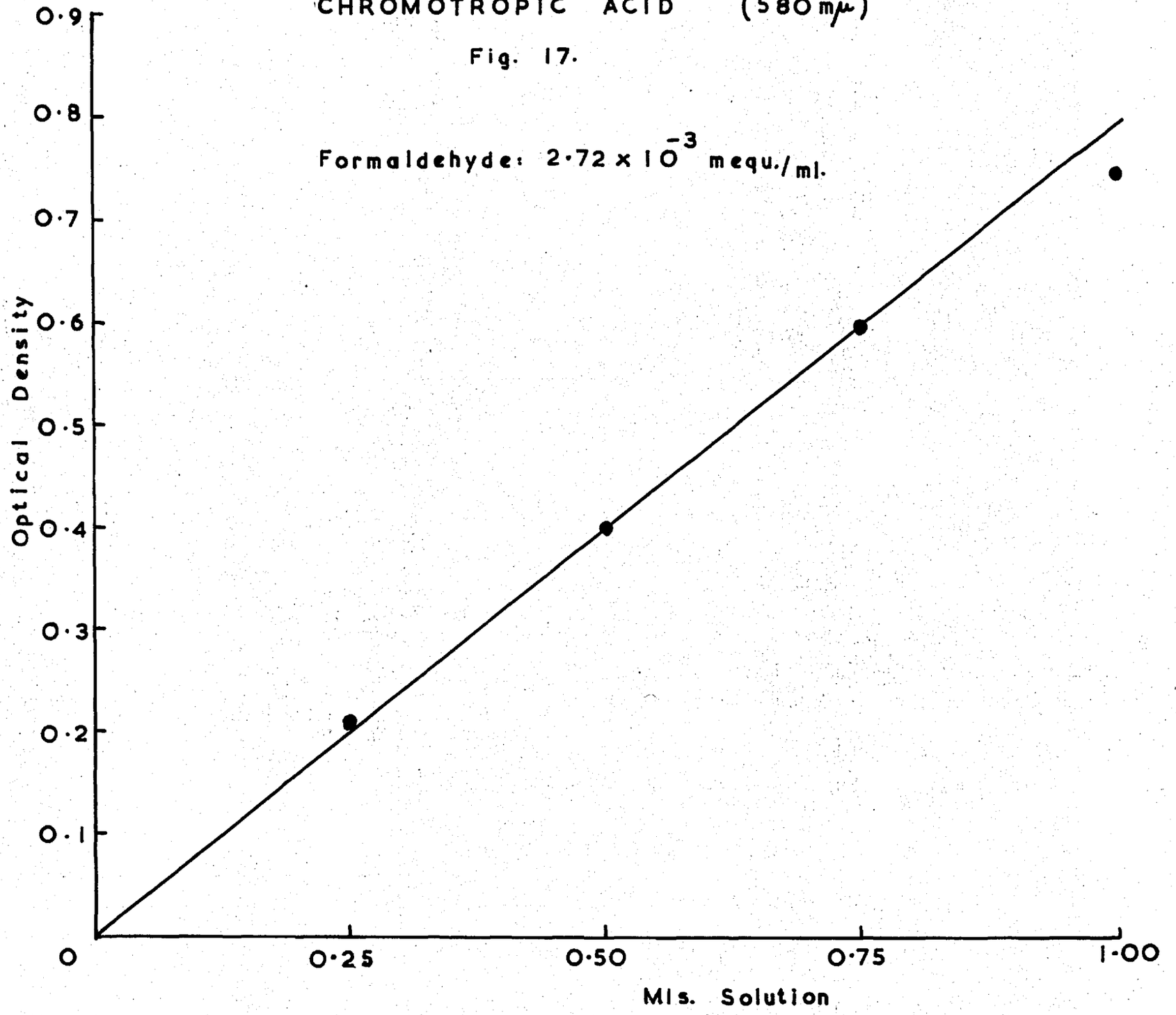
0.005 m.equ. ammonia gives an optical density = 0.50

Procedure

Add to a 50 ml. volumetric flask, 25 ml. of saturated boric acid solution containing from 10 - 300 µg ammonia. Whilst swirling the flask to ensure good mixing add in order, 5 ml. saturated chlorine water (freshly prepared), and 5 ml. of .8% phenol solution. Heat on a steam bath for 3 minutes, remove and cool in iced water. Add 5 ml. of 3M sodium hydroxide and dilute to volume. Read the absorbance of the blue colour at 625 mµ against a reagent blank. A calibration curve has been obtained using 10^{-3} molar Analar ammonium chloride (Fig. 16). This method is rapid to apply and reproducible to within 5%.

FORMALDEHYDE ANALYSIS USING CHROMOTROPIC ACID (580 mμ)

Fig. 17.



f) Quantitative Analysis for Formaldehyde

A colorimetric method for the estimation of formaldehyde in the presence of other aldehydes involving the use of Schiff's reagent in strong sulphuric acid (135, 136) has the disadvantage that it is not accurate within 5% and the reagent is unstable. Eegriwe (137) has proposed the use of chromotropic acid (1:8 - dihydroxynaphthalene 3:6 - disulphonic acid) as a specific reagent in spot tests for detection of formaldehyde. This reaction has been developed as a quantitative method (138, 139) and used here.

Procedure

To 1 ml. of sample containing 20 - 80 µg formaldehyde in a 50 ml. volumetric flask is added 50 mg. solid chromotropic acid. A further 5 ml. concentrated sulphuric acid is added, and the mixture heated in a water bath for one hour. The solution is cooled and made up to 50ml. with distilled water. The violet colour develops quickly, and is measured against a reagent blank at 580 mµ. The colour is stable for 24 hours.

A calibration curve has been obtained (Fig. 17) using 10^{-3} molar Analar formaldehyde solution. The reproducibility of this procedure is found to be within 2 - 3% over the range 0 - 0.002 m.equ/ml.

C. RESULTS AND OBSERVATIONS

The results of a systematic irradiation of resin samples in the hydroxide form up to 500 Mr are tabulated in Table 9 and presented in Figs. 18 and 19.

(i) Loss in Strong Base Capacity

Irradiation produces a marked loss in the strong base capacity. Table 9 shows that the strong base capacity falls 78% between 0 - 500 Mr. This value may be compared with corresponding values obtained with the resin in other salt forms. Table 10 compares the strong base capacity loss measured in the hydroxide and chloride form, with strong base capacity loss in the nitrate form observed by Natarajan (140). This shows that the hydroxide form is less stable to radiation than the chloride and nitrate forms, the effect being most marked up to 100 Mr. Chloride and nitrate appear to be equally stable to irradiation, but the hydroxide form decomposes rapidly up to 100 Mr then less rapidly up to 500 Mr. This may be explained by the fact that the hydroxide resin was not completely regenerated (i.e. 60% hydroxide form and 40% chloride form initially), and decomposition is only rapid whilst hydroxide is being destroyed,

TABLE 9

IRRADIATIONS IN THE HYDROXIDE FORM

No.	Dose (Mr)	Capacity (m.equ/g)				Basic Products in the Leach (m.equ/g)						Formal-dehyde (mequ/g)	Chloride in leach (mequ/g)
		Hyd-roxide	Weak Base	Strong Base	Total	Ter-tiary	Second-ary	Prim-ary	Ammonia	Total	Total Nitrogen (Volatile)		
1	4.93	2.09	0.22	3.75	3.97	0.07	0.01	0.01	-	0.09	-	-	-
2	8.45	1.78	0.23	3.72	3.95	0.11	0.02	0.01	-	0.14	0.14	-	-
3	18.50	1.98	0.32	3.60	3.92	0.21	0.03	0.02	-	0.26	0.27	-	-
4	43.30	1.90	0.34	3.27	3.61	0.44	0.12	0.04	0.01	0.61	0.50	0.01	-
5	88.00	1.27	0.49	2.92	3.41	0.66	0.22	0.05	0.02	0.95	0.91	0.02	-
6	146.00	0.48	0.64	2.65	3.29	0.86	0.31	0.12	0.08	1.37	1.10	0.02	0.22
7	307.00	0.37	0.95	1.65	2.60	0.94	0.43	0.32	0.28	1.97	1.62	0.01	0.80
8	500.00	0.15	1.13	0.87	2.00	1.10	0.41	0.41	0.55	2.47	2.50	0.01	1.35
9	-	2.30	0.20	4.00	4.20	-	-	-	-	-	-	-	-

TABLE 10

PER CENT STRONG BASE CAPACITY LOSS

Dose (Mr)	Chloride	Nitrate (140)	Hydroxide
100	10	11	30
380+	40*	43	67
500	-	54	78

* Result from Table 5

\+ 1 watt.hr.g. radiation absorbed

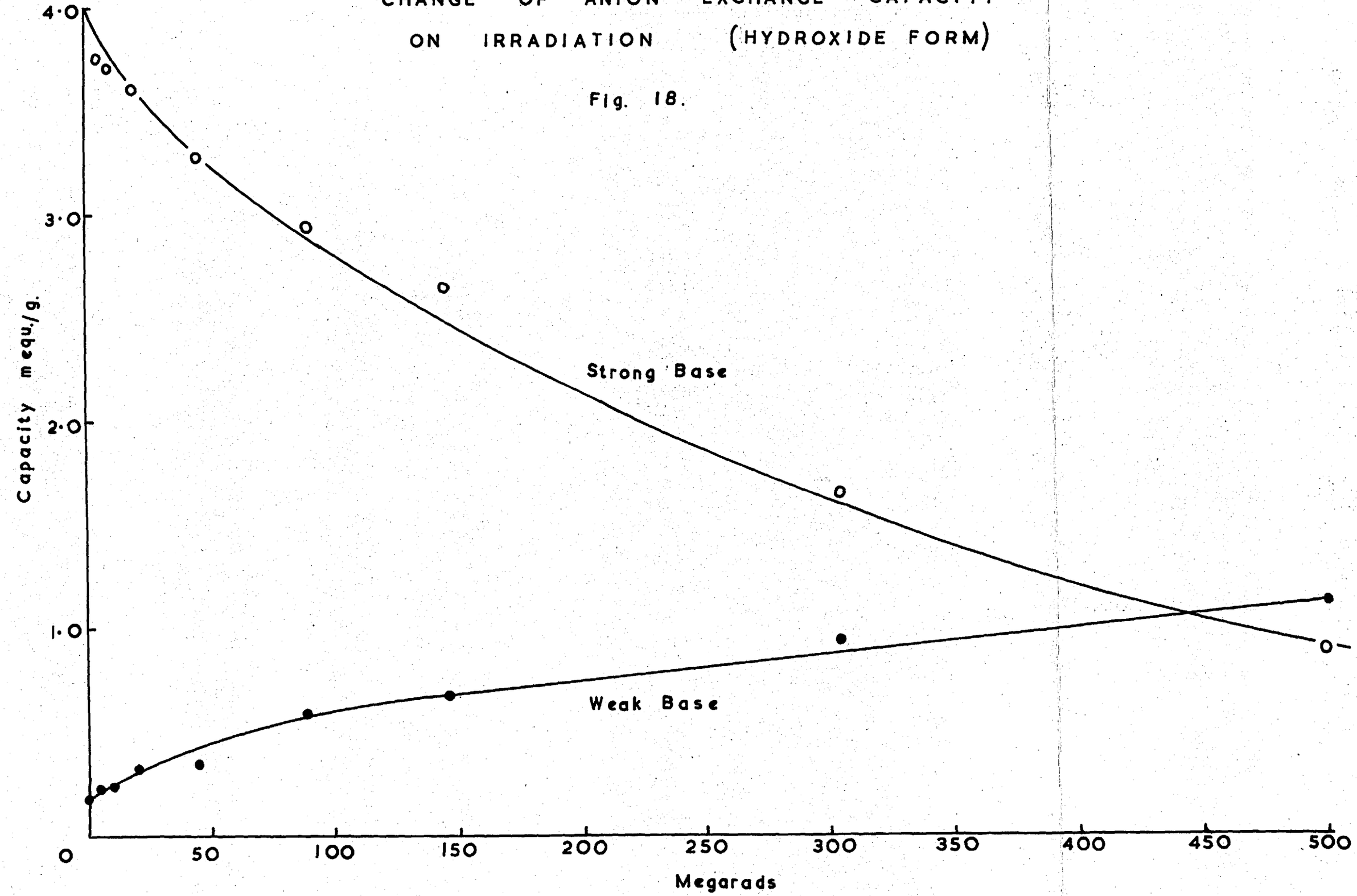
(up to 100 Mr) after which the resin contains predominantly chloride groups, these being more resistant. This ~~would be~~ was borne out by the fact that free chloride was not detected in leach solutions until the total dose received was 146 Mr. At 500 Mr, practically all the hydroxide groups have been destroyed, and further decomposition will remove only chloride groups. It is anticipated that on further irradiation, strong base capacity will continue to decrease as the chloride functional groups are lost.

(ii) Gain in Weak Base Capacity

Fig. 18 shows that there is an appreciable increase in the weak base capacity on irradiation

CHANGE OF ANION EXCHANGE CAPACITY
ON IRRADIATION (HYDROXIDE FORM)

Fig. 18.



corresponding to the loss of methyl groups from the quaternary methyl amino structure. The weak base capacity increases from 0.2 - 0.9 m.equ/g. over the range 0 - 500 Mr. This observation corresponds with a similar result obtained by Fisher (93) who observed a marked difference between the loss in total capacity and the loss of quaternary capacity. The rate of increase of weak base capacity is less than the rate of increase of basic products in the leach and would indicate that the formation of weak base groups is a secondary effect. The primary effect appears to be the loss of functional groups, to produce aliphatic amines and ammonia. It must be noted that after 500 Mr, the exchange capacity of the resin comprises 56% weak base and 44% strong base groups.

(iii) Formation of Basic Products

It has been shown that the loss of total exchange capacity can be accounted for by the formation of basic products in the leach solution. Furthermore, the presence of tertiary, secondary and primary aliphatic amines and ammonia represent practically all of the total nitrogenous products in the leach.

High molecular weight organic amines, which

TABLE 11

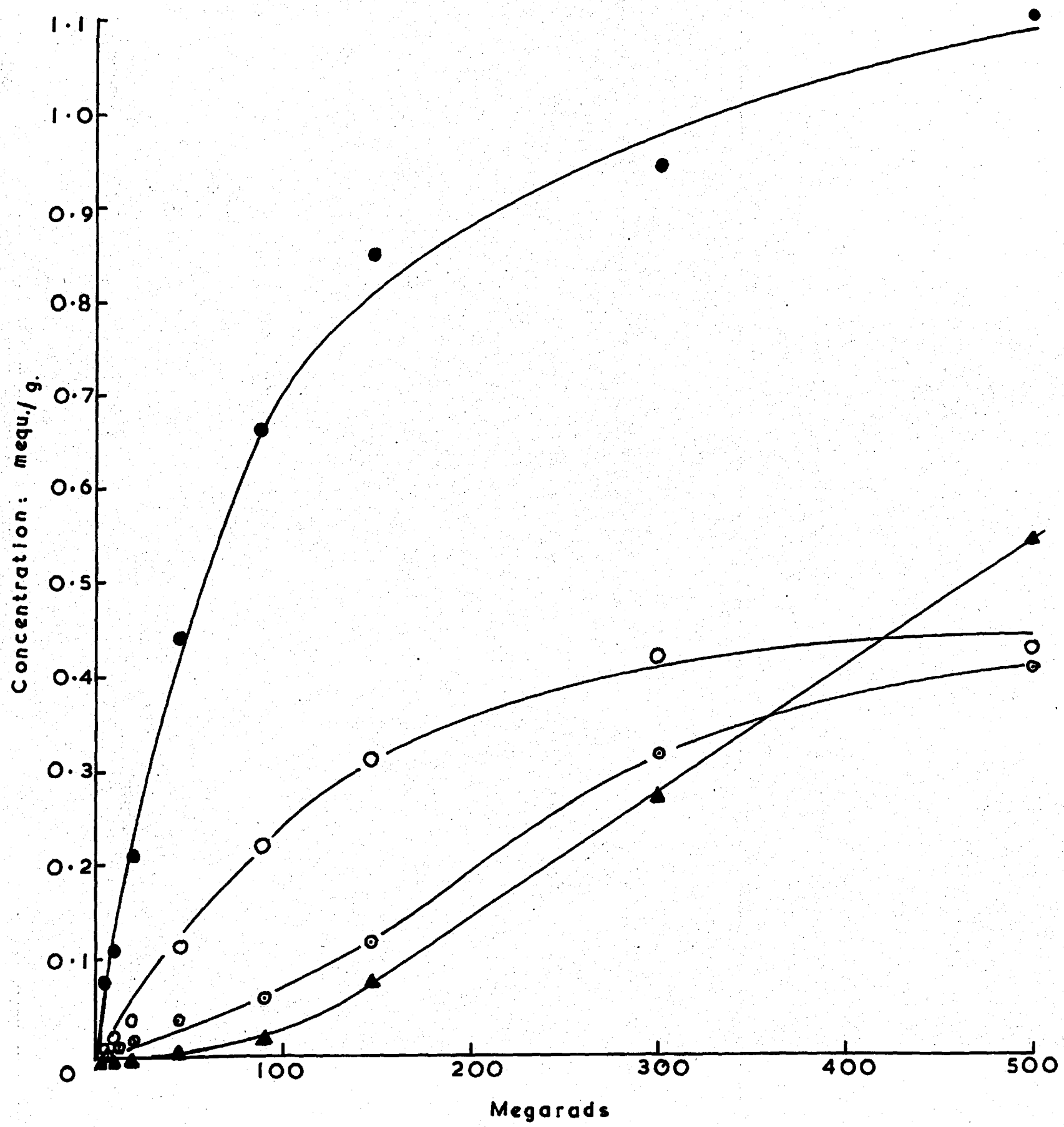
MEASURED G VALUES FOR BASIC PRODUCTS

Dose (Mr)	Tertiary Amine	Secondary Amine	Primary Amine	Ammonia
0	14.23	3.09	0.48	0
50	5.78	2.29	0.77	0
100	2.68	1.73	1.06	0.77
150	1.56	1.16	1.16	1.31
200	1.05	0.77	1.35	1.31
300	0.78	0.39	0.77	1.31
400	0.58	0.19	0.58	1.31
500	0.47	0.09	0.19	1.31

$$G\ \text{Value} = \frac{\text{no. of molecules product formed}}{\text{100 eV. radiation energy absorbed in the system.}}$$

CONCENTRATION OF BASIC PRODUCTS IN THE LEACH

Fig. 19.



could arise by rupture of the polystyrene skeleton, do not appear to be formed, as estimations by the Kjeldahl method agreed, within experimental error, to values obtained by estimating the total volatile base on steam distillation.

Tertiary Amine

The production of tertiary amine is rapid at the beginning of irradiation, as may be seen from G value determinations (Table 11). The initial reaction (up to 0.1 Mr) may be a chain reaction dependent on oxygen, and possibly continues up to 50 Mr (G = 14.23) in the absence of oxygen. Tertiary amine is formed by breaking of the C - N bond between the functional group and the polymer chain. Subsequently the tertiary amine is broken down to secondary amine.

Secondary Amine

Secondary amine is also formed at the start of irradiation as a primary product (Fig. 19), i.e. by

1) decomposition of the weak base groups initially present on the polymer chain and

2) formation from tertiary amine, resulting from decomposition of quaternary groups.

The yield of secondary amine decreases (Table 9) on further irradiation, as it becomes converted to

primary amine.

Primary Amine and Ammonia

No ammonia and only traces of primary amine are detected in the initial stages of the reaction when tertiary amine formation is predominant, i.e. up to 50 Mr. The formation of primary amine and ammonia increases in the latter stages of the reaction, as tertiary and secondary amines are being decomposed, and both strong and weak base capacity is lost. The concentration of ammonia increases as the basic products are degraded, and ammonia itself is not destroyed any further. At 500 Mr it is seen that leach solutions contain mainly tertiary amine and free ammonia in excess of primary and secondary amines. Ammonia formation seems to be the last step in the degradation. The formation of further degradation products such as nitrite and hydroxylamine (141), by radiolysis of ammonia, was not detected in the spot analysis of the leach solutions.

(iv) Effect of Dose-Rate

Results in Table 9 were performed at a constant dose-rate of 0.61 Mr/hr, samples being irradiated from a few days up to several weeks. Irradiation of resin samples in the hydroxide form have also been

TABLE 12

DOSE RATE DEPENDENCE

Distance (cms.)	Dose Rate	Total Dose (Mr)	Capacity (m.equ/g)		Basic Products (m.equ/g)				Total
			Strong Base	Weak Base	Tertiary	Secondary	Primary	Ammonia	
3	0.61	55.5	3.11	0.42	0.47	0.11	0.04	0.01	4.16
6	0.18	65.0	2.94	0.45	0.51	0.13	0.04	0.01	4.08
BLANK			3.80	0.22	-	-	-	-	4.02

carried out at dose-rates varying by a factor of 4, (Table 12).

The results show that there appears to be no dose-rate dependence in the range investigated.

Dose-rate effects are of significance in the following three cases:

1) reactions propagated by chain mechanism
2) reactions depending on the availability of oxygen
3) irradiations of very dilute solutions for long periods at high doses.

In the case of irradiated resins, a chain mechanism only accounts for the reaction up to 100,000 rads when all the oxygen is used up, after which the system is essentially oxygen-free. The basic products are produced in concentrated medium, e.g. at 500 Mr 2.5 m.equ. of base is present in approximately 5 ml. of solution (concentration 0.5 N). It is unlikely therefore, that such a system is dose-rate dependent. It is of interest that Bednar et al (107) have reported that the decomposition of cation exchangers is independent of dose-rate, over a range of 4.83×10^4 to 1.62×10^5 rads/hr.

(v) Physical Damage to Resins

Irradiation does not appear to destroy the

cross-linked polystyrene network. A mass balance, between the sum of total capacity and basic products released and the total capacity of the unirradiated resin, agrees within the limits of experimental accuracy. There does not therefore seem to be a significant weight loss on irradiation, e.g. no more than 10% at 500 Mr. Small changes in weight may take place due to loss of functional groups, e.g. 10 - 20% weight loss might be expected if all the functional groups are removed from the polystyrene chain.

The polystyrene chain is resistant to irradiation. Experiments have shown that polystyrene becomes less soluble, i.e. more highly cross-linked when irradiated in a reactor (142). It is feasible that in the case of resins containing a 7 - 9% cross-linked polystyrene skeleton, there will be further cross-linking on irradiation, causing the resin beads to shrink. Degradation of the polystyrene network by chain scission occurs to a lesser extent than the production of cross-links, i.e. ratio of chain scission:cross-linking is 0.35 and this would explain the fact that high molecular weight organic fragments do not occur in the leach.

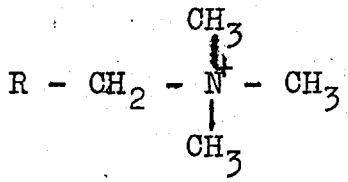
It has been observed that at the highest doses

the resin particles tend to clump together and bed down during column operation. This leads to a large pressure drop in the bed and results in a marked drop in the flow rate.

D. DISCUSSION AND REACTION MECHANISMS

The primary decomposition reaction is the formation of tertiary amine by rupture of the C - N bond between the functional group and the polymer chain. The bond energies of triethylamine and trimethylamine are shown in Table 13, together with the dissociation energies for selected aliphatic and aromatic amines.

The mean C - N bond energy for aliphatic amines is usually taken as 72.8 k cal., whereas the dissociation energy for this bond varies with the size of the group attached to the N atom. The phenyl group attracts electrons from the C - N bond, weakening it and lowering the dissociation energy, e.g. from 102 k cal. for ammonia to 59.1 k cal. for benzylamine. A quaternary ammonium compound, of the resin type



where R represents the polystyrene chain, contains

TABLE 13

C-N BOND ENERGIES (143)

Amines	Bond Energy (k cal.)	Dissociation Energy (k cal.)
$CH_3 - NH_2$	68.1	—
$(CH_3)_2 - NH$	65.7	—
$(CH_3)_3 - N$	—	—
$C_2H_5 - NH_2$	68.4	—
$(C_2H_5)_2 - NH$	71.3	—
$(C_2H_5)_3 - N$	73.4	—
$H - NH_2$	—	102.0
$CH_3 - NH_2$	—	80.0
$C_6H_5.CH_2 - NH_2$	—	59.1

four C - N bonds. The C - N bonds in the trimethyl-amino functional group have bond energies of about 72.8 k cal. whereas the C - N bond to the polystyrene chain (i.e. R - CH_2 -), by analogy to Table 13, has a bond energy of less than 72.8 k Cal., and probably in the region of 59.1 k cal. This would appear to indicate that the latter is the weakest bond, and is likely to be the most sensitive to radiation.

A plausible free radical mechanism may be postulated for the production of tertiary amine by chain reaction in the presence of oxygen in the solution.

Reaction 1

$$R - CH_2 - \overset{CH_3}{\underset{CH_3}{\overset{|}{\underset{|}{N^+}}}} - CH_3\bar{O}H \longrightarrow R - \dot{C}H_2 + \cdot N^+(CH_3)_3 + \bar{O}H$$

$$R - \dot{C}H_2 + O_2 \longrightarrow R.CH_2O_2^{\bullet}$$

$$R.CH_2O_2^{\bullet} + R - \underset{H}{CH} - \overset{+}{N}(CH_3)_3\bar{O}H \longrightarrow R.CH_2O_2H + R - \underset{\bullet}{CH} - \overset{+}{N}(CH_3)_3\ \bar{O}H$$

$$R - \underset{\bullet}{CH} - \overset{+}{N}(CH_3)_3\bar{O}H + O_2 \longrightarrow R - \underset{O_2^{\bullet}}{CH} - \overset{+}{N}(CH_3)_3\bar{O}H$$

$$R - \underset{O_2^{\bullet}}{CH} - \overset{+}{N}(CH_3)_3\bar{O}H + R - \underset{H}{CH} - \overset{+}{N}(CH_3)_3\bar{O}H \longrightarrow R - \underset{O_2H}{CH} - \overset{+}{N}(CH_3)_3\bar{O}H + R - \underset{\bullet}{CH} - \overset{+}{N}(CH_3)_3\bar{O}H$$

$$R - \underset{\underset{O_2H}{|}}{CH} - \overset{+}{N}(CH_3)_3\bar{O}H \longrightarrow R - CHO + :N(CH_3)_3 + H_2O_2$$

This reaction mechanism is sustained until the available oxygen is used up.

Baumann (144) has shown that hydrogen peroxide reacts with the anion exchange resin to give a hydroperoxide grouping, which decomposes to regenerate the resin in the hydroxide form and liberate oxygen (Reaction 2). This reaction could explain why hydrogen peroxide is not observed quantitatively in the leach solutions.

Reaction 2

$$R - CH_2 - \overset{+}{N}(CH_3)_3\bar{O}H + H^+\bar{O_2}H \longrightarrow R - CH_2 - \overset{+}{N}(CH_3)_3.\bar{O_2}H + H_2O$$

$$R - CH_2 - \overset{+}{N}(CH_3)_3\bar{O_2}H \longrightarrow R - CH_2 - \overset{+}{N}(CH_3)_3\bar{O}H + \tfrac{1}{2}O_2$$

Reaction 1 shows the direct breaking of the C - N bond leading to a free radical mechanism in the presence of oxygen. A similar reaction would take place by indirect action, i.e. initial radiolysis of water to give $H^\bullet$ and $OH^\bullet$ radicals:

Reaction 3

$$H_2O \longrightarrow H^{\bullet} + OH^{\bullet} + (H_2 + H_2O_2)$$

$$\left.\begin{matrix} H^{\bullet} \\ OH^{\bullet} \end{matrix}\right\} + R - CH_2 - \overset{+}{N}(CH_3)_3\bar{O}H \longrightarrow R - \underset{\bullet}{C}H - \overset{+}{N}(CH_3)_3\bar{O}H + \left.\begin{matrix} H_2 \\ H_2O \end{matrix}\right\}$$

$$R - \underset{\bullet}{C}H - \overset{+}{N}(CH_3)_3\bar{O}H + O_2 \longrightarrow R - \underset{\bullet O_2}{C}H - \overset{+}{N}(CH_3)_3\bar{O}H$$

$$R - \underset{\bullet O_2}{C}H - \overset{+}{N}(CH_3)_3\bar{O}H + R - \underset{H}{C}H - \overset{+}{N}(CH_3)_3\bar{O}H$$

$$\longrightarrow R - \underset{O_2H}{C}H - \overset{+}{N}(CH_3)_3\bar{O}H + R - \underset{\bullet}{C}H - \overset{+}{N}(CH_3)_3\bar{O}H$$

$$\downarrow$$

$$RCHO + :N(CH_3)_3 + H_2O_2$$

These reactions can only occur whilst oxygen is available. The following calculation shows when the oxygen is used up.

From Reactions 1 and 3

For 1 mole $N(CH_3)_3$ formed, 1 mole O_2 is used up. However, 1 mole $N(CH_3)_3$ formed produces 1 mole H_2O_2, and 1 mole H_2O_2 regenerates ½ mole O_2. Thus to form 1 mole $N(CH_3)_3$, ½ mole O_2 is required.

From Table 11 the initial G-value for tertiary

amine formation is 15. $\therefore$ G for oxygen consumption

$= 7.5$

i.e. 7.5 oxygen mols. used up per 100 eV absorbed.

If the initial oxygen concentration in water at $25^{o}C = 0.25 \times 10^{-3}$ M.

$$\text{oxygen molecules/}_{ml} = 0.25\times10^{-3}\times\frac{6.023\times10^{23}}{10^{3}}$$

$$\therefore \text{ radiation energy to use up oxygen} = 0.25\times10^{-3}\times\frac{6.023\times10^{23}}{10^{3}}\times\frac{100}{7.5}\ \text{eV/ml}$$

$$= 32{,}500 \text{ rads}$$

$$\text{As } \left[1 \text{ rad} = 6.24\times10^{13} \text{ eV/g in water}\right].$$

However, it has been shown that G for production of tertiary amine is of the order of 5 - 15 up to a total dose of 50 Mr. It is unlikely that oxygen diffusion can account for this and therefore the following two mechanisms could continue the reaction when all the oxygen is used up.

i) a free radical chain mechanism in the absence of oxygen

ii) a high yield non-chain reaction.

Lemmon et al (145) have discussed the radiolysis of the quaternary ammonium compound choline chloride $\left[(CH_3)_3 \overset{+}{N}. CH_2.CH_2OHCl\right]$. It has been shown that this

compound, when irradiated in a solid crystalline form, decomposes with an exceptionally high G value e.g. G = 1250 for C^{14} beta radiation and G = 175 for Co^{60} gamma radiation, where the difference is due to a dose rate effect. The main products were shown to be acetaldehyde and trimethylamine, resulting from the rupture of the C - N bond, holding the functional group. A series of choline analogues did not give the high G-value reactions. It was also found that choline chloride, in solution and at high temperatures, gave a G-value of 2 - 3 for Co^{60} gamma radiation. A chain mechanism has been suggested by the authors, to explain their findings, and by applying this mechanism to the radiation decomposition of resins, it is possible to postulate a chain reaction in the absence of oxygen.

Reaction 4

$$R - CH_2 - \overset{+}{N}(CH_3)_3\bar{O}H \xrightarrow{(-e)} \left[R - \overset{+}{C}H_2 - \overset{+}{N}(CH_3)_3\bar{O}H\right]$$

$$\downarrow$$

$$R\overset{+}{C}H_2 + \overset{+}{N}(CH_3)_3 + \bar{O}H$$

$$R - \overset{+}{C}H_2 + \bar{O}H \longrightarrow R.CH_2OH$$

$$\overset{+}{N}(CH_3)_3 + R - CH_2 - \overset{+}{N}(CH_3)_3\bar{O}H$$

$$\longrightarrow :N(CH_3)_3 + \left[R - \overset{+}{C}H_2 - \overset{+}{N}(CH_3)_3\bar{O}H\right]$$

The group remaining on the resin after irradiation is therefore postulated as an alcohol and not an aldehyde as in Reactions (1 - 3).

A high yield reaction, in the absence of oxygen, may be of the thermal Hofmann degradation type to form tertiary amine directly as follows.

Reaction 5

$$R - CH_2 - \overset{+}{N}(CH_3)_3\overset{-}{O}H \longrightarrow R.CH_2OH + N(CH_3)_3$$

The mechanism of such a reaction may be explained by the formation of an intermediate carbonium ion (146).

$$R - CH_2 - \overset{+}{N}(CH_3)_3\bar{O}H \longrightarrow R.\overset{+}{C}H_2 + N(CH_3)_3 + \bar{O}H$$

$$R - \overset{+}{C}H_2 + \bar{O}H \longrightarrow R.CH_2OH + N(CH_3)_3$$

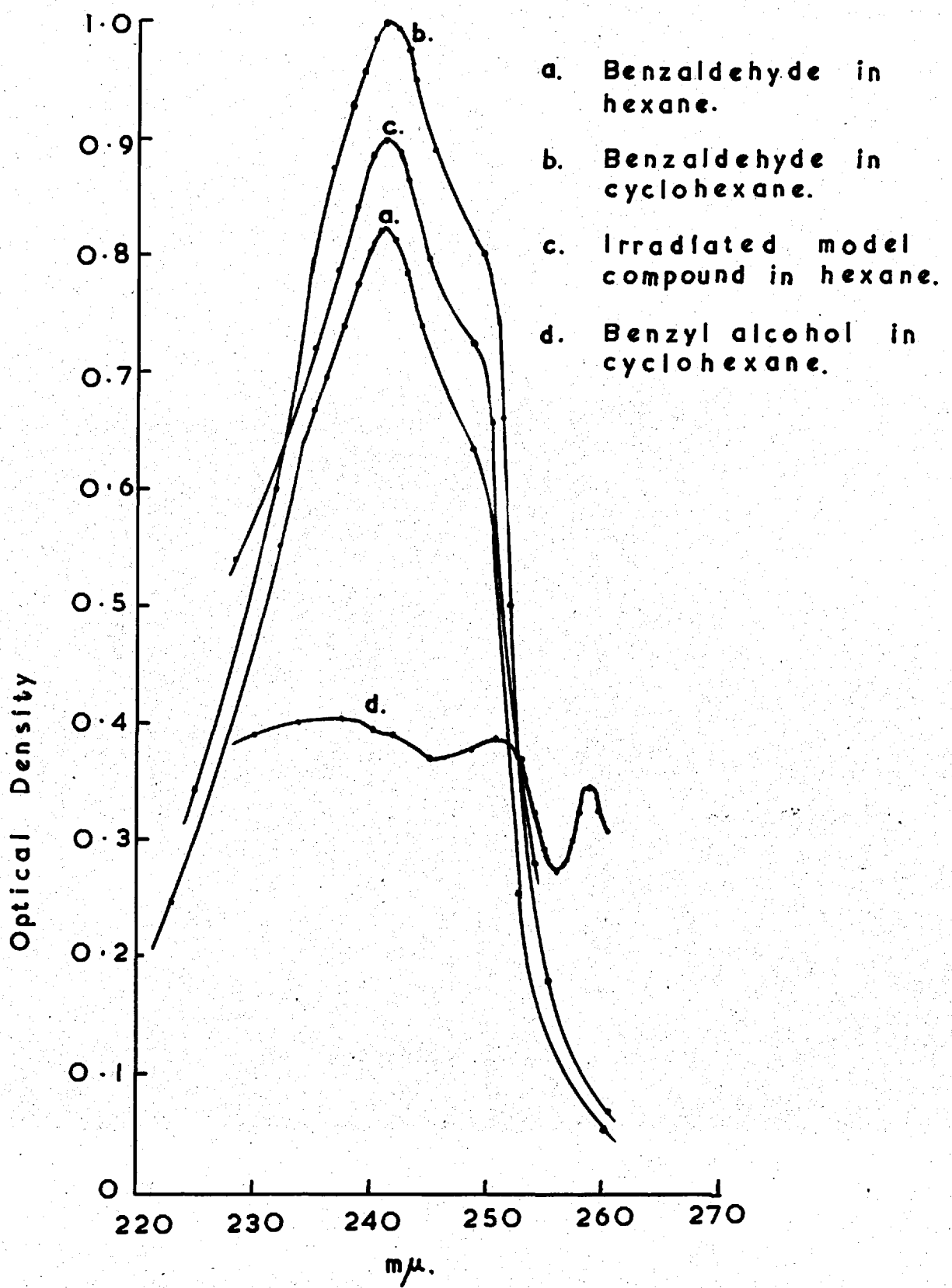
The C - N bond is broken, resulting in electron transfer to form the organic cation, which combines to form an alcohol.

The group remaining on the resin after irradiation is probably an alcohol or an aldehyde. It is difficult to characterise this group experimentally with irradiated resin samples, and so a model compound was irradiated as follows:

Irradiation of the Model Compound

A 4% aqueous solution of benzyl trimethyl-ammonium hydroxide $\left[C_6H_5CH_2\overset{+}{N}(CH_3)_3\bar{O}H\right]$ was irradiated

SPECTRUM OF IRRADIATED MODEL COMPOUND Fig. 21.



at doses of up to 10^6 rads. The aqueous solution, which became slightly cloudy on irradiation, was shaken with n-hexane to extract the decomposition products. The organic layer was washed with dilute acid to remove the basic products formed, i.e. tertiary and secondary amines.

The spectrum of the organic layer was measured from 220 - 270 mμ, and a peak was found at 241 mμ (Fig. 21). The unirradiated quaternary compound extracted into n-hexane gave zero optical density over the range 220 - 270 mμ. The peak obtained with the irradiated model compound, corresponded with the peak absorption of benzaldehyde in ethanol, reported in the literature. To check this, solutions of benzaldehyde and benzyl alcohol were extracted into n-hexane and cyclohexane, and their absorption peaks measured. Fig. 21 shows that the spectrum of the irradiated model compound is almost identical with that of benzaldehyde but does not resemble the spectrum of benzyl alcohol.

A 2:4 dinitrophenyl hydrazone derivative of the unknown compound was also prepared, and this gave a peak at 450 - 470 mμ in the visible region. This compares with the same derivative prepared with benzaldehyde, which resulted in a peak at 460-480 mμ.

Although this work has been mainly qualitative, it would appear that benzaldehyde is the most likely product when the model compound is irradiated. Further work is required on a more quantitative basis, to show the yield of all products at doses up to 10^6r, and to show conclusively that benzyl alcohol is not formed.

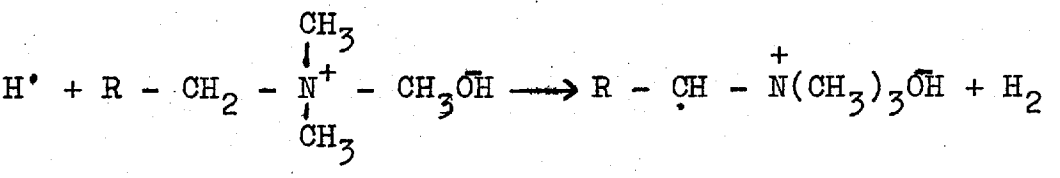
On the basis of the model compound work, it is necessary to provide a mechanism, which will explain the possible formation of an aldehyde grouping on the resin and produce tertiary amine as a product in the absence of oxygen. The following chain mechanism may be suggested.

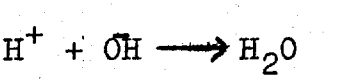
Reaction 6

(a) $R - \underset{H}{CH} - \overset{+}{N}(CH_3)_3\bar{O}H \longrightarrow R - \dot{C}H - \overset{+}{N}(CH_3)_3\bar{O}H + H^{\bullet}$

(b) $\left.\begin{matrix} H^{\bullet} \\ OH^{\bullet} \end{matrix}\right\} + R - CH_2 - \overset{CH_3}{\underset{CH_3}{N^+}} - CH_3\bar{O}H \longrightarrow R - \dot{C}H - \overset{CH_3}{\underset{CH_3}{N^+}} - CH_3\bar{O}H + \left.\begin{matrix} H_2 \\ H_2O \end{matrix}\right\}$

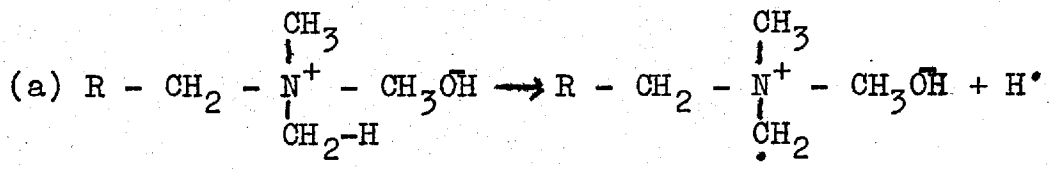
$R - \dot{C}H - \overset{CH_3}{\underset{CH_3}{N^+}} - CH_3\bar{O}H + H_2O \longrightarrow R - CHO + \overset{CH_3}{\underset{CH_3}{N}} - CH_3 + H^{\bullet} + H^+$

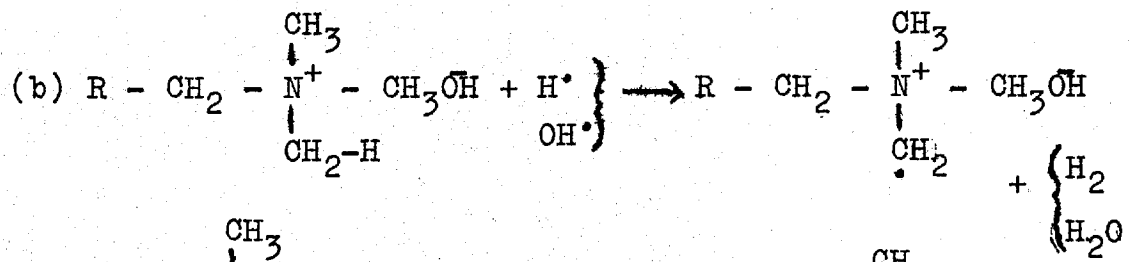


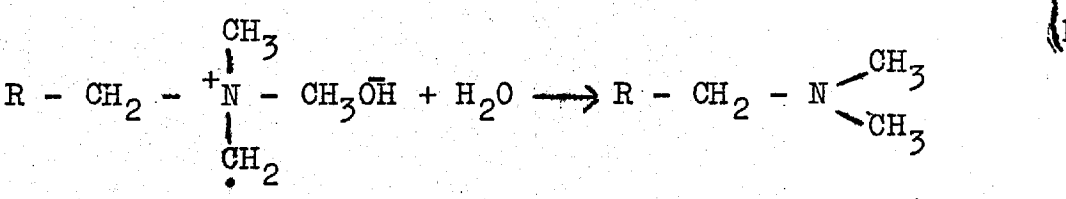


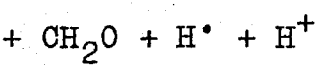
Either step (a) direct or (b) indirect could initiate the reaction.

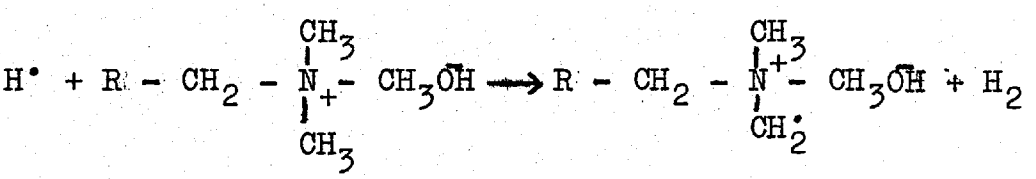
Reaction 7

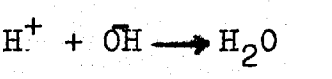










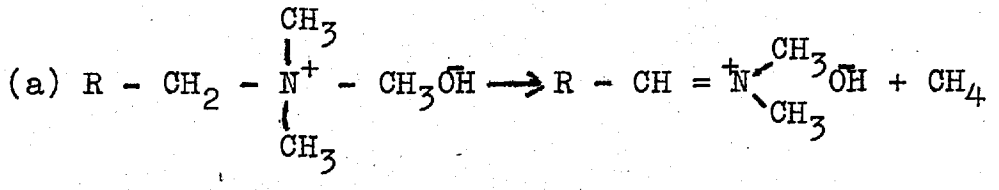


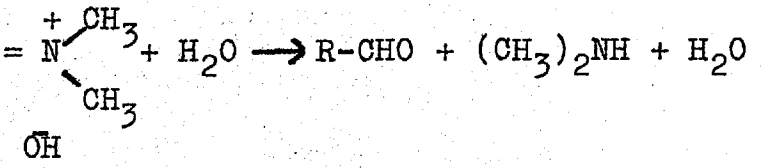
Reaction 7 would explain the increase in weak base capacity of the resin, with the formation of

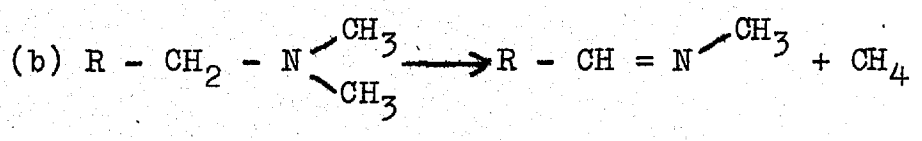
formaldehyde in the leach solution.

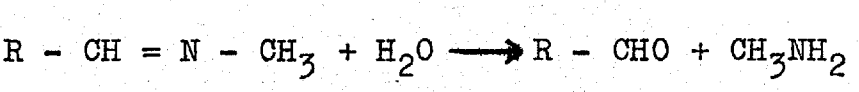
A more typical reaction of amino compounds is to decompose by the formation of an intermediate imine, which is unstable and hydrolyses to form an aldehyde and an aliphatic amine.

Reaction 8







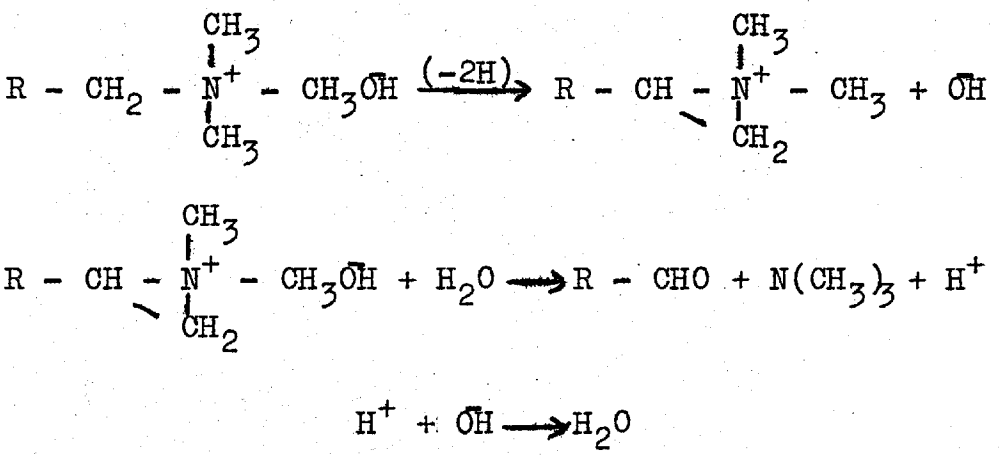


Secondary and primary amines can be formed by Reaction 8, directly from the quaternary and tertiary structure, resulting in the production on the resin of an aldehyde group. Methane is liberated as a gaseous product, and is not detected in the aqueous leach analysis.

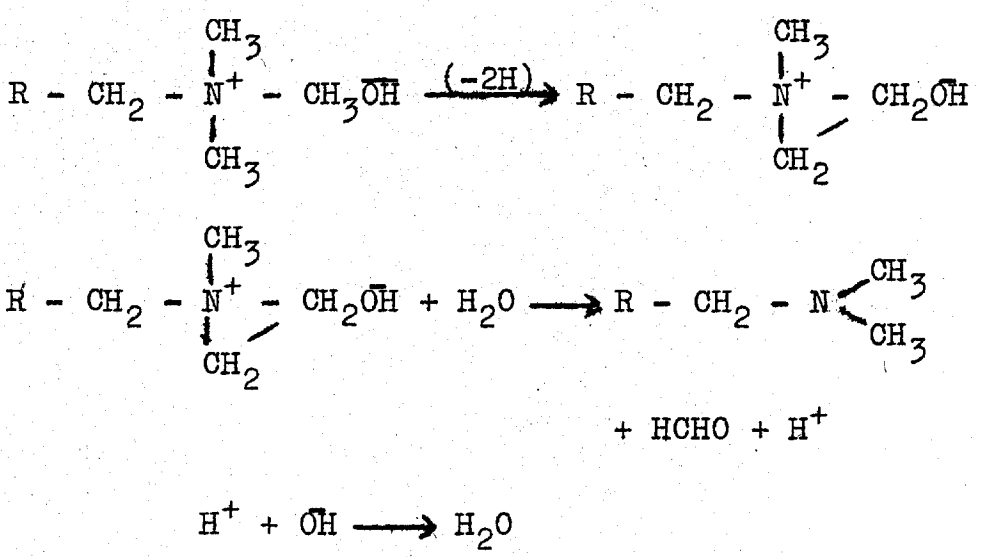
Further reactions, common to amino-compounds are the removal of molecular hydrogen, to give an aldehyde

and the corresponding amine.

Reaction 9



Reaction 10



Reaction 9 would also explain the formation of Trimethylamine and an aldehyde, whereas Reaction 10 accounts for the formation of weak base groups. These molecular reactions are possibly more likely to

occur than Reactions 6 and 7 outlined previously.

The radiolysis of the tertiary, secondary and primary amines in the leach solutions, at high doses in the absence of oxygen, may also be explained by an analogous mechanism, i.e. removal of molecular hydrogen or methane to give an intermediate imine, which consequently hydrolyses.

Reaction 11

$$\begin{matrix} H \\ | \\ N \\ | \\ CH_3 \end{matrix} - CH_3 \xrightarrow{(-2H)} CH_2 = N(CH_3)$$

$$CH_2 = N(CH_3) + H_2O \longrightarrow HCHO + CH_3NH_2$$

$$CH_3NH_2 \xrightarrow{(-2H)} CH_2 = NH$$

$$CH_2 = NH + H_2O \longrightarrow HCHO + NH_3$$

Reaction 12

$$\begin{matrix} CH_3 \\ | \\ N \\ | \\ CH_3 \end{matrix} - CH_3 \longrightarrow CH_3N = CH_2 + CH_4$$

$$CH_3N = CH_2 + H_2O \longrightarrow CH_3NH_2 + HCHO$$

$$\begin{matrix} H \\ | \\ N \\ | \\ CH_3 \end{matrix} - CH_3 \longrightarrow HN = CH_2 + CH_4$$

$$HN = CH_2 + H_2O \longrightarrow HCHO + NH_3$$

Reactions 11 and 12 show that tertiary, secondary and primary amines can be decomposed step-wise to give ammonia as a final product.

The formaldehyde formed in each of the stages above may take part in further reactions with the aliphatic bases, particularly primary and secondary amines to give hydroxy methyl derivatives, which readily further react to form bis alkylamino - or bis dialkylamino derivatives. These reactions take place in alkaline solution.

Reaction 13

$$CH_3NH_2 + HCHO \longrightarrow CH_3NH.\ CH_2OH$$

$$(CH_3)_2NH + HCHO \longrightarrow (CH_3)_2N.\ CH_2OH$$

Reaction 14

$$CH_3NH.CH_2OH + CH_3NH_2 \longrightarrow CH_3.NH.CH_2NH.CH_3 + H_2O$$

$$(CH_3)_2N.CH_2OH + (CH_3)_2NH \longrightarrow (CH_3)_2N.CH_2.N.(CH_3)_2 + H_2O$$

These reactions may explain why such low yields of formaldehyde are detected in the aqueous leach solutions.

Conclusion

The reaction mechanisms presented above have been proposed to explain the more important experimental observations, but they are in the main still speculative. The great difficulty is that most of the reactions are based on the nitrogenous products released, because little is known about the residual grouping remaining on the resin, which appears to be insoluble in all organic solvents. A more extensive study on a model compound of the type discussed, although not strictly analogous, would be helpful. Gas analysis would show if methane, hydrogen or other gaseous products are liberated on irradiation.

SECTION 16

THERMAL STABILITY IN THE HYDROXIDE FORM

A. INTRODUCTION

B. EXPERIMENTAL

C. RESULTS AND DISCUSSION

A. INTRODUCTION

In many operations, where anion exchange resins in the hydroxide form are to be used, e.g. demineralisation, it is recommended that process solutions should be kept below 60°C. It has been suggested that the thermal instability of the resin may in some way contribute towards the radiation decomposition. Thus, Fisher (93) postulated that a heating effect, observed when resins are irradiated with cobalt-60 gamma radiation, could result in decomposition, equal in magnitude to that produced by the radiation itself. A local heating effect of this type is unlikely, since resin samples are not in contact with the source capsule, and the maximum radiation energy (i.e. 1.5 watt hr/g) is absorbed over a period of weeks. It is, however, of interest to investigate the properties of the resins at elevated temperatures and compare the results with those for irradiated resins.

Wheaton and Baumann (147) and Swetz (148) have shown that a resin in the chloride form, when heated at 100°C for 16 hours does not lose appreciable capacity. Marinsky and Potter (149) observed a loss of capacity at temperatures of 117° and 135°C when resin samples are heated in ampoules.

They further found that the reaction obeyed first order kinetics, and that basic, but unidentified, decomposition products were formed.

The present study, relates the changes in anion exchange capacity to the basic products released when resin samples in the hydroxide form are maintained at boiling water temperature for up to one week.

B. EXPERIMENTAL

An aqueous slurry, containing approximately 1.0 g. of the resin in the hydroxide form, was placed in a 50 ml. round-bottomed distillation flask, fitted with a short air-condenser dipping into a receiver containing 5 - 6 ml. of distilled water. The resin sample was refluxed at 95 - 100°C, by heating the flask in an oil-bath. Volatile products are collected by dissolving them in a small gas trap fitted to prevent backsuction between the distillation flask and the air condenser.

The dissolved volatile products and aqueous leach liquor, after heating of the resin, were combined and analysed for individual basic products, i.e. tertiary and secondary amines, using the procedures outlined in Section 15.

TABLE 14

LOSS OF CAPACITY ON HEATING AT BOILING WATER TEMPERATURE

		Hours of heating			
		0	4	26	120
Capacity	Strong Base	4.20	3.85	3.51	3.05
	Weak Base	0.20	0.20	0.41	0.44
	Total (a)	4.40	4.05	3.92	3.49
Basic Products	Tertiary	-	0.30	0.46	0.79
	Secondary	-	-	-	10^{-3}
	Total Amines (b)	-	0.30	0.46	0.79
	Total Nitrogen	-	0.27	0.42	0.76
Sum Total (a+b)		4.40	4.35	4.38	4.28
% Loss in Capacity		-	8.00	11.00	21.00

Both the strong and weak base capacity of the resin was determined after heating, and compared with the capacity of blank samples, kept at room temperature (25°C) during the period of heating.

C. RESULTS AND DISCUSSION

The capacity measurements and analysis of basic products of resin specimens heated 4, 26 and 120 hours are shown in Table 14.

The results show that heating at approximately 100°C produces a distinct change in capacity, resulting from a loss in quaternary capacity and a small increase in the weak base capacity. Tertiary amine appears to be the only basic product produced. These reactions can be explained by Hofmann degradation.

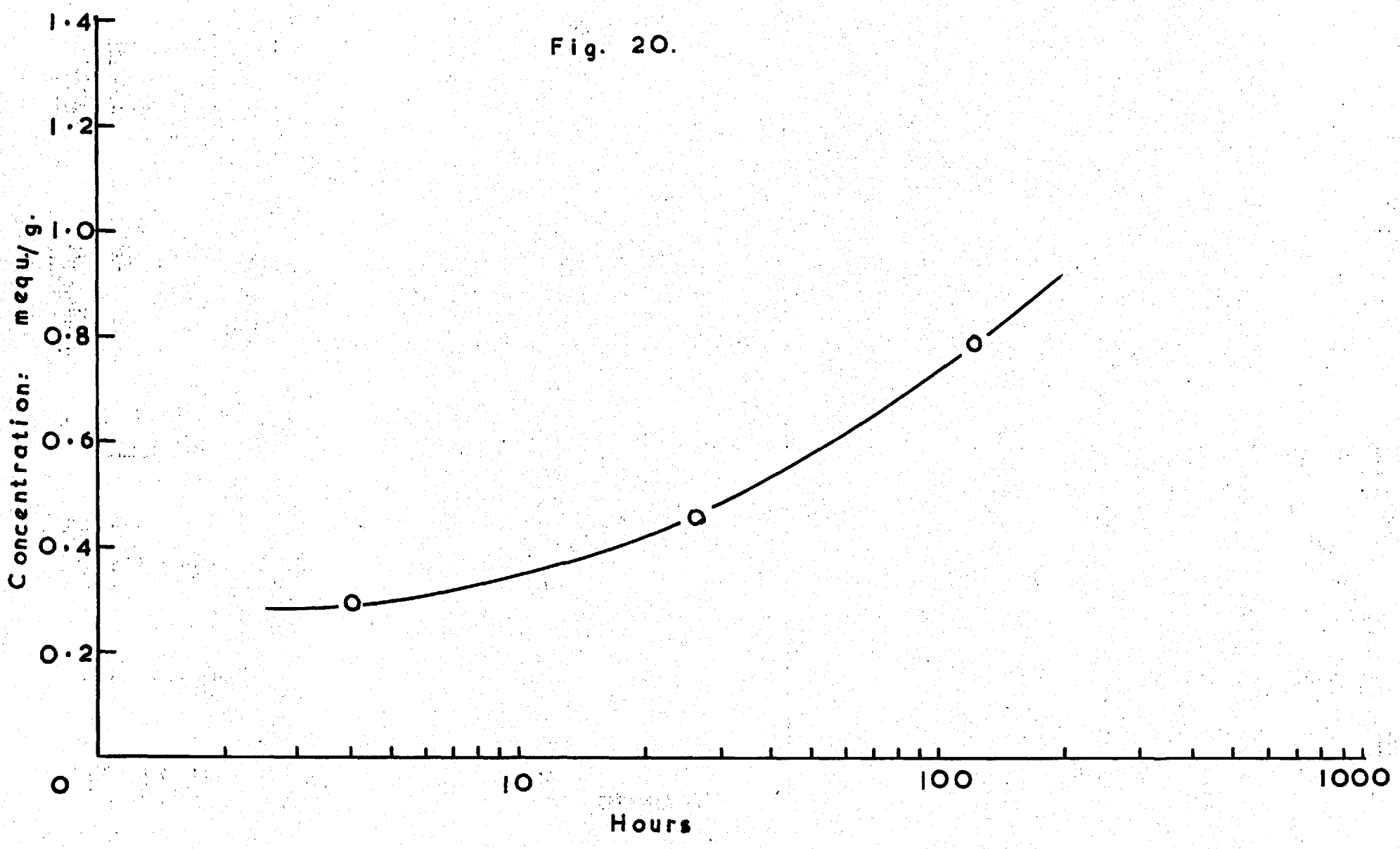
i) $R - CH_2 - \overset{+}{N}(CH_3)_3\bar{O}H \longrightarrow R - CH_2 - OH + N(CH_3)_3$

ii) $R - CH_2 - \overset{+}{N}(CH_3)_3\bar{O}H \longrightarrow R - CH_2 - N(CH_3)_2 + CH_3OH.$

The total loss in quaternary capacity over 120 hrs. is 28%, whereas the loss in total capacity over the same range is 21%. This is explained by a slight conversion of strong base to weak base capacity. Accordingly, it would seem that 70% of the decomposition is by reaction 1 (above) and 30% by reaction 2.

YIELD OF TERTIARY AMINE ON HEATING AT 100°C

Fig. 20.



The formation of tertiary amine accounts for all the nitrogen present in the leach solution, and this is confirmed by the fact that only trace quantities of secondary amines are detected after 120 hrs. The build-up of tertiary amine is shown in Fig 20, the concentration beginning to rise after 120 hrs.

Baumann (150) in a recent paper, has presented results which confirm the observations found in this work. Resins heated at 95°C, were found to decompose by two distinct processes, one accounting for a 15% loss in capacity over a period of 3 days, the other a slower decomposition, this reaction having a half-life of 43 days. Both the fast and slow reactions occur by Hofmann degradation, the production of tertiary amine corresponding to 60% of the decomposition. The tertiary base was estimated by adsorbing it on a cation exchanger, and measuring the change in the cation exchange capacity. This would however, give results corresponding to the total anions released on heating, but Baumann showed good agreement between loss in capacity and tertiary amine formed and concluded that no other base was formed.

It is clear therefore, that the resin undergoes

a rapid loss of capacity over a period of 5 days, by a mechanism which is not analogous to the radiation decomposition mechanism. Baumann shows that further heating produces a slower decomposition, lasting 43 days, after which the resin is useless for chemical processing. This work would indicate that if resins were irradiated at temperatures of 100°C, then the rate of decomposition would increase at first, but would later follow the radiation degradation pattern more closely. Thermal decomposition would therefore be expected to contribute only a small amount to the total loss of capacity at high doses and at temperatures of up to 100°C.

APPENDIX I

C A L C U L A T I O N O F R E S U L T S

A. CAPACITY CALCULATIONS

Volhard Titration Method

Normality of solutions:

i) Silver nitrate = 0.0953

ii) Ammonium Thiocyanate = 0.0961

Weight of resin sample = 1.13 g.

Ammonia Leach - 10 ml. sample + 10 ml. 0.0953 $AgNO_3$ (50 ml. total solution)

Back titrate against 0.0961 NH_4CNS

mls. before titration	mls. after titration	titre
0	9.45	9.45
0	9.45	9.45
	Mean	9.45

$\therefore$ 9.45 mls. 0.0961 N NH_4CNS

$$= \frac{9.45 \times 0.0961}{0.0953} \text{ mls. } 0.0953\text{N} AgNO_3$$

$$= 9.51 \text{ mls. } 0.0953 \text{ N } AgNO_3$$

Excess silver nitrate = (10.00 - 9.51) mls.

= 0.49 mls.

Concentration of chloride ions = 0.49 x 0.0953 x 5

= 0.234 m.equ.

Weak base capacity $= \frac{0.234}{1.13}$ m.equ/g.

$= \underline{0.21 \text{ m.equ/g.}}$

Sodium Sulphate Leach

50 ml. total solution.

10 ml. sample + 10 ml. 0.0953 N $AgNO_3$

Back titrate against 0.0961 N NH_4CNS

mls. before titration	mls. after titration	titre
0.	0.45	0.45
0.45	0.90	0.45
	Mean	0.45

$\therefore$ 0.45 mls. 0.0961 N NH_4CNS

$= \frac{0.45 \times 0.0961}{0.0953}$ mls. 0.0953N.$AgNO_3$

$= \underline{0.46 \text{ mls.}}$

Excess silver nitrate $= (10.00 - 0.46)$

$= \underline{9.54 \text{ mls.}}$

Concentration of chloride ion $= 9.54 \times 0.0953 \times 5$

$= 4.54$ m.equ.

Strong base capacity $= \frac{4.54}{1.13}$ m.equ/g

$= \underline{4.22 \text{ m.equ/g}}$

B. TOTAL NITROGEN DETERMINATIONS

Volume of aqueous leach = 50 ml.

Weight of resin = 0.92 g

Strength of acid = 0.11 N

Strength of alkali = 0.12 N

Take 5 ml. aliquot and distil into 10 ml. 0.11 N hydrochloric acid.

Now 10 ml. 0.11 N acid ≡ 9.2 ml. 0.12 N alkali.

After steam distillation, 8.50 ml. alkali required to neutralise distillate.

∴ Excess alkali = 9.2 - 8.50

= 0.7 mls.

∴ Concentration of products in distillate = 0.7 x 0.12 x 10

= 0.84 m.equ.

Concentration of nitrogen in leach $= \frac{0.84}{0.92}$ m.equ/g

$= \underline{0.91 \text{ m.equ/g}}$

C. TO CALCULATE CONCENTRATION OF TERTIARY AND SECONDARY AMINES IN A MIXTURE USING FIGS. 13 AND 14

Volume of amine solution = 50 ml.

Weight of resin sample = 1.10 g

Analysis

Tertiary Amine

Vol. of aliquot (ml.)	Optical Density
0.2	0.41
0.2	0.39
	Mean = 0.40

Secondary Amine

Vol. of aliquot (ml.)	Optical Density
0.5	0.73
0.5	0.75
	Mean = 0.74

Using Fig. 14 to calculate secondary amine concentrations.

Optical Density = 1.0 is equivalent to a

Concentration = 1.68×10^{-3} m.equ.

∴ Concentration of secondary amine in 50 ml. solution

$$= \frac{0.74 \times 1.68 \times 10^{-3} \times 50}{0.5} \text{ m.equ.}$$

$$= 0.12 \text{ m.equ.}$$

Concentration of secondary amine $= \frac{0.12}{1.10}$

$= \underline{0.11 \text{ m.equ/g}}$

Using Fig. 13. to calculate tertiary amine concentration.

1) Correct for dimethylamine in sample.

Optical density = 1.0 is equivalent to a

Concentration = 2.20×10^{-2} m.equ. dimethylamine.

In 0.2 ml. sample, contribution of dimethylamine to optical density value $= \frac{0.12}{50} \times 0.2 \times \frac{1}{2.2 \times 10^{-2}}$

$= \underline{0.02}$

2) Corrected value of optical density for tertiary amine estimation is (0.40 - 0.02) = 0.38.

From Fig. 13.

Optical density = 1.0 when

Concentration = 5.53×10^{-3} m.equ. for trimethylamine.

$\therefore$ tertiary amine in 50 ml. solution $= \frac{0.38 \times 5.53 \times 10^{-3} \times 50}{0.2}$

$= \underline{0.53 \text{ m.equ}}$

$\therefore$ Concentration of tertiary amine $= \frac{0.53}{1.1}$ m.equ/g

$= \underline{0.47 \text{ m.equ/g}}$

B I B L I O G R A P H Y

1. Parry, Atomics, 1, 159-66, 177, (1950)
2. Manowitz, Nucleonics, 9, 10, (1951)
3. Stein and Beard, Nuclear Power, 2, 501, (1957)
4. Jefferson, Nuclear Power, 2, 506, (1957)
5. Brucer, Nucleonics, 12, 8, (1954)
6. Grimmett, Radiology, 59, 19, (1952)
7. Hall, Ind. Chemist, 35, 577, (1959)
8. Kuhl, Sparrow and Manowitz, Nucleonics, 13, 128, (1955)
9. Anon., Nuclear Power, 4, 110, (1959)
10. Brynjolfsson and Holm, I.A.E.A. Conference, Warsaw 1959, Paper 75
11. Seligman, Geneva Conference, 20, 5, (1958)
12. Eastwood, West and Wiblin, Ibid, 19
13. Voyodic and Stone, ARF - 1150 - 3, (1959)
14. Charlesby and Flint, Atomics, 6, 100, (1955)
15. Eastwood, Nucleonics, 13, 52, (1955)
16. Atkins, Accessory Equipment and Procedures for use of a 1,500 Curie Cobalt-60 Gamma Ray Source, WADC - TN - 55 - 302, (1956)
17. Atkins, Design of a High Intensity Gamma Irradiation Facility, WADC - TR - 56 - 452, (1956)

18. Atkins, Wolfsberg, Lorentz and Smith, Design and use of a 23,000 Curie Cobalt-60 Facility, WADC - TR - 57 - 498, (1957)

19. Bauman, Nucleonics, 15, 96, (1957)

20. Ghormley and Hochanadel, Rev. Sci. Instr., 22, 473, (1951)

21. Greenfield, Silverman and Dickinson, Nucleonics, 10, 65, (1952)

22. Blomgren, Hart and Markheim, Rev. Sci. Instr., 24, 298, (1953)

23. Valyi-Nagy, I.A.E.A. Conference, Warsaw 1959

24. Firestone and Willard, Rev. Sci. Instr., 24, 904, (1953)

25. Kuhl, Singleton and Manowitz, Nucleonics, 13, 42, (1955)

26. Breger, Belynsky and Prokudin, J. Nuclear Energy, 4, 504, (1957)

27. Jones, High Intensity Gamma Irradiation Facilities at the Knolls Atomic Power Laboratory, KAPL - 1773, (1957)

28. Colichmann, Mallow and Jarrett, Nucleonics, 15, 115, (1957)

29. Chapiro, Cottin, Haissinsky, Magat and Vermeil, J. Phys. Radium, 14, 687, (1953)

30. Burton, Ghormley and Hochanadel, Nucleonics, 13, 74, (1955)

31. Johnson, Brucer, Steinmann and Cagnat, Nucleonics, 14, 119, (1956)

32. Aitken, Dyne and Trapp, Nucleonics, 15, 100, (1957)

33. Firsov, J. Nuclear Energy, 5, 425, (1957)

34. Shwarz and Allen, Nucleonics, 12, 58, (1954)

35. Callinan, Elec. Eng., 74, 510, (1955)

36. Manowitz, Nucleonics, 11, 18, (1953)

37. Obricki, Ball and Davidson, Nucleonics, 11, 52, (1953)

38. Nehemias, Brownell, Meinke and Coleman, Chem. Eng. Prog., 49, 569, (1953)

39. Brownell, Meinke, Nehemias and Harmer, Amer. J. Phys., 22, 511, (1954)

40. Breger, Belynsky, Karpov and Prokudin, Radioisotopes in Scientific Research, Vol 1, Page 122, Pergamon Press, (1958)

41. Anon., Nuclear Power, 2, 508, (1957)

42. Murray, Dove and Roberts, Radioisotopes in Scientific Research, Vol 1, Page 139, Pergamon Press, (1958)

43. Danno, I.A.E.A. Conference, Warsaw 1959

44. Callan, J. Amer. Concrete Inst., 25, 17, (1953)

45. Creutz and Downes, J. App. Phys.,, 20, 1236, (1949)

46. Foster, J. Amer. Concrete Inst., 25, 45, (1953)

47. Glen, Civil Eng., 21, 657, (1951)

48. Gugelot and White, J. App. Phys., 21, 369, (1950)

49. Kennerdy, Wyckoff and Snyder, Concrete as a Protective Barrier for Gamma Rays from Cobalt-60, NBS Journal of Research, 44, 157, (1950)

50. Price, Horton and Spinney, Radiation Shielding, Pergamon Press, (1957)

51. Ruddy, Gamma Shielding for Engineering Reference, AECU - 1211, (1951)

52. Harrison, Shielding Calculations Glove Box Symposium, (1957)

53. Goldstein and Wilkins, Final Calculations on the Penetration of Gamma Rays, NYO 3075

54. Rockwell, Reactor Shielding Design Manual, TID 7004

55. Taylor, Application of Gamma Ray build-up data to Shield Design

56. Code of Practice against Radiation Hazards,

I Imperial College of Science and Technology, Dec. 1958, (third revised edition, June 1960)

57. Murray, U.K.A.E.A., Private Communication

58. Murray, U.K.A.E.A., Private Communication

59. Irving, Shell Research Ltd., Private Communication

60. Pulsford and Washtell, Nuclear Power, 2, 58, (1957)

61. Taylor, Nuclear Power, 2, 503, (1957)

62. Fricke and Morse, Phil. Mag., 7, 129, (1929)

63. Miller, J. Chem. Phys., 18, 79, (1950)

64. Dewhurst, J. Chem. Phys., 19, 1329, (1951)

65. Weiss, Nucleonics, 10, 28, (1952)

66. Davidson, Goldblith and Proctor, Nucleonics, 11, 22, (1953)

67. Hochanadel and Ghormley, J. Chem. Phys., 21, 880, (1953)

68. Lazo, Dewhurst and Burton, J. Chem. Phys., 22, 1370, (1954)

69. Hardwick, Can. J. Chem., 30, 17, (1952)

70. Bastian, Weberling and Palilla, Anal. Chem., 25, 284, (1953)

71. Farmer, J. Chem. Soc., , 3248, (1954)

72. Weiss, Allen and Schwarz, Geneva Conference, Paper 155, (1955)

73. Haybittle, Saunders and Swallow, J. Chem. Phys., 25, 1213, (1956)

74. Gilat and Stein, Geneva Conference, Vol 29, 43, (1958)

75. Rosinger, Ibid, 21, 209, (1958)

76. Taimuty, Towle and Peterson, Nucleonics, 17, 103, (1959)

77. Harlan and Hart, Nucleonics, 17, 102, (1955)

78. Nickolic and Wright, Nucleonics, 13, 104, (1955)

79. Henley, Nucleonics, 11, 41, (1953)

80. Hart, Koch and Taimuty, Geneva Conference, 21, 188, (1958)

81. Taimuty, Glass and Deaver, Ibid, 21, 204, (1958)

82. Kuhl, Manowitz and Rosenzweig, Curie Evaluation of Hollow Cylindrical Sources, BNL - 260, (1953)

83. Lewis, Nehemias, Harmer and Martin, Nucleonics, 12, 40, (1954)

84. Smith and Atkins, Nucleonics, 14, 25, (1956)

85. Saunders, Morehead and Daniels, J. Am. Chem. Soc., 75, 3096, (1953)

86. Magat and Reinisch, J. App. Rad. Isotopes, 1, 194, (1956)

87. Kovalev, J. App. Rad. Isotopes, 3, 113, (1958)

88. Ferguson, Geneva Conference, paper 551, (1955)

89. Ryan and Wheelwright, Ind. Eng. Chem., 51, 60, (1959)

90. Cathers, Geneva Conference, paper 743, (1955)

91. Hammond, Geneva Conference, paper 724, (1955)

92. Higgins, Radiation Damage to Ion Exchange Resin, ORNL - 1325, (1953)

93. Fisher, Effect of Gamma Radiation on Ion Exchange Resins, RMO 2528, (1954)

94. Wedemeyer, The Stability of Ion Exchange Resins to X-rays, PhD. Thesis, Vanderbilt University, (1953)

95. Nikashina, Breger, Senyavin and Gordievskii, Int. J. App. Rad. - and Isotopes, 4, 201, (1959)

96. Nikashina et al, Khim. Prom. (573), 1959

97. Costachel and Furnica, The Chemical Modification of Ion Exchange Resins under the action

of Ionising Radiation, Geneva Conference, paper 1294, (1958)

98. Costachel, Furnica and Dragut, Studii si. cercetari de chimie, 7, 409, (1959)

99. Furnica and Dragut, Studii cercetari de chimie, 7, 399, (1959)

100. Costachel, Furnica and Grigorescu, Referat. Zhur. Khin., 2, 4080, (1959)

101. Shigematsu, and Oshio, Bull. Inst. Chem. Research, Kyoto University, 36, 349, (1959)

102. Nater, Geneva Conference, paper 1476, (1958)

103. Tsuan Man Wei, Ai Chernova, and Proskurnin, Atomnaya Energ., 5, 573, (1958)

104. Polevdov, Nikashina, Gordiyevskii, Senyavin and Breger, Nanch. Doklady, Vysshei Shkoly Khim.i Khim. Tekhnol, 4, 761, (1958)

105. Semushin and Kuzin, Zhur. priklad. Khim, 32, 2193, (1959)

106. Utley, Diss. Abs., 20, 1198, (1959)

107. Pesek and Bednar, Jaderna Energ. 6, 267, (1960)

108. Kraus and Nelson, Geneva Conference, paper 837 (1955)

109. Kunin, and McGarvey, Ind. Eng. Chem., 41, 1265, (1949)

110. Kunin, Anal. Chem., 21, 87, (1949)

111. Lindsay and D'Amico, Ind. Eng. Chem., 43, 1085, (1951)

112. Wheaton and Baumann, Ind. Eng. Chem., 43, 1088, (1951)

113. Feigl, Spot Tests in Organic Analysis, Elsevier Publishing Co., (1956)

114. Waddington, Ph.D. Thesis, University of London, (1956)

115. Feigl and Anger, Mikrochim Acta, 1, 138, (1937)

116. Rimini, L'Orosi, 22, 40, (1899)

117. Fisher and Kunin, Anal. Chem., 27, 1191, (1955)

118. Mizuch and Savchenko, Org. Chem. Ind. USSR, 7, 24, (1940)

119. Weber and Wilson, J. Biol. Chem., 35, 385, (1918)

120. Aycock, Eisenbraun and Shracher, J. Am. Chem. Soc., 73, 1351, (1951)

121. Blumrich and Bandel, Angew. Chem., 54, 374, (1941)

122. Dyer, J. Fisheries Research Board Can., 7, 576, (1950)

123. Richter, Lee and Hill, J. Biochem., 35, 1225, (1941)

124. Clark and Morgan, Mikrochim Acta, 20, 966, (1956)

125. English, Anal. Chem., 23, 344, (1957)

126. Cullis, and Waddington, Anal. Chim. Acta, 15, 158, (1956)

127. Stanley, Baun and Gove, Anal. Chem., 23, 1779, (1951)

128. Critchfield and Johnson, Anal. Chem., 28, 436, (1956)

129. Milun, Anal. Chem., 29, 1502, (1957)

130. Persez and Poirier, Bull. Soc. Chim., France, 754, (1953)

131. Snell and Snell, Colorimetric Methods of Analysis, Volume 2, (1949)

132. Gove, Baum and Stanley, Anal. Chem., 23, 721, (1951)

133. Crowther and Large, Analyst, 81, 64, (1956)

134. Bolleter, Bushman and Tidwell, Anal. Chem., 33, 593, (1961)

135. Deniges, Compt. rend., 150, 529, (1910)

136. Blaedel and Blacet, Anal. Chem., 13, 449, (1941)

137. Eegriwe, Z. Anal. Chem., 22, 110, (1937)

138. Bricker and Johnson, Anal. Chem., 17, 400, (1945)

139. Salterfield, Wilson and Leclair, Anal. Chem., 26, 1792, (1954)

140. Natarajan, Private Communication

141. Rigg, Weiss and Schales, J. Chem. Soc., 3034, (1952)

142. Charlesby, J. Polymer Sci., 11, 513, 521, (1953)

143. Cottrell, Strength of the Chemical Bond, Butterworth, (1956)

144. Baumann, A.E.C. Research and Development Report, DP 477, April 1960

145. Lemmon, Nucleonics 11, 44, (1953)
J. Am. Chem. Soc., 77, 4139, (1955)
J. Am. Chem. Soc., 80, 2730, (1958)

146. Burton and Praill, Quarterly Rev., 6, 302, (1952)

147. Wheaton, and Baumann, Ind. Eng. Chem., 43, 1088, (1951)

148. Swetz, Ind. Eng. Chem., 47, 1020, (1955)

149. Marinsky and Potter, A.E.C.U. - 3348, (1954)

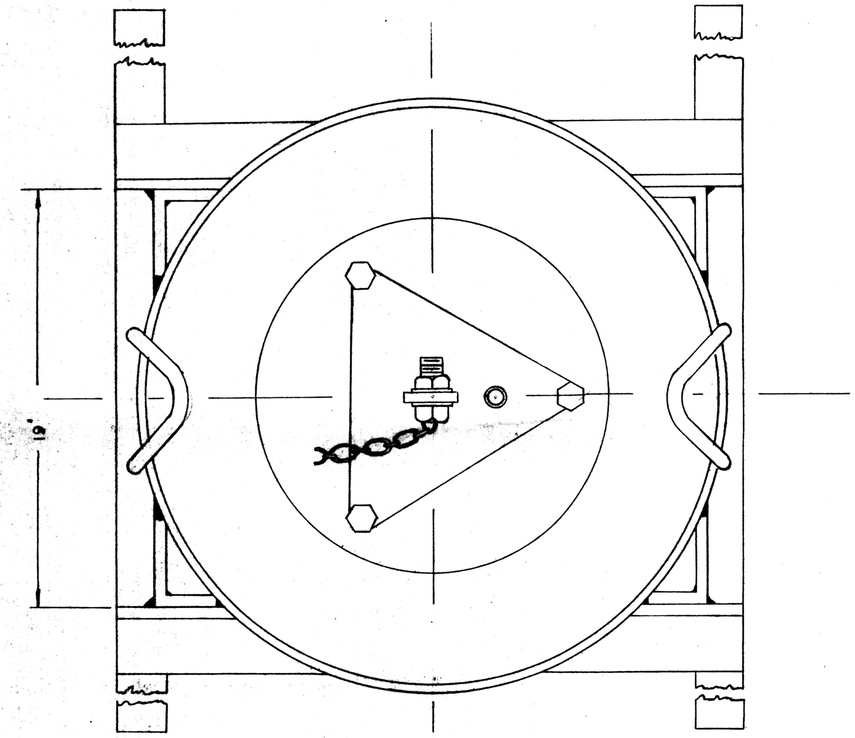
150. Baumann, J. Chem. Eng. Data, 5, 376, (1960)

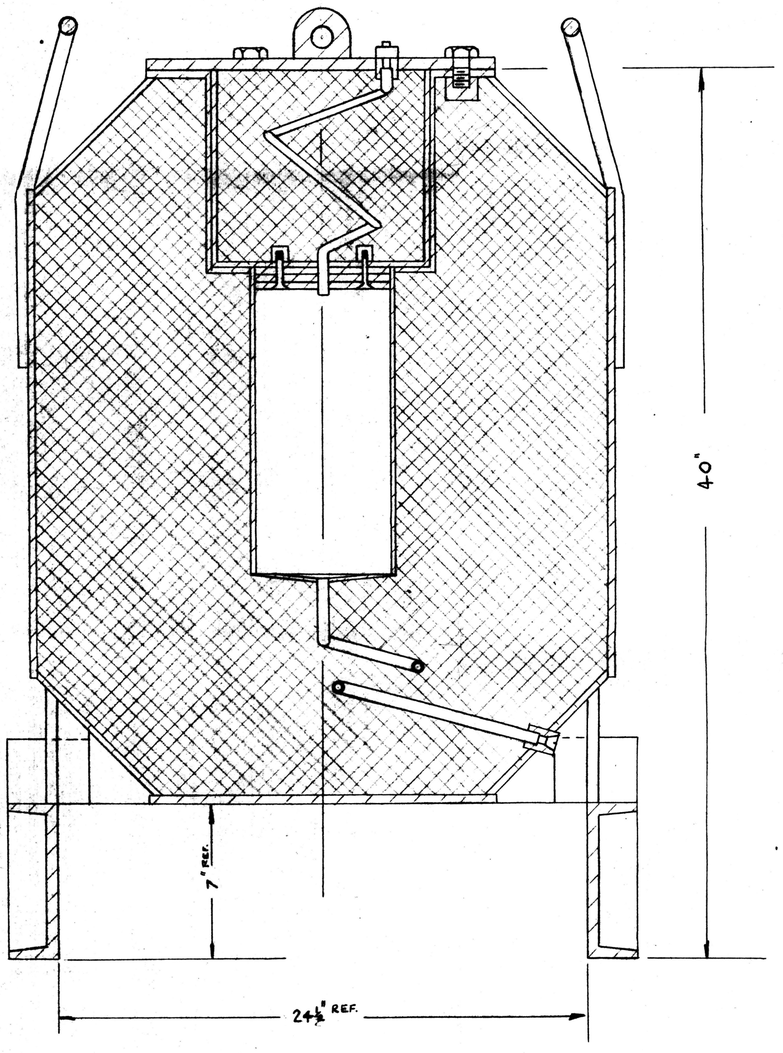
Geneva Conference (1955):

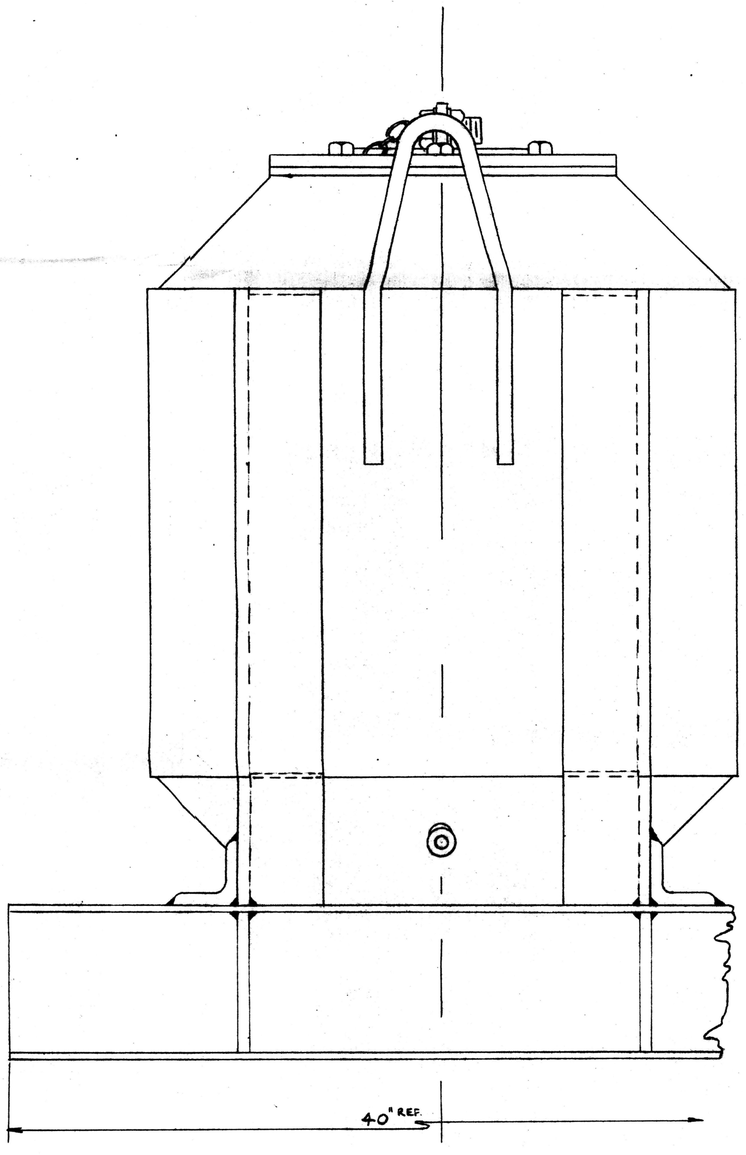
Proceedings of the First Geneva Conference on the Peaceful Uses of Atomic Energy.

Geneva Conference (1958):

Proceedings of the Second Geneva Conference on the Peaceful Uses of Atomic Energy.







NOTE : MAXIMUM CAPACITY 39,000 CURIES. Co 60

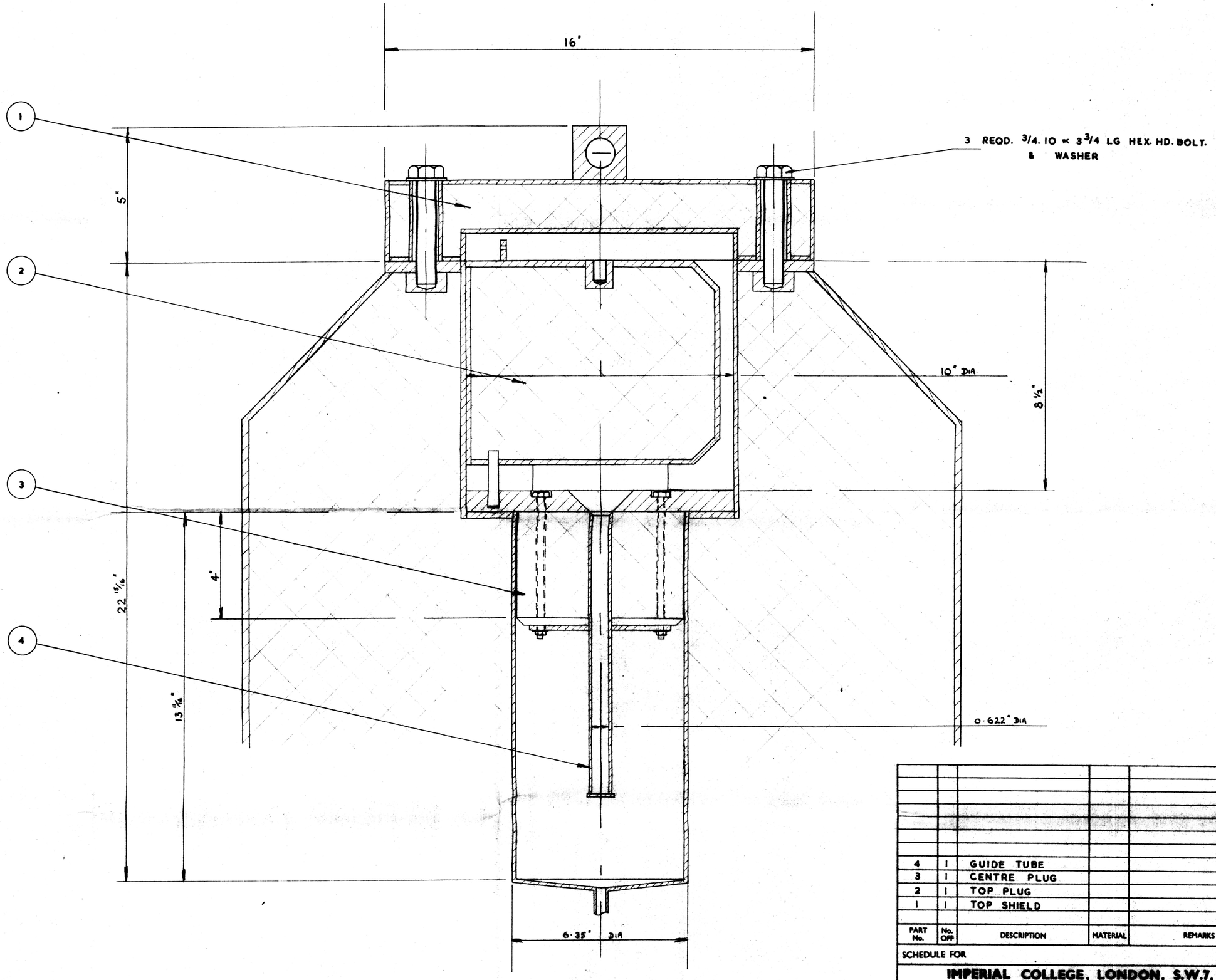
PART No.	No. OFF	DESCRIPTION	MATERIAL	REMARKS

SCHEDULE FOR

IMPERIAL COLLEGE, LONDON. S.W.7.
CHEMICAL ENGINEERING DEPARTMENT

TITLE
STANDARD SHIPPING CONTAINER

SCALE 1/4 FULL SIZE	DRAWN BY M. Street	DATE
JOB No.	DRG. No. N.T. 1.	



PART No.	No. OFF	DESCRIPTION	MATERIAL	REMARKS
4	1	GUIDE TUBE		
3	1	CENTRE PLUG		
2	1	TOP PLUG		
1	1	TOP SHIELD		

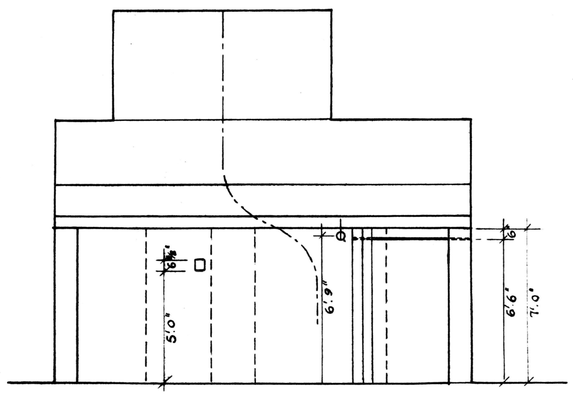
SCHEDULE FOR

IMPERIAL COLLEGE, LONDON. S.W.7.
CHEMICAL ENGINEERING DEPARTMENT

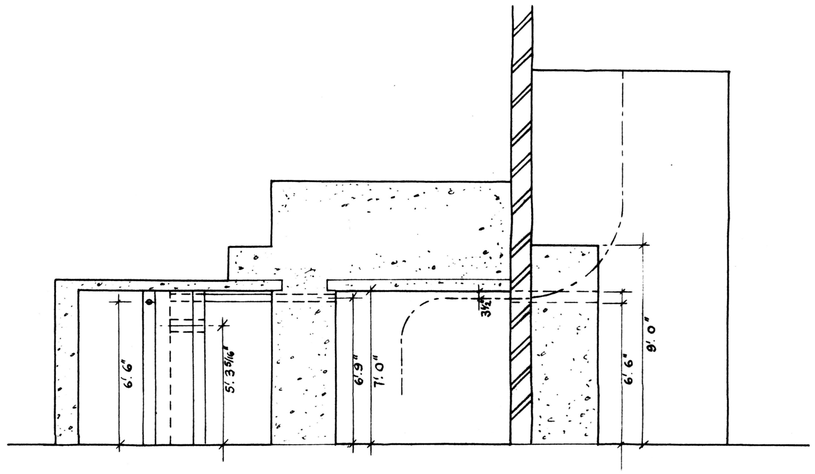
TITLE **MODIFIED PLUG FOR LEAD CONTAINER**

SCALE 1/2 FULL SIZE | DRAWN BY M. Streat | DATE

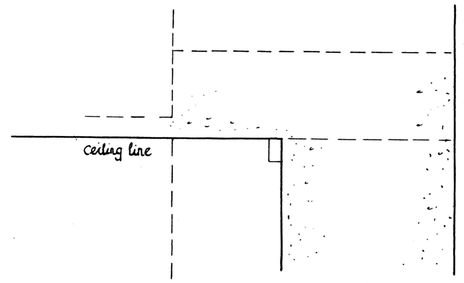
JOB No. | DRG. No. NT. 2.



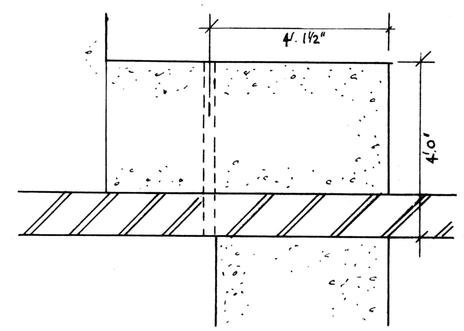
SECTION A - A



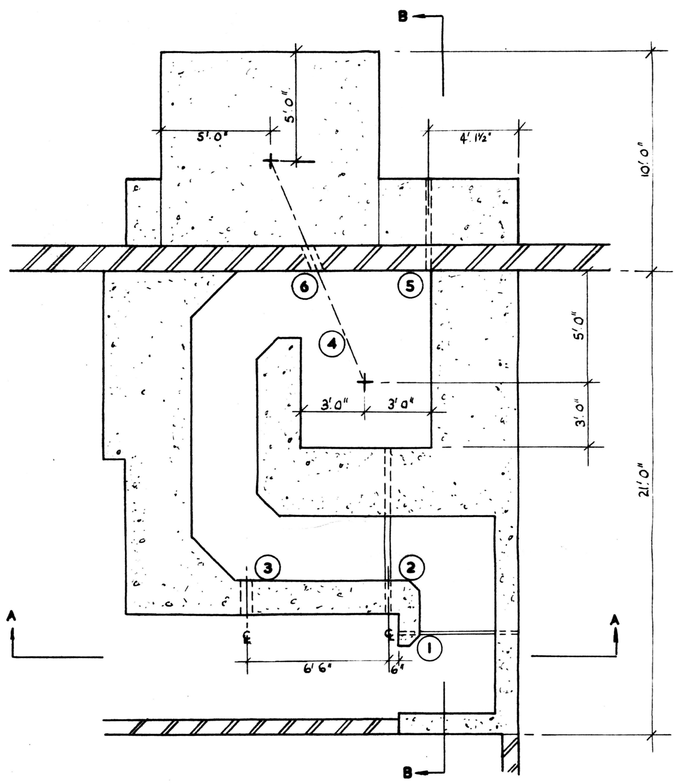
SECTION B - B



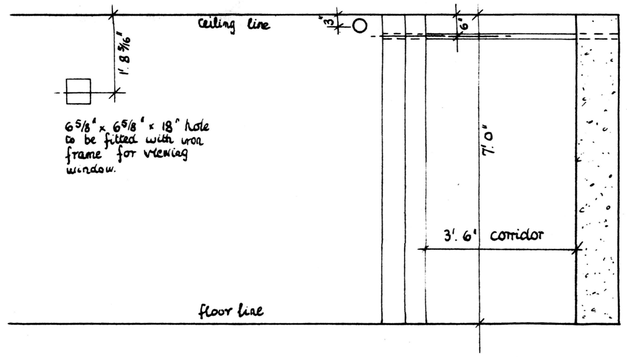
ELEVATION



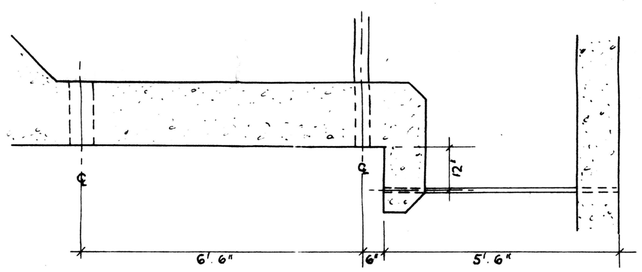
PLAN DETAIL. 5.



PLAN



ELEVATION



PLAN DETAIL. 1.

PART No.	No. OFF	DESCRIPTION	MATERIAL	REMARKS
1	1	1" DIA. TUBE	M.S.	
2	1	4" DIA. TUBE	M.S.	
3	1	6⅝" x 6⅝" HOLE		WINDOW FRAME
4	1	1" O.D. 16 SWG TUBE	S.S.	GUIDE TUBE
5	1	6" x 3" x 4'. 0" DUCT		
6	1	6" DIA. PIPE	C. I.	

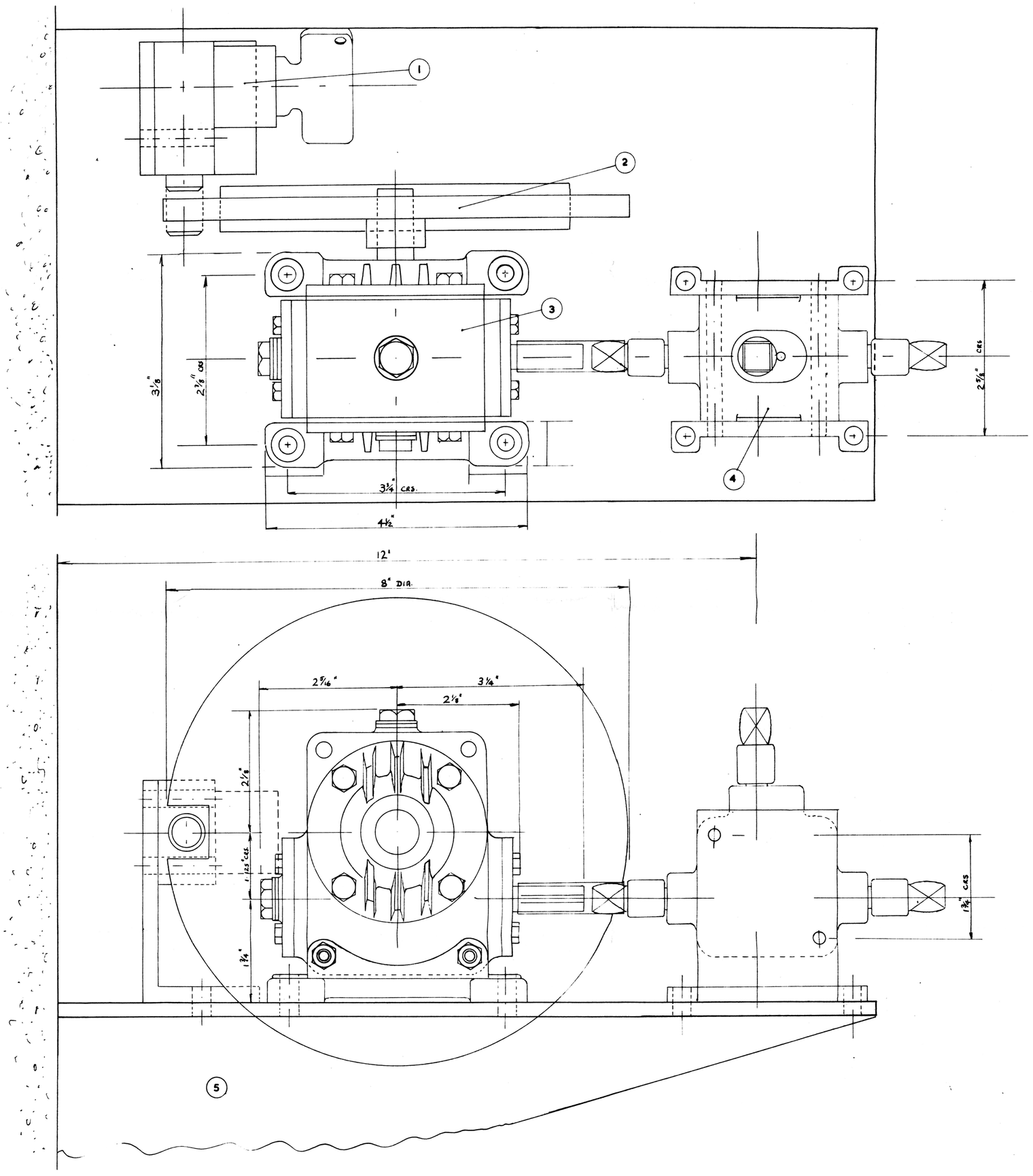
SCHEDULE FOR

IMPERIAL COLLEGE, LONDON. S.W.7.
CHEMICAL ENGINEERING DEPARTMENT

TITLE
CONCRETE SHIELD

SCALE 1/4 TO 1 FT., 1/2 TO 1 FT. | DRAWN BY M. Street | DATE 11. 6. 59.

JOB No. | DRG. No. NT. 3.



PART No.	No. OFF	DESCRIPTION	MATERIAL	REMARKS
1	1	CASTELL LOCK		TYPE K
2	1	BRASS DISC		8 DIA 3/8
3	1	CROFTS WORM GEAR BOX		REDUCTION 25/1
4	1	BEVEL BOX		TELEFLEX
5	1	INTELOCK SUPPORT		

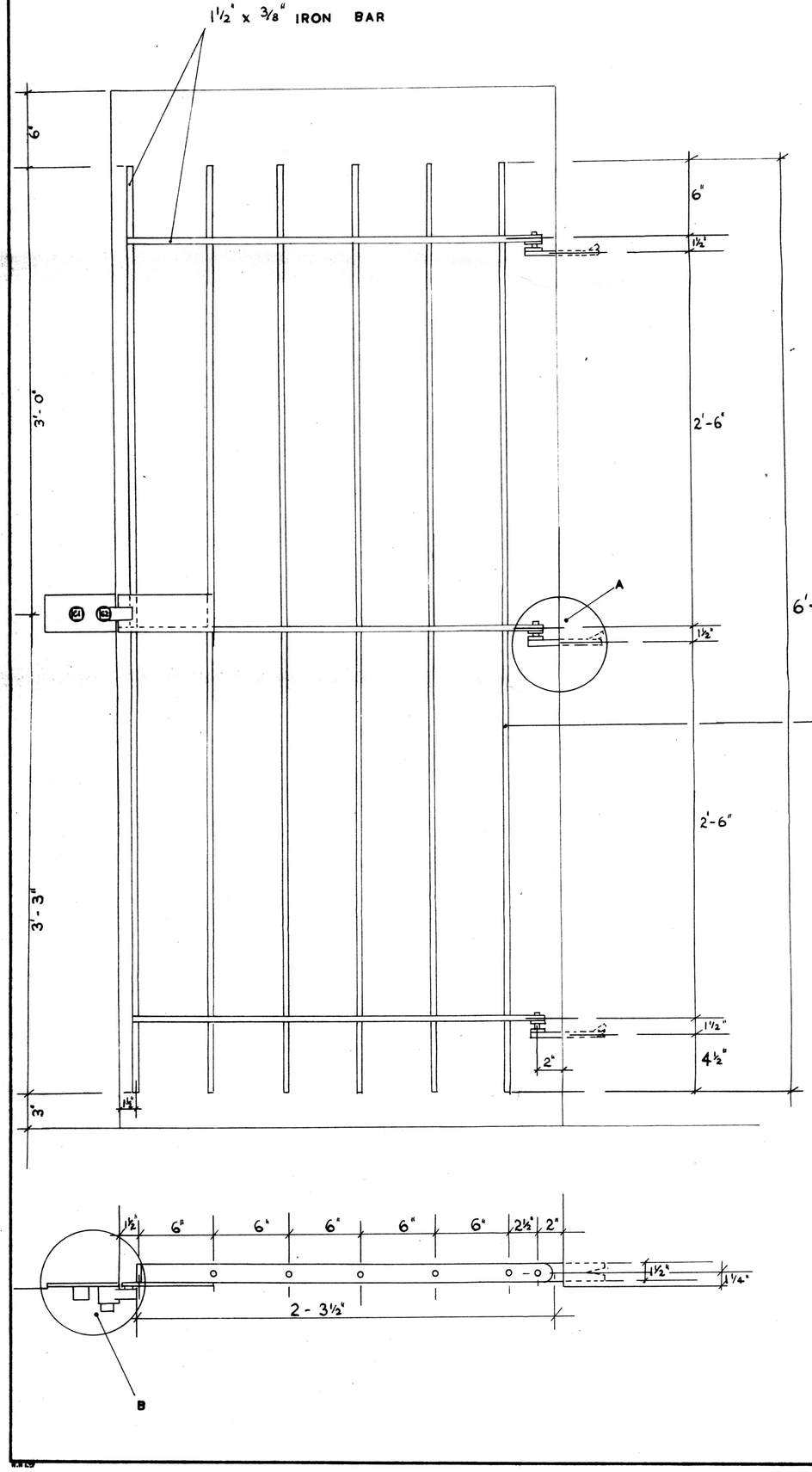
SCHEDULE FOR

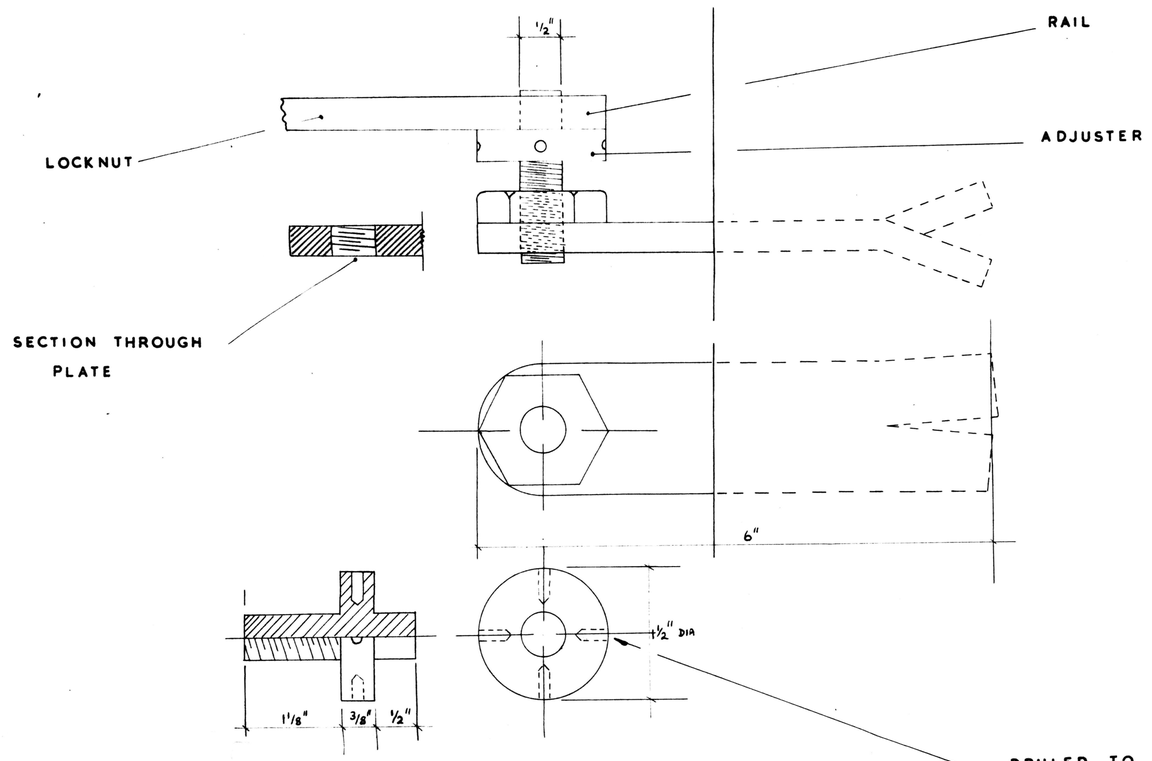
IMPERIAL COLLEGE, LONDON. S.W.7.
CHEMICAL ENGINEERING DEPARTMENT

TITLE

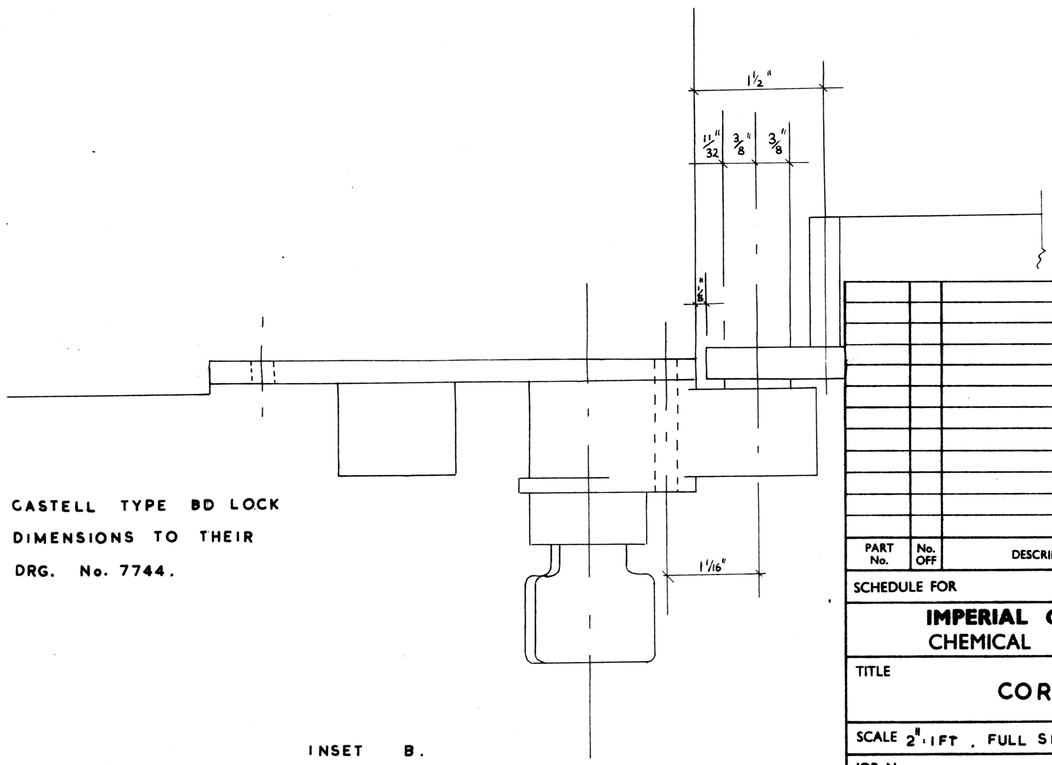
SOURCE INTERLOCK

SCALE FULL SIZE	DRAWN BY M. Sheat	DATE 3. 7. 59
JOB No.	DRG. No. NT. 4.	





INSET A.



CASTELL TYPE BD LOCK
DIMENSIONS TO THEIR
DRG. No. 7744.

INSET B.

PART No.	No. OFF	DESCRIPTION	MATERIAL	REMARKS
				GATE TO BE MANUFACTURED TO DRAWING WITH 7½" x 3" CATCH PLATE WELDED TO POSITION ON SITE TO GIVE ⅛" CLEARANCE.

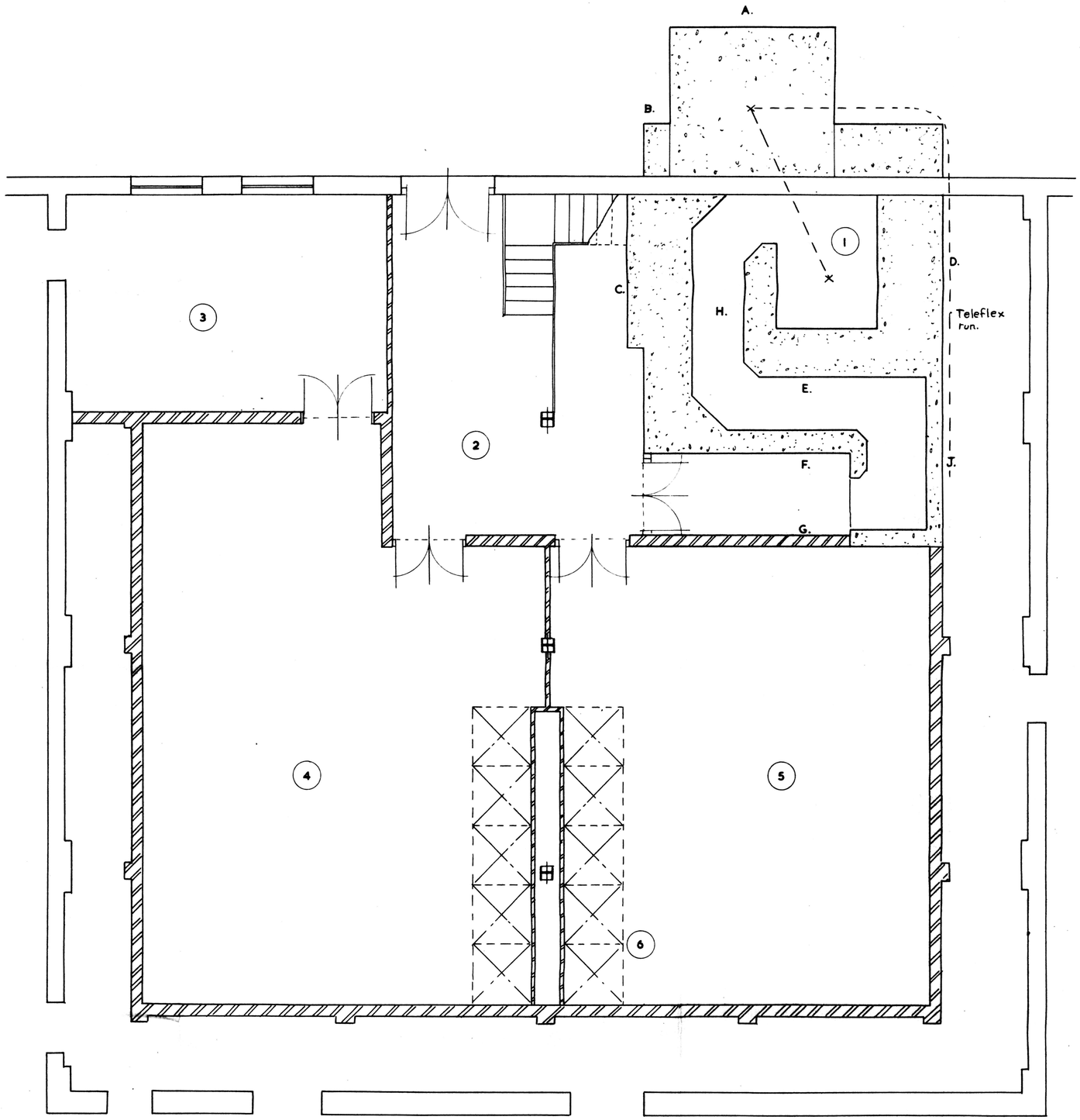
SCHEDULE FOR

IMPERIAL COLLEGE, LONDON, S.W.7.
CHEMICAL ENGINEERING DEPARTMENT

TITLE

CORRIDOR GATE

SCALE 2" : 1 FT. FULL SIZE	DRAWN BY M. Street. DATE 22. 6. 59.
JOB No.	DRG. No. N T. 5.



PART No.	No. OFF	DESCRIPTION	MATERIAL	REMARKS
	1	SOURCE ROOM		
	2	ENTRANCE HALL		
	3	COUNTING ROOM		
	4	ACTIVE LAB.		
	5	RESEARCH LAB.		
	6	FUME HOODS		

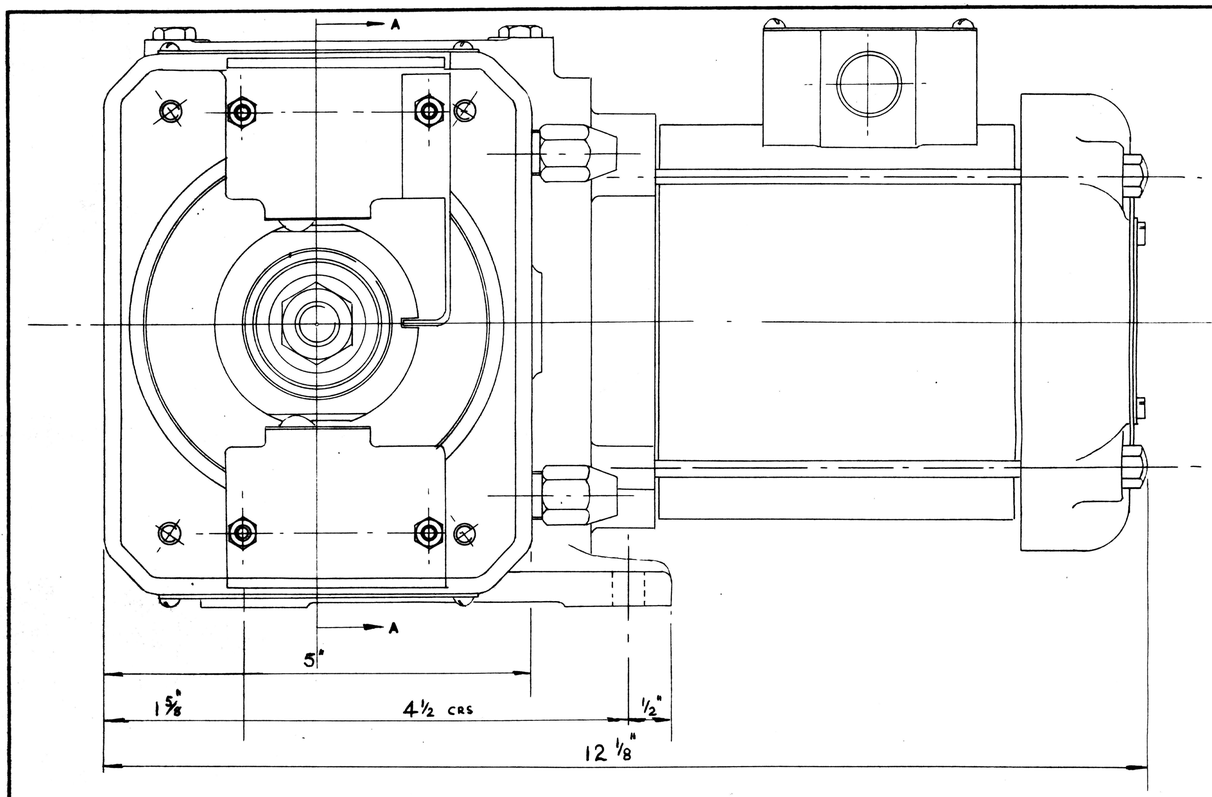
SCHEDULE FOR

IMPERIAL COLLEGE, LONDON. S.W.7.
CHEMICAL ENGINEERING DEPARTMENT

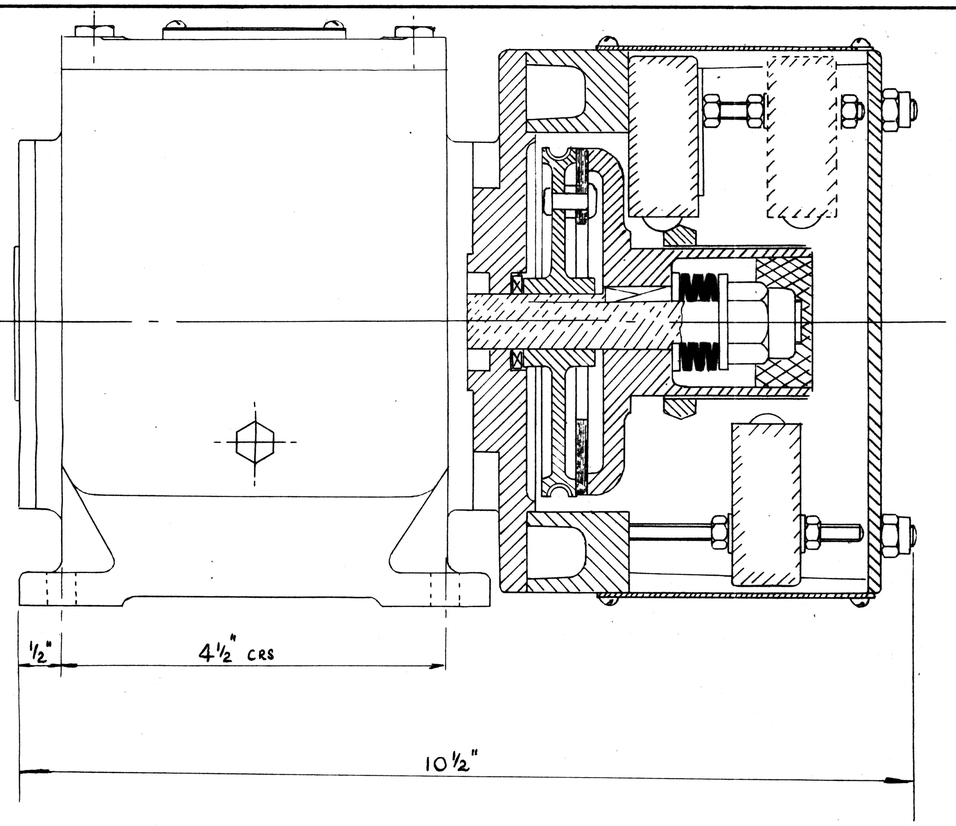
TITLE

NUCLEAR TECHNOLOGY LABS.

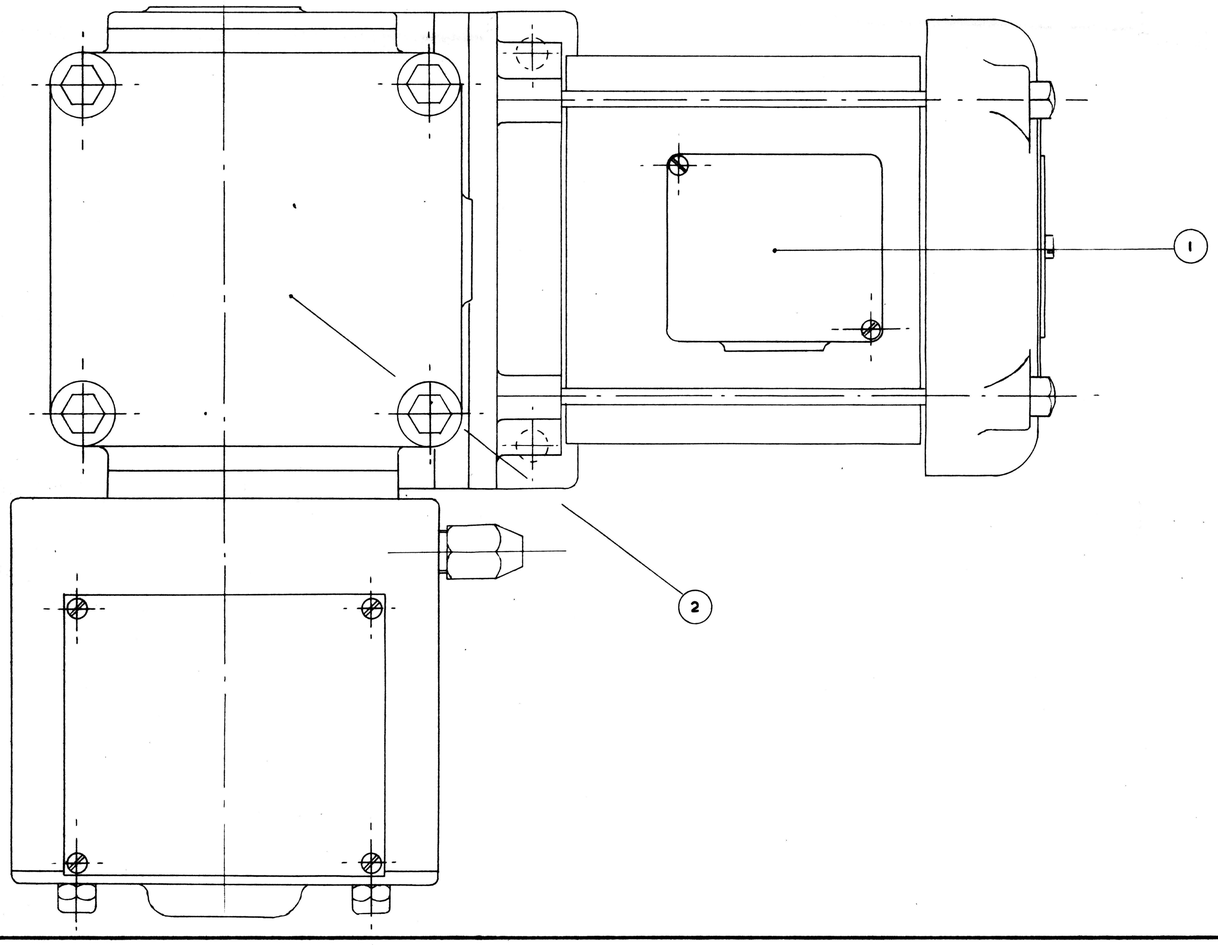
SCALE 1/4" TO 1 FT	DRAWN BY M. Short DATE 22. 6. 59.
JOB No.	DRG. No. N T. 6.



VIEW OF DRIVE UNIT WITH COVER REMOVED.



SECTION A-A THROUGH DRIVE UNIT SHOWING SLIPPING CLUTCH ARRANGEMENT.



PART No.	No. OFF	DESCRIPTION	MATERIAL	REMARKS
	1.	3 PHASE ELECTRIC MOTOR 2800 R.P.M.		
	2.	40/1 REDUCTION GEARBOX ASSEMBLY.		

SCHEDULE FOR

IMPERIAL COLLEGE, LONDON. S.W.7.
CHEMICAL ENGINEERING DEPARTMENT

TITLE
TELEFLEX DRIVE MOTOR

SCALE FULL SIZE	DRAWN BY M. Great.	DATE 9. 9. 60.
JOB No.	DRG. No. NT. 7.	